

Towards Defining the Role of CNS  
Circuits in Control of Energy  
Homeostasis

**Inaugural-Dissertation**

zur Erlangung des Doktorgrades

der Mathematisch-Naturwissenschaftlichen Fakultät  
der Universität Köln

vorgelegt von  
Simon Heß  
aus Adenau

Köln 2011

Berichterstatter: **Prof. Dr. Peter Kloppenburg**  
**Prof. Dr. Jens Brüning**

Tag der mündlichen Prüfung: 19.10.2011

# Contents

<b>Abbreviations</b>	<b>ix</b>
<b>Abstract</b>	<b>x</b>
<b>Zusammenfassung</b>	<b>xii</b>
<b>1 Introduction</b>	<b>1</b>
1.1 The central nervous system in control of energy homeostasis . . . . .	2
1.2 Insulin and leptin signaling in the CNS . . . . .	5
1.3 The ventromedial hypothalamus (VMH) . . . . .	7
1.4 The dopaminergic system in control of energy homeostasis . . . . .	10
1.4.1 Dopamine and the anatomy of the dopaminergic system . . . . .	11
1.4.2 Physiology of dopaminergic signaling . . . . .	13
1.4.3 The role of the dopaminergic system in food reward . . . . .	16
1.5 The fat mass and obesity-associated protein ( <i>Fto</i> ) . . . . .	20
1.6 Technical aspects . . . . .	21
1.6.1 The perforated patch clamp technique . . . . .	21
1.6.2 Pore-forming agents . . . . .	22
1.7 Objectives . . . . .	29
<b>2 Materials and Methods</b>	<b>32</b>
2.1 Animal care . . . . .	32
2.2 Brain slice preparation . . . . .	32
2.3 Patch-clamp recordings . . . . .	33
2.3.1 Whole cell recordings . . . . .	35
2.3.2 Measurements of postsynaptic currents . . . . .	35
2.3.3 Perforated-patch clamp recordings . . . . .	36
2.3.4 Single cell labeling . . . . .	36

2.3.5	Drugs . . . . .	37
2.3.6	Data analysis . . . . .	38
<b>3</b>	<b>Results</b>	<b>39</b>
3.1	The perforated patch technique . . . . .	39
3.1.1	Whole cell vs. perforated-patch clamp . . . . .	39
3.1.2	Technical considerations . . . . .	44
3.1.3	Ionophores . . . . .	45
3.2	Regulation of SF-1 neurons in the ventromedial hypothalamus by fuel sensing signals . . . . .	47
3.2.1	Properties of SF-1 neurons . . . . .	47
3.2.2	Insulin hyperpolarizes and decreases the firing rate of SF-1 neurons	50
3.2.3	Ablation of insulin receptors in SF-1 neurons alters synaptic connectivity in HFD mice . . . . .	53
3.3	Regulation of mesencephalic dopaminergic midbrain neurons by fuel sensing signals . . . . .	55
3.3.1	Properties of mesencephalic dopaminergic neurons . . . . .	55
3.3.2	Insulin activates the PI3-kinase pathway and increases the activity of mesencephalic dopaminergic neurons . . . . .	58
3.3.3	The excitatory effect of insulin on mesencephalic dopaminergic neurons is cell-intrinsic . . . . .	62
3.3.4	Wortmannin reverses the excitatory effect of insulin . . . . .	64
3.4	Regulation of mesencephalic dopaminergic midbrain neurons by the obesity-associated Fto gene . . . . .	66
3.4.1	Fto alters cocaine-induced responses of mesencephalic dopaminergic neurons . . . . .	66
3.4.2	Fto regulates D <sub>2</sub> -receptor-dependent control of firing in mesencephalic DA neurons in a cell-autonomous manner . . . . .	70
3.4.3	D <sub>2</sub> R-signaling is necessary for cocaine-induced ‘rebound’ . . . . .	72
3.4.4	Fto affects the pacemaker efficacy in mesencephalic dopaminergic neurons of cocaine-sensitized animals . . . . .	74

<b>4</b>	<b>Discussion</b>	<b>78</b>
4.1	The Perforated-Patch Configuration revisited . . . . .	78
4.2	The ventromedial hypothalamus in control of energy homeostasis . . . . .	80
4.2.1	Properties of SF-1 neurons . . . . .	81
4.2.2	Insulin signaling modulates the neuronal activity of SF-1 neurons and alters the synaptic connectivity in HFD mice . . . . .	82
4.2.3	Outlook . . . . .	85
4.3	Regulation of mesencephalic dopaminergic neurons by feeding-related signals . . . . .	87
4.3.1	Properties of mesencephalic dopaminergic neurons . . . . .	88
4.3.2	Insulin signaling modulates the neuronal activity and alters the synaptic connectivity of mesencephalic dopaminergic neurons . . . . .	90
4.3.3	Outlook . . . . .	92
4.4	Regulation of mesencephalic dopaminergic midbrain neurons by the obesity- associated Fto gene . . . . .	95
4.4.1	Fto alters cocaine-induced responses of mesencephalic dopamin- ergic neurons . . . . .	95
4.4.2	Fto regulates D <sub>2</sub> -receptor-dependent control of firing in mesen- cephalic DA neurons in a cell-autonomous manner . . . . .	97
4.4.3	Fto affects the pacemaker efficacy in mesencephalic dopaminergic neurons of cocaine-sensitized animals . . . . .	98
4.4.4	Outlook . . . . .	99
<b>5</b>	<b>Appendix</b>	<b>101</b>
5.1	SK currents decrease during whole cell recordings . . . . .	101
5.2	Insulin activates the PI3-kinase pathway . . . . .	102
5.3	Population response of mesencephalic DA neurons upon insulin treatment	103
5.4	Fto regulates the activity of the dopaminergic circuitry . . . . .	104
5.5	Fto regulates D <sub>2</sub> -receptor-dependent control of firing in mesencephalic DA neurons in a cell-autonomous manner . . . . .	104

<b>List of Figures</b>	<b>108</b>
<b>List of Tables</b>	<b>109</b>
<b>Bibliography</b>	<b>110</b>
<b>Danksagung</b>	<b>130</b>
<b>Erklärung</b>	<b>132</b>
<b>Teilpublikationen</b>	<b>133</b>
<b>Curriculum Vitae</b>	<b>136</b>

# Abbreviations

AB	Antibody
AADC	Aromatic amino acid decarboxylase
AC	Adenylate cyclase
ACTH	Adrenocorticotrophic hormone
AgRP	Agouti-related protein
ARC	Arcuate nucleus
ATP	Adenosine triphosphate
BBB	Blood-brain-barrier
BMI	Body mass index
CA	Catecholamine
cAMP	cyclic adenosine monophosphate
CART	Cocaine-amphetamine regulated transcript
CNQX	6-Cyano-7-nitroquinoxaline-2,3-dione (AMPA/kainate receptor antagonist)
CNS	Central nervous system
CPP	Conditioned place preference
CPu	Caudate putamen
D2R	Dopamine type 2 receptor
DA	Dopamine/dopaminergic
DAG	diacylglycerine
DAP-5	DL-2-amino-5-phosphopentanoic acid (NMDA receptor antagonist)
DARPP-32	32 kD dopamine and cAMP-regulated phosphoprotein
DAT	Dopamine transporter
DR	Dopamine receptor
DBH	Dopamine $\beta$ -decarboxylase

DMH	Dorsomedial hypothalamus
DMSO	Dimethyl sulfoxide
DMT2	Diabetes mellitus type 2
FFA	Free fatty acids
GABA	$\gamma$ -Aminobutyric acid
GHRH	Growth hormone-releasing hormone
GIRK	G-Protein activated inwardly rectifying potassium channel
GPCR	G-Protein coupled receptor
GR	Ghrelin receptor
HFD	High-fat diet
i.c.v.	intracerebroventricular
IP <sub>3</sub>	Inositoltrisphosphate
IR	Insulin receptor
IRS	Insulin-receptor-substrate
JAK2	Janus kinase 2
K <sub>ATP</sub>	ATP-dependent potassium channel
LepR	Leptin receptor
LH	Lateral hypothalamus
MC3/4	Melanocortin receptor 3 and 4
MSN	Medium spiny neuron
NA	Numerical aperture
NAc	Nucleus accumbens
NCD	Normal chow diet
NPY	Neuropeptide Y
PDK	Phosphatidylinositol-dependent kinase
PFC	Prefrontal cortex
PI3K	Phosphatidylinositol-3-kinase
PIP	Phosphatidylinositolphosphate

PIP <sub>2</sub>	Phosphatidylinositol-4,5-bisphosphate
PIP <sub>3</sub>	phosphatidylinositol-3,4,5-bisphosphate
PKC	Protein kinase C
PLC	Phospholipase C
PTX	Picrotoxin (GABA <sub>A</sub> receptor antagonist)
POMC	Proopiomelanocortin
PP-1	Protein phosphatase 1
PTEN	Phosphatase and tensin homolog
PVN	Paraventricular nucleus
RRA	Retrochubral area
R <sub>S</sub>	Series resistance
SF-1	Steroidogenic factor 1
SNP	single nucleotide polymorphisms
SNpc	Substantia nigra <i>pars compacta</i>
TH	Tyrosine hydroxylase
TRPC	Transient receptor potential channel
VMAT2	Vesicular monoamine transporter 2
VMH	Ventromedial hypothalamus
VTA	Ventral tegmental area
WD	Working distance
WHO	World health organization

# Abstract

Healthy individuals are able to maintain a steady body weight over a long period of time due to an active process called energy homeostasis in which food intake is matched to energy expenditure with great precision. Once this tightly regulated system becomes unbalanced, weight gain and, on a longer time scale, obesity will develop. The control of energy homeostasis is accomplished by neuronal circuits within the CNS. These circuits, are able to modulate food intake and energy expenditure in response to various peripheral signals related to energy stores.

Among the peripheral signals which have been found to directly act on the CNS circuits in control energy of homeostasis is the pancreas-derived hormone insulin (Brüning *et al.* , 2000). Although, most studies focused on the role of insulin in neurons of the arcuate nucleus of the hypothalamus (ARC), insulin receptors are also expressed in other brain areas involved in the control of energy homeostasis such as the ventromedial hypothalamus (VMH) and the mesencephalon (Havrankova *et al.* , 1978).

In this thesis, the effect of insulin signaling on the electrophysiological properties of SF-1 neurons of the VMH and dopaminergic neurons of the mesencephalon was investigated. Perforated-patch recordings were performed to characterize insulin's effect on the single-cell level and whole cell recordings were performed to investigated insulin signaling dependent alterations on a network level.

In the VMH, insulin directly hyperpolarizes a subset of SF-1 neurons via a PI3-kinase signaling cascade. The reduction in firing rate is largely dependent on the activation of ATP-dependent potassium channels ( $K_{ATP}$ ). In contrast, insulin did not reduce the firing rate of SF-1 neurons in which the insulin receptor was specifically deleted. On a network level, ablation of insulin receptors in SF-1 neurons alters the synaptic connectivity in mice subjected to a high-fat diet (HFD). Ablation of the insulin receptor results in the increase of excitatory drive on anorexigenic POMC neurons in the ARC. Accordingly, mice with a SF-1 neuron specific ablation of the insulin receptor are at least in part protected against HFD-induced alterations of metabolic parameters.

In the mesencephalic dopaminergic circuitry, insulin stimulates the neuronal activity of a subset of dopaminergic neurons. The excitatory effect of insulin is cell-intrinsic and is mediated via PI3K-dependent signaling. Ablation of the insulin receptor in dopaminergic neurons abolished this response. Furthermore, this ablation decreases the excitatory input on dopaminergic neurons. Thus, insulin signaling is involved in the establishment or maintenance of excitatory synaptic connections in mesencephalic dopaminergic neurons.

In spite of the dysregulation of fuel-related signals, variations of certain genetic factors are also associated with the development of obesity and obesity-associated comorbidities like type 2 diabetes. Among those variations, single nucleotide polymorphisms within the *FTO* gene showed one of the most robust correlations with an increase in body mass index (Frayling *et al.* , 2007). The role of Fto was investigated in mesencephalic dopaminergic neurons using the perforated-patch configuration.

Ablation of Fto in mesencephalic dopaminergic neurons leads to profound alterations in cocaine-evoked responses in such a way that the cocaine-induced inhibition was strongly reduced in Fto-deficient mice. This altered response is also seen in mice with a Fto-deletion specifically in dopaminergic neurons showing the effect of Fto is cell-autonomous. Further pharmacological characterization could demonstrate that Fto regulates the activity of dopaminergic neurons via alterations of dopamine receptor type 2 signaling. This notion is further supported by behavioral experiments and quantitative realtime PCR. In summary, these findings reveal an Fto-dependent alteration of the function of the mesencephalic dopaminergic circuitry.

# Zusammenfassung

Aufgrund des aktiven Prozesses der Energie-Homöostase bleibt das Körpergewicht bei gesunden Individuen über lange Zeit auf einem konstanten Niveau. Nahrungsaufnahme und Energieverbrauch sind in diesem System präzise reguliert. Gerät dieser Regelkreis aus dem Gleichgewicht, kann dies zu einer Gewichtszunahme und über einen längeren Zeitraum zu Fettleibigkeit führen.

Die Energiehomöostase wird durch zentrale neuronale Netzwerke kontrolliert. Diese Netzwerke integrieren und verarbeiten periphere Signale, die in Abhängigkeit des Energiestatus ausgeschüttet werden. Dazu gehört das im Pankreas ausgeschüttete Hormon Insulin, welches neben vielfältiger peripherer Wirkungen auch direkt die ZNS-abhängige Kontrolle der Energiehomöostase beeinflusst (Brüning *et al.*, 2000). Insulinrezeptoren werden in einer Reihe zentralnervöser Strukturen wie dem ventromedialen Hypothalamus (VMH) und dem Mesencephalon exprimiert (Havrankova *et al.*, 1978). Die meisten Studien über die Rolle des Rezeptors konzentrierten sich bislang jedoch auf den Nucleus arcuatus (ARC).

In der vorliegenden Arbeit wurde daher die Wirkung von Insulin auf die elektrophysiologischen Eigenschaften von SF-1 Neuronen des VMH und auf dopaminerge Neurone im Mesencephalon der Maus mittels der *patch-clamp*-Technik untersucht. Eines der wichtigsten Ergebnisse dieser Studien ist die durch Insulin verursachte, PI3-Kinase abhängige Hyperpolarisation und damit Inhibition einer Unterpopulation von SF-1 Neuronen im VMH. Weiterhin konnte gezeigt werden, dass der inhibitorische Effekt von Insulin hauptsächlich auf die Aktivierung ATP-abhängiger Kaliumkanäle ( $K_{ATP}$ ) zurückzuführen ist. Im Gegensatz dazu ändert sich die Aktivität von SF-1 Neuronen mit einer spezifischen Deletion des Insulinrezeptors nach Insulinapplikation nicht. Auf der Netzwerkebene konnte mittels whole cell patch-clamp Messungen gezeigt werden, dass die Deletion des Insulinrezeptors einen Einfluss auf die synaptische Konnektivität im VMH von Mäusen hat, die zuvor mit einer fettreichen Diät (HFD) gefüttert wurden. Bei diesen Mäusen führt die Rezeptordeletion zu einem erhöhten exzitatorischen Ein-

gang auf POMC-Neurone des ARC, deren Aktivität einen Appetit-zügelnden Einfluss hat. Somit sind Mäuse mit einer SF-1-spezifischen Insulinrezeptordeletion zumindest teilweise gegen HFD-induzierte Veränderungen metabolischer Parameter geschützt.

Im dopaminergen System des Mesencephalon konnte gezeigt werden, dass Insulin die elektrische Aktivität einer Unterpopulation dopaminergener Neurone erhöht. Weiterhin konnte gezeigt werden, dass dieser Insulin-Effekt auf die Aktivierung des PI3-Kinase Signalweges zurückzuführen ist. Insulinrezeptordeletion in dopaminergen Neuronen hebt den Insulin-Effekt auf und führt zu einer Abnahme exzitatorischer Eingänge auf dopaminerge Neurone. Zusammenfassend konnte gezeigt werden, dass das Hormon Insulin die Aktivität dopaminergener Neurone beeinflusst. Es ist an der Etablierung und Aufrechterhaltung exzitatorischer Eingänge auf dopaminerge Zellen beteiligt.

Neben der Dysregulation peripherer Signale spielen auch Variationen bestimmter genetischer Faktoren eine Rolle bei der Entstehung von Fettleibigkeit. Die genetische Prädisposition begünstigt daher die Entstehung von Fettleibigkeit und die Manifestation mit Fettleibigkeit verbundener Krankheiten wie Typ 2 Diabetes. Einzelnukleotid-Polymorphismen (SNPs) innerhalb des *FTO*-Gens zeigten dabei die stärksten Korrelationen mit einem erhöhten body mass index (Frayling *et al.*, 2007). Mittels nicht-invasiver *perforated-patch*-Messungen an Gehirnschnitten von Mäusen wurde in dieser Arbeit die Rolle des *Fto* Gens in dopaminergen Neuronen des Mesencephalon untersucht.

Es konnte gezeigt werden, dass die Deletion von *Fto* zu tiefgreifenden Veränderungen auf Kokain-vermittelter Effekte führt. Die Kokain-induzierte Inhibition dopaminergener Neurone war in ubiquitär *Fto*-deletierten Mäusen geringer als in Kontrolltieren. Dieser Effekt trat auch in Mäusen auf, die eine *Fto*-Deletion exklusiv in dopaminergen Neuronen besaßen. Das deutet darauf hin, dass es sich um einen zellautonomen Effekt handelt. Anhand einer pharmakologischen Charakterisierung konnte gezeigt werden, dass die *Fto*-abhängigen Veränderungen der Aktivität dopaminergener Zellen auf Veränderungen des Dopaminrezeptor Typ 2-abhängigen Signalweges zurückzuführen ist. Diese Ergebnisse wurden durch quantitative realtime PCR und Verhaltensversuche unterstützt. Zusammenfassend zeigen die Ergebnisse, dass *Fto* die Funktion des dopaminergen Systems beeinflusst.

# 1 Introduction

**O**BESITY is a health condition which has dramatically increased over the last decades and is now being regarded as an epidemic of global proportions. First noted in the United States, obesity has spread to other industrialized countries and is becoming a major health threat in economically developing nations such as China, Mexico and Brazil (Caballero, 2007; Popkin & Gordon-Larsen, 2004). In 2008, 1.5 billion adults worldwide with an age of 20 years and older were overweight (defined as body mass index (BMI)  $\geq 25$  kg/m<sup>2</sup>; World Health Organization (WHO), 2007) and of these, nearly 500 million adults were obese (BMI  $\geq 30$  kg/m<sup>2</sup>; WHO fact sheet no. 311). These alarming numbers have also been appreciated in a report by the WHO Regional Office for Europe which states that “excess body weight poses one of the most serious health challenges of the 21<sup>st</sup> century for the WHO European Region” (WHO, 2009).

Hand in hand with the pandemic occurrence of overweight and obesity, associated co-morbidities like hypertension, stroke, cancer or diabetes mellitus type 2 (DMT2) are steadily increasing (Huxley *et al.* , 2009; Mosher *et al.* , 2009; Must *et al.* , 1999; Osmond *et al.* , 2009). Furthermore, a large body of evidence indicates that obesity and obesity-linked diseases like DMT2 negatively affect brain function (reviewed in Bruce-Keller *et al.* , 2009). Obesity leads to accelerated cognitive aging and age-related neurodegenerative diseases, such as Alzheimer’s and Parkinson’s disease (reviewed in Luchsinger & Mayeux, 2007; O’Rahilly, 2009; Yaffe, 2007). Therefore, factors contributing to the development of obesity are of great interest. Genetic predispositions in combination with environmental and behavioral factors, such as a sedentary lifestyle and unlimited availability of highly nutritious energy-dense food result in a mismatch of food intake versus energy expenditure — the root cause of overweight and obesity. Once this tightly regulated and fine-tuned system becomes unbalanced, weight gain, and on a longer time scale, obesity will develop (Morton *et al.* , 2006).

Hence, it is of greatest importance to define the homeostatic control mechanisms

involved in regulation of body weight and energy homeostasis in order to gain a full understanding of the development of obesity and related co-morbidities.

## 1.1 The central nervous system in control of energy homeostasis

Owing to environmental factors like emotions, time of day, convenience etc., energy intake as well as expenditure is subjected to day-to-day fluctuations. Despite these short-term imbalances, healthy individuals are able to maintain a steady body weight over very long time periods. This phenomenon reflects an active process called energy homeostasis in which cumulative food intake is matched with great precision to energy expenditure.

Nearly 60 years ago, Kennedy (1953) was the first who postulated that signals proportional to the amount of body fat modulate food intake and energy expenditure, thus maintaining energy homeostasis. A series of pioneering lesion studies in which different regions of the hypothalamus were destroyed demonstrated the pivotal role of the central nervous system (CNS) in the maintenance of energy homeostasis. Lesions of the ventromedial hypothalamus (VMH), paraventricular nucleus (PVN) and the dorsomedial hypothalamus (DMH) caused hyperphagia (excessive food intake) and obesity (Brobeck & Tepperman, 1943; Hetherington, 1940, 1944), whereas lesions of the lateral hypothalamus (LH) led to hypophagia (reduced food intake; Brobeck, 1951). Further evidence in favor of Kennedy's hypothesis came from parabiosis<sup>1</sup> studies on hypothalamic lesioned rats. Rats with lesions in the VMH were merged with normal rats. While the animals which lacked the VMH developed obesity, the normal counterparts developed hypophagia and weight loss. These experiments demonstrated for the first time the presence of a satiety-mediating signal which provides a negative-feedback in proportion to body fat mass (Hervey, 1959).

During the following decades, the peripheral hormones insulin and leptin were identified as signals to convey the energy status to the brain. While insulin is produced in pancreatic  $\beta$ -cells, leptin is derived from adipocytes. Both hormones are secreted proportional to body fat content and cross the blood-brain-barrier (BBB) via a saturable

---

<sup>1</sup>*parabiosis* – two animals are merged by surgical means allowing the exchange of humoral factors.

mechanism (Banks, 2006; Baura *et al.* , 1993). Insulin, as well as leptin, are satiety mediating (anorexigenic) and have been demonstrated to act directly on CNS neurons along with nutrients (i.e. glucose) and nutrient-related factors, such as free fatty acids (FFA; Brüning *et al.* , 2000; He *et al.* , 2006; Ibrahim *et al.* , 2003; Parton *et al.* , 2007; see figure 1.1). One of the brain regions with the highest expression of insulin and leptin receptors (IR, LepR) is the hypothalamus (see figure 1.1; Marks *et al.* , 1990). Within the hypothalamus, the arcuate nucleus (ARC) is anatomically uniquely positioned at the base of the hypothalamus. Here, the BBB is highly permeable and thus neurons which reside in the ARC are directly exposed to a large variety of bloodborne peripheral hormones (e.g. leptin, insulin) and other fuel-related signals. Two neuronal subpopulations within the ARC are integral parts of a neuronal circuit called 'melanocortin system' and are one of the best characterized pathways involved in the neuronal control of feeding and energy expenditure.

The first subpopulation expresses the anorexigenic peptides cocaine-amphetamine regulated transcript (CART) and the large precursor peptide proopiomelanocortin (POMC) which is further cleaved into melanocortins ( $\alpha$ -,  $\beta$ -,  $\gamma$ -MSH),  $\beta$ -endorphin and adrenocorticotrophic hormone (ACTH). The second subpopulation expresses the hunger mediating (orexigenic) peptides agouti-related protein (AgRP) and neuropeptide Y (NPY).

Current models suggest that POMC/CART neurons are stimulated by elevated levels of insulin and leptin which triggers the release of melanocortins. Of these,  $\alpha$ - and  $\beta$ -MSH have been shown to potently reduce food intake and increase energy expenditure by activating melanocortin receptors (MC3/4R; Adan *et al.* , 1994). In contrast, AgRP/NPY neurons become activated by decreasing levels of insulin/leptin. While NPY stimulates anabolic circuits, AgRP is a natural inverse agonist of MC3/4Rs and thereby reduces the effect of POMC-derived melanocortins on these receptors (Cone *et al.* , 1996; Stanley *et al.* , 1986). Furthermore, AgRP/NPY neurons provide unidirectional GABAergic (inhibitory) input on POMC/CART neurons, thereby tonically inhibiting POMC/CART-derived satiety signals. POMC/CART as well as AgRP/NPY neurons project to a wide array of hypothalamic (i.e. PVN, LH, VMH and DMH) and

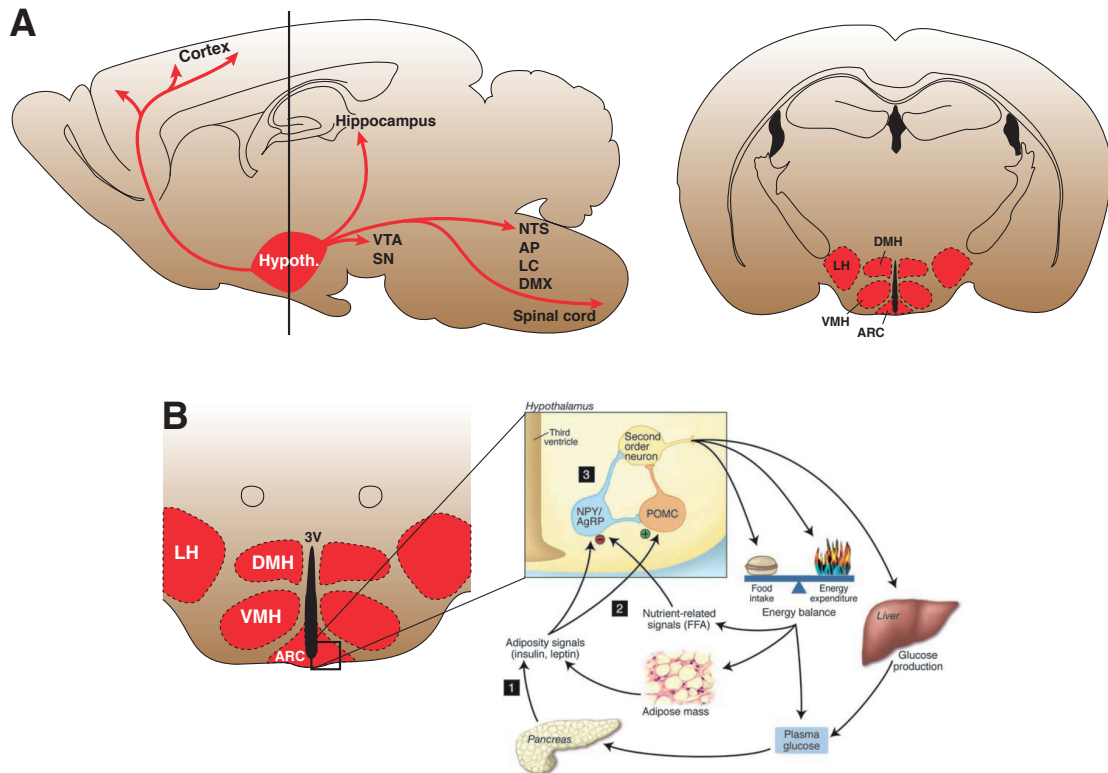


**Figure 1.1:** Diagram of hypothalamic projections and the melanocortin system. (A) *left* Saggital view of a mouse brain showing projections from the hypothalamus to target brain areas (*red arrows*). AP, area postrema; DMX, dorsal motor nucleus of the vagus; LC, locus coeruleus; NTS, nucleus of the solitary tract; SN, substantia nigra; VTA, ventral tegmental area. *right* Coronal section of the mouse brain (vertical bar in A, *left*) showing the hypothalamic regions in control of energy homeostasis (not shown: PVN). ARC, nucleus arcuatus; DMH, dorsomedial hypothalamus; LH, lateral hypothalamus; PVN, paraventricular nucleus; VMH, ventromedial hypothalamus. (B) The melanocortin system. Food intake and energy expenditure are regulated by the brain in response to afferent input and signals from peripheral tissue, such as peripheral hormones like insulin and leptin and/or nutrient-related signals like FFA and glucose. In the ARC, a small neuronal network consisting of POMC and AgRP neurons integrates these signals accordingly. As a result, the output of “second-order neurons” is modulated which regulate food intake and energy expenditure. AgRP, agouti-related protein; FFA, free fatty acid; POMC, proopiomelanocortin; NPY, neuropeptide Y (Adapted from Gao & Horvath, 2007; Paxinos & Franklin, 2008; Schwartz & Porte, 2005).

extrahypothalamic regions (Belgardt & Brüning, 2010; Cone, 2005). Here, POMC and AgRP neurons are reported to exert their effects on feeding via modulating the activity of “second-order neurons” located downstream of the ARC which in turn integrate and convey information to other brain regions such as the midbrain and the periphery. However, the exact whereabouts of these neurons as well as the implicated neuronal circuits in which these neurons act remain elusive.

## 1.2 Insulin and leptin signaling in the CNS

Insulin is a peptide hormone which is produced in pancreatic  $\beta$ -cells and its release is triggered by increased glucose concentrations (Polonsky, 2005). After its discovery in 1923, insulin's role in control of energy homeostasis was largely underestimated at first. It was thought to only act in the periphery, for instance in liver, muscle, or fat tissue without having any effect on the brain. However, almost 60 years later, it could be demonstrated in a primate model that insulin was able to reduce food intake and body weight when delivered to the brain by chronic intracerebroventricular (i.c.v.) infusion (Woods *et al.*, 1979). Further evidence emerged that insulin circulates in proportion to body fat mass (Bagdade *et al.*, 1967; Considine *et al.*, 1996) and that circulating insulin is transported across the BBB via a saturable mechanism (Baura *et al.*, 1993) rendering insulin a key hormonal signal implicated in the CNS control of energy homeostasis (reviewed in Schwartz & Porte, 2005). In addition, studies in organisms like fruit flies (*Drosophila melanogaster*) point to an evolutionary conserved role for insulin's action as an metabolic regulator (Garofalo, 2002). Initially, detailed knowledge of the insulin signaling cascade had been derived from peripheral tissue cells like muscle cells, pancreatic  $\beta$ -cells, adipocytes and hepatocytes. During the last decade, it has been shown that insulin signaling works largely the same way in CNS neurons (Niswender *et al.*, 2003).

The insulin receptor belongs to the family of receptor tyrosine kinases and is a disulfide-bonded dimer consisting of an  $\alpha$ - and  $\beta$ -subunit. Upon activation by insulin, the intracellular  $\beta$ -subunit gets trans-autophosphorylated at multiple tyrosine residues thereby creating the binding site for insulin-receptor-substrate (IRS1 – 4) molecules, which then become phosphorylated by the intrinsic IR tyrosine kinase. In turn, IRS bind to and activates the 85kDa regulatory subunit (p85) of the phosphatidylinositol-3-kinase (PI3K) which releases the 110 kDa catalytic subunit (p110) from complex. Catalytically active PI3K is relocalized to the membrane and catalyzes the conversion of phosphatidylinositol-4,5-bisphosphate (PIP<sub>2</sub>) into phosphatidylinositol-3,4,5-bisphosphate (PIP<sub>3</sub>). Of note, the synthesis of PIP<sub>3</sub> and therefore PI3K signaling is negatively regulated by the 'phosphatase and tensin homolog' (PTEN) which dephosphorylates PIP<sub>3</sub> to PIP<sub>2</sub>. PIP<sub>3</sub>

can exert immediate effects on neuronal activity by binding to ion channels, but also activates phosphatidylinositol-dependent kinase 1 (PDK1) which activates downstream targets such as protein kinase B (PKB a.k.a. AKT) and protein kinase C (PKC; Belgardt & Brüning, 2010; Niswender & Schwartz, 2003; Plum *et al.*, 2006b; Taniguchi *et al.*, 2006). In the ARC, insulin hyperpolarizes POMC as well as AgRP neurons via a PI3K-dependent process which leads to an increase of the open probability of ATP-dependent potassium channels ( $K_{ATP}$ ) following the local accumulation and binding of PIP<sub>3</sub> (Köner *et al.*, 2007; Plum *et al.*, 2006a; Shyng & Nichols, 1998). Conversely, it has also been demonstrated that insulin depolarizes a subset of AgRP neurons in the ARC; however the involved ion channels have not yet been identified (Claret *et al.*, 2007). Besides immediate effect on neuronal excitability in hypothalamic neurons, insulin also plays a pivotal role in transcriptional regulation. As mentioned before, insulin signaling leads to the activation of PKB. Activation of PKB results in phosphorylation and nuclear exclusion of the forkhead transcription factor FOXO1 giving way for the binding of the signal transducer and activator of transcription (STAT3) to the POMC gene and subsequent POMC transcription (Belgardt *et al.*, 2008). Consequently, generation of POMC leads to increased  $\alpha$ -MSH levels resulting in a reduction of food intake.

Compared to insulin, the adipocyte-derived peptide hormone leptin is secreted by adipocytes, circulates proportional to the body fat mass (Frederich *et al.*, 1995) and has only been detected in several mammal species which suggests that it has evolved more recently (Doyon *et al.*, 2001). Leptin is the product of the *ob* gene and was first cloned in 1994 (Zhang *et al.*, 1994). Its anorexigenic effect was demonstrated in a series of experiments where chronic peritoneal injections of leptin were able to rescue the obese phenotype of *ob/ob* mice by normalizing metabolic parameters to values of lean controls (Pellemounter *et al.*, 1995). Similar to insulin, leptin crosses the BBB via a saturable mechanism (Banks *et al.*, 1996).

The LepR belongs to the family of cytokine receptors and consists of a single membrane spanning domain. While several isoforms exist, only the full length isoform is capable of initiating intracellular signaling. Upon activation by leptin, LepRs trigger the activation of janus kinase 2 (JAK2) which in turn phosphorylates the LepRs on several

residues creating a binding site for STAT3 molecules. STAT3 is also phosphorylated by JAKs and translocates to the nucleus following dimerization. Here, STAT3 induces the transcription of target genes – and in the case of POMC neurons – the POMC gene. A negative feedback mechanism is provided by the suppressors of cytokine signaling (SOCS) which are activated in response to STAT3 activation (Banks *et al.*, 2000; Belgardt & Brüning, 2010; Niswender & Schwartz, 2003). Similar to insulin, leptin also has immediate effects on neuronal activity. In the ARC it has been demonstrated that POMC neurons depolarize and increase their firing rate upon leptin stimulation (Cowley *et al.*, 2001). Conversely, it has also been reported that leptin hyperpolarizes glucose-responsive ARC and VMH neurons by activating  $K_{ATP}$  channels (Spanswick *et al.*, 1997). Evidence suggests that leptin’s excitatory effects are mediated by transient receptor potential channels (TRPC1,4,5), a non-selective cation channel in a PI3K-dependent process (Hill *et al.*, 2008; Qiu *et al.*, 2010). In fact, it has been reported that LepR-activated JAK2 phosphorylates IRS which in turn activates PI3K. Subsequently, PI3K activates phospholipase C (PLC)  $\gamma$ 1 resulting in opening of TRPC (Qiu *et al.*, 2010).

Since insulin’s and leptin’s immediate effects on neuronal firing are both PI3K-dependent, several studies suggest a “cross-talk” between insulin and leptin (Carvalho *et al.*, 2005; Mirshamsi *et al.*, 2004; Niswender *et al.*, 2001). A recent report by Williams *et al.* (2010) has shown that IRs and LepR are differentially expressed in individual POMC neurons of the ARC suggesting that the cross-talk between leptin and insulin occurs within a network of cells rather than within individual POMC neurons.

### 1.3 The ventromedial hypothalamus (VMH)

Early studies on the role of the CNS in control of energy homeostasis have identified the VMH as one of the key brain regions mediating anorexigenic effects (see 1.1). Despite the notion for the VMH’s central importance in maintaining energy homeostasis, research focus shifted from the VMH to the ARC after the detection of the melanocortin system with the fuel-sensing POMC and AgRP neurons as two of its main components. However, recent molecular and genetic experiments have led to increasing interest in the feeding-related neuronal circuits which reside within the boundaries of the VMH.

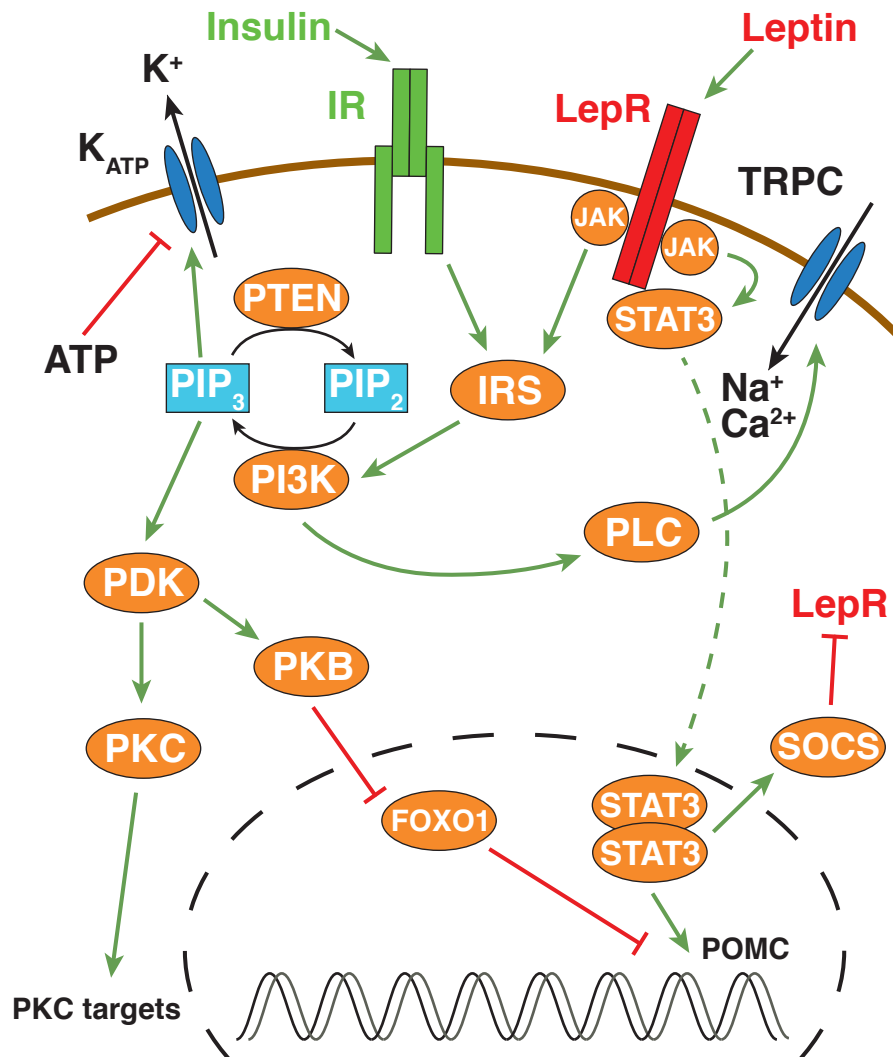


**Figure 1.2:** Overview of insulin and leptin signaling pathways (adapted from Belgardt & Brüning, 2010; Niswender *et al.*, 2003; Qiu *et al.*, 2010). Green arrows signify activation, red arrows inhibition; K<sub>ATP</sub>, ATP-dependent potassium channel; FOXO1, forkhead transcription factor 1; IRS, insulin-receptor-substrate; JAK, janus kinase; IR, insulin receptor; LepR, leptin receptor; PDK1, phosphatidylinositol-dependent kinase 1; PIP<sub>2</sub>, phosphatidylinositol-4,5-bisphosphate; PIP<sub>3</sub>, phosphatidylinositol-3-4,5-trisphosphate; PKB, protein kinase B; PKC, protein kinase C; PLC, phospholipase C; SOCS, suppressors of cytokine signaling; STAT3, signal transducer and activator of transcription; TRPC, transient receptor potential channel.

For instance, expression studies have shown that brain-derived neurotrophic factor (BDNF) is highly expressed in VMH neurons (Xu *et al.*, 2003). BDNF is an important regulator of glucose and lipid metabolism and genetic deficiency in BDNF or its receptor leads to obesity (Xu *et al.*, 2003). The studies on the BDNF effect in the VMH also revealed that the anorexigenic BDNF signaling is not dependent on the melanocortin system because BDNF was still able to reduce feeding in MC4R-deficient mice (Xu *et al.*, 2003). Furthermore, immunohistochemical studies revealed that LepRs are highly ex-

pressed in VMH neurons and that leptin signaling directly modulates BDNF expression exclusively in VMH neurons. (Elmqvist *et al.* , 1998b). Leptin leads to an increase of BDNF transcripts whereas the reduction of leptin by fasting leads to a decrease (Komori *et al.* , 2006).

Efforts have been made to identify and characterize neuronal subpopulations within the VMH. Several studies revealed that neurons in the VMH can be separated by their responsiveness towards glucose. The glucose-responsive (GR) subpopulation of VMH neurons increase their activity in response to elevated glucose levels. In contrast to non-GR neurons, the activity of GR neurons is acutely modulated by peripheral hormones such as leptin and insulin (Miki *et al.* , 2001; Spanswick *et al.* , 1997, 2000). Apart from the categorization based on physiological characteristics, 'genetic' markers for neuronal subpopulations are mandatory. Genetic manipulation of specific neurons allows the selective perturbation of defined neuronal circuits and the subsequent assessment of these manipulations in awake, unrestrained animals. In this regard, the utilization of the steroidogenic factor 1 (SF-1) as a genetic marker for VMH neurons has provided valuable insights on the influence of the VMH on the maintenance of energy homeostasis.

SF-1 is a nuclear receptor which is expressed in several peripheral tissues (i.e. adrenalcortex, testis, ovary, placenta, adipose tissue) and the brain (Parker & Schimmer, 1997). Within the brain, immunohistochemical analysis revealed that SF-1 is almost exclusively found in neuronal subpopulations of the VMH with the strongest localization in the dorsomedial part of the VMH (Shinoda *et al.* , 1995). Mice lacking SF-1 suffer from a failure to normally develop adrenal glands and gonads and also have an abnormally developed VMH (Ikeda *et al.* , 1995; Luo *et al.* , 1994). These mice, when rescued from lethality by adrenal transplantation, developed severe obesity resulting from both hyperphagia and reduced energy expenditure (Majdic *et al.* , 2002). Dhillon *et al.* (2006) showed that SF-1 neurons depolarize and increase their activity upon leptin treatment in contrast to non-SF-1 neurons in the VMH which respond with a hyperpolarization. Additionally, disrupted leptin signaling in SF-1 neurons leads to obesity comparable to the body weight phenotype of mice which specifically lack the LepR in POMC neurons (Balthasar *et al.* , 2004). Interestingly, mice with a combined POMC, SF-1-specific LepR

knockout developed an increased body weight phenotype that was approximately the sum of that observed in either knockout mouse. This leads to the conclusion that leptin simultaneously acts on neuronal circuits within the VMH and the ARC and that leptin signaling in the VMH and ARC is independent from each other.

Output projections of the VMH have been thoroughly characterized by immunohistochemical means and show a diverse innervation pattern of many brain regions (Canteras *et al.* , 1994). Despite this, the question still remains of the functional nature of the connections between the VMH and other feeding-related brain areas, and how exactly VMH neurons modulate their target neurons. Sternson and colleagues (2005) demonstrated for the first time by using laser scanning photostimulation in rodent brain slices that neurons which are located in the medial VMH (mVMH) provide a strong glutamatergic (excitatory) input on POMC neurons of the ARC. Conversely, NPY neurons of the ARC receive only a sparse excitatory input from the lateral VMH (latVMH). However, interactions between VMH neurons and their targets are still only poorly understood. Thus, future work is required to better understand the impact of VMH signaling on energy homeostasis.

## **1.4 The dopaminergic system in control of energy homeostasis**

The hypothalamus harbors the homeostatic system which integrates various energy store related hormonal and neuronal signals thereby maintaining energy homeostasis by matching food intake to energy expenditure. However, under certain conditions, the homeostatic system fails to adequately regulate food intake which might consequently result in the development of obesity. Recent advances in research on feeding related circuits in the hypothalamus have already pointed out that differences in hormonal signaling and genetic factors determine the individual's susceptibility to obesity (Morton *et al.* , 2006; O'Rahilly, 2009). However, these findings cannot fully explain the development of the obesity epidemic during the last decades.

One explanation for this phenomenon might be that the neuronal circuits in control of energy homeostasis have evolved under conditions where food was not abundantly available. In this light, additional neuronal circuits which are capable of overriding

the homeostatic system might have co-evolved. As a consequence, further food intake would be promoted in times of plenty. The dopaminergic (DA) system which mediates the rewarding aspects of food and/or food predictive cues has been hypothesized to be one of the systems eligible to override the homeostatic system under certain circumstances (Palmiter, 2007).

#### 1.4.1 Dopamine and the anatomy of the dopaminergic system

Dopamine, as well as noradrenaline and adrenaline, belong to the catecholamine (CA) class of monoamines. Dopamine and noradrenaline are the two primary CAs in the brain and were first identified in the brain nearly five decades ago by formaldehyde histofluorescence (Carlsson & Falck, 1962). Catecholaminergic neurons are localized in seventeen discrete cell groups which are distributed from the medulla oblongata to the olfactory bulb and retina. They were subsequently labeled 'A1 – A17' according to the nomenclature introduced by Dahlström & Fuxe (1964) which is still widely in use.

All CAs share the same synthesis pathway which starts with L-tyrosine. L-tyrosine is converted into L-DOPA by tyrosine hydroxylase (TH) and further converted into dopamine by the aromatic amino acid decarboxylase (AADC). Subsequently, dopamine serves as a precursor for the synthesis of noradrenaline by the dopamine  $\beta$ -decarboxylase (DBH) which in turn can further be catalyzed to adrenaline by the phenylethanolamine-*N*-methyl transferase. Advances in immunohistochemical techniques involving antibodies for CA-synthesizing enzymes and various CA neuron-specific components, such as the dopamine transporter (DAT) or the vesicular monoamine transporter 2 (VMAT2), rendered it possible to characterize and distinguish between the different CAs more accurately. These studies revealed a distribution pattern for dopaminergic (DA) neurons from the mesencephalon to the olfactory bulb and retina (A8 – A17; see figure 1.3A).

The main source for brain dopamine is the DA neurons which are located in the mesencephalon (Bentivoglio & Morelli, 2005). Initially, DA neurons of the mesencephalon were identified as a single continuous cell layer extending from the median to the lateral part of the mesencephalon (Dahlström & Fuxe, 1964). These neurons were further

subdivided into separate cell groups (A8 – A10) according to anatomically established brain regions (A8: retrorubral area [RRA]; A9: substantia nigra *pars compacta* [SNpc]; A10: ventral tegmental area [VTA]; see figure 1.3B,C).

These neuronal populations have been associated with three different systems: The *nigrostriatal*, the *mesolimbic* and *mesocortical* systems. The A9 cell group (SNpc), which contains >70% of all DA neurons, projecting to the dorsal striatum (the caudate putamen [CPu]) along the *nigrostriatal* pathway. The A10 neurons within the VTA projecting to the nucleus accumbens (NAc), the amygdala, the hippocampus, and the olfactory tubercle via the *mesolimbic* pathway and to the prefrontal cortex (PFC) via the *mesocortical* pathway. The A8 cell group being a dorsal and caudal extension of the A9 cell group contributes to all three pathways (Björklund & Dunnett, 2007).

Generally, the three DA pathways are associated with different functions. The *nigrostriatal* pathway is associated with motor function since degeneration of DA neurons in the SNpc causes depletion of striatal dopamine resulting in severe motor dysfunctions such as bradykinesia and rigidity, hallmarks of Parkinson's disease (Burns *et al.*, 1983; Iversen & Iversen, 2007). In contrast, the *mesolimbic* and *mesocortical* pathways are usually thought to be involved in complex processes like motivation, reinforcement, reward seeking behavior. Dysfunction of DA signaling along these pathways can lead to pathological conditions like addiction and schizophrenia (Kauer, 2004; Wise, 2006).

Many studies have shown that the three pathways are anatomically and functionally distinct from each other, for instance, DA neurons projecting to the striatum rarely send collaterals to extrastriatal areas, but the cells of origin do not necessarily have to be localized in the SNpc. Moreover, it has been shown by anterograde and retrograde tracing experiments that A9 (SNpc) and A10 (VTA) DA neurons have overlapping projection targets (Björklund & Dunnett, 2007), and a large body of evidence suggests that all DA systems participate in reward-related behavior and addiction (Wise, 2009). On the cellular level, subsets of SNpc and VTA neurons have demonstrated the same characteristic responses towards reward and reward-related cues which has led to pooled electrophysiological data (Schultz, 1998), despite their heterogeneous electrophysiological properties (Margolis *et al.*, 2006; Neuhoff *et al.*, 2002; Wolfart *et al.*, 2001).

Thus, the ‘classical’ model with its strict ‘division of duties’ between A9 (SNpc) and A10 (VTA) DA neurons is rather an oversimplification meaning that the mesencephalon constitutes a continuum in which DA neurons projecting to striatal or corticolimbic targets are intermingled.

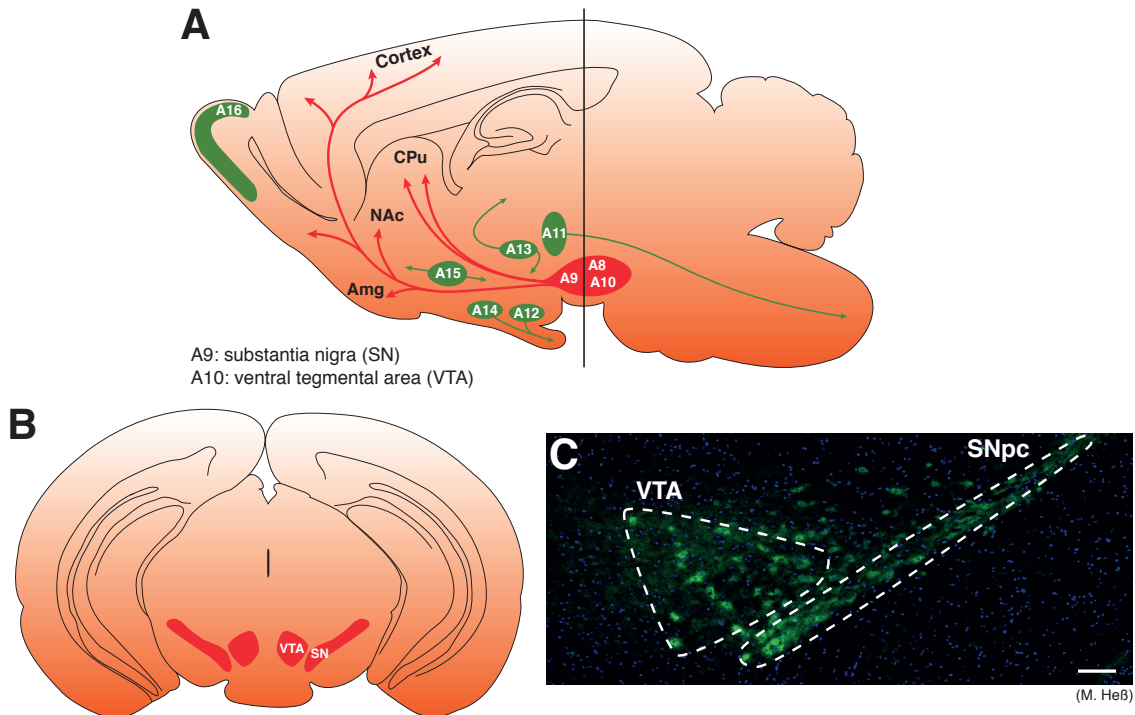


**Figure 1.3:** Distribution of dopaminergic cell groups in the rodent brain. (A) Sagittal view of DA cell groups and their projections in the rodent brain. DA neurons are confined to distinctive cell groups (A8 – A17) from the mesencephalon to the olfactory bulb (Dahlström & Fuxe, 1964). Cell groups in red show the localization and projections of mesencephalic DA neurons. (modified from Björklund & Dunnett, 2007; Paxinos & Franklin, 2008). (B) Coronal section at the level of the vertical bar in the left panel showing the localization of the VTA (A10) and SNpc (A9; modified from M. Heß, Paxinos & Franklin, 2008). (C) Immunohistochemistry for TH labeling DA neurons in the mesencephalon. Dashed lines show the borders of VTA and SNpc. Green (TH), DA neurons; blue (DAPI), DNA. Scale bar: 100  $\mu$ m (modified from M. Heß). Amg, amygdala; CPU, caudate putamen; DA, dopaminergic; NAc, nucleus accumbens; SNpc, substantia nigra *pars compacta*; TH, tyrosine hydroxylase, VTA, ventral tegmental area.

### 1.4.2 Physiology of dopaminergic signaling

In spite of the rather small number of DA neurons (400,000 – 600,000 neurons in humans which equates  $\sim$ 1% of the total amount of neurons; Björklund & Dunnett, 2007), DA signaling unfolds its potential by divergent projections within the target areas meaning that every DA neuron connects to approx. 300 – 400 target neurons (Schultz, 1998).

Dopamine exerts its cellular effects via G-protein coupled receptors (GPCRs) which can be separated into two classes: the D1- and D2-like family. Dopamine receptor dependent activation of intracellular signaling cascades modulates a large variety of cellular targets such as voltage-/ligand-gated ion channels, ion pumps or transcription factors (see figure 1.4; Calabresi *et al.* , 2007; Greengard *et al.* , 1999. These dopamine-mediated alterations in cell-intrinsic properties play a pivotal role in reward, learning and drug addiction (Hyman *et al.* , 2006; Kauer & Malenka, 2007; Robinson & Berridge, 1993; Schilström *et al.* , 2006).

Initially, dopamine receptors were separated into D1-like and D2-like receptors based on their differential regulation of adenylate cyclase (AC) which catalyzes the conversion of adenosine triphosphate (ATP) to cyclic adenosine monophosphate (cAMP; Keibian & Calne, 1979). However, further advances in molecular biological techniques led to the discovery of multiple dopamine receptor subtypes which are either 'D1-like' (D1 and D5) or 'D2-like' (D2, D3 and D4) based on their structural, pharmacological and biochemical properties (Beaulieu & Gainetdinov, 2011; Missale *et al.* , 1998).

D1-like receptors are exclusively expressed postsynaptically on target cells of mesencephalic DA neurons, such as medium spiny neurons (MSNs) in the striatum (Bentivoglio & Morelli, 2005). D1Rs activate the  $G_{\alpha_s/olf}$  family of G-proteins leading to an increase in cAMP concentration via activation of AC. Subsequently, elevated cAMP levels lead to the activation of protein kinase A (PKA), and the phosphorylation of the '32 kD dopamine and cAMP-regulated phosphoprotein' (DARPP-32). This in turn, regulates a large variety of downstream targets via inhibition of protein phosphatase-1 (PP-1; see figure 1.4; Greengard, 2001; Hervé & Girault, 2005).

D2-like receptors exist in two splice variants (D2L, D2S) with the D2L variant being predominantly expressed in postsynaptic target cells and the D2S variant being mostly presynaptically expressed as an autoreceptor in mesencephalic DA neurons (Bentivoglio & Morelli, 2005; Giros *et al.* , 1989; Khan *et al.* , 1998). Furthermore, the D2S variant possesses a higher sensitivity to dopamine over D2L receptors which renders D2R-dependent effects on dopamine-associated brain functions more complex. Unlike D1Rs, D2Rs have the opposite effect on cAMP production and downstream targets via

activation of the  $G\alpha_{i/o}$  G-protein causing AC inhibition. Furthermore, D2Rs modulate ion channel function in a more direct fashion than D1Rs via activation of the  $G\beta\gamma$  subunit of the G-protein (Hervé & Girault, 2005). D2R-dependent activation of  $G\beta\gamma$  has been demonstrated to directly inhibit L- and N-Type  $Ca^{2+}$  channels and to activate G-Protein activated inwardly rectifying potassium channels (GIRKs; see figure 1.4; Hervé & Girault, 2005; Uchida *et al.*, 2000). A specific GIRK splice variant (GIRK2) is highly expressed in the mesencephalon (Karschin *et al.*, 1996). Therefore, D2 autoreceptors provide an important feedback mechanism to control the firing rate of DA neurons and the synthesis and release of dopamine in response to extracellular dopamine levels.

The firing rate of mesencephalic DA neurons determines how much dopamine is released in the respective target areas. *In vivo*, dopaminergic neurons show three main patterns of activity: 1.) an inactive (hyperpolarized) state which is present in >50% of mesencephalic DA neurons (Grace & Bunney, 1984); 2.) a slow (2 – 10 Hz), irregular single-spike or ‘tonic’ firing pattern which is driven by an intrinsic pacemaker and 3.) a burst or ‘phasic’ firing pattern (Freeman *et al.*, 1985; Grace & Bunney, 1984; Overton & Clark, 1997). A large body of evidence suggests that the activity of DA neurons code for the “reward prediction error”<sup>2</sup>, such that an unpredicted reward triggers DA neuron burst firing (positive prediction error – “better than expected”), a reward as expected is reflected by tonic firing (“as expected”), and when the reward is “worse than expected” (negative prediction error) DA neurons stop firing (Schultz, 1998, 2007). On a synaptic level, it has been hypothesized that tonic firing of DA neurons provides a stable baseline level of extrasynaptic dopamine which preferentially stimulates the highly sensitive presynaptic D2Rs, whereas burst firing of DA neurons induces a fast, high amplitude, transient signal which is confined within the synapse owing to the reuptake by high-affinity DAT (Floresco *et al.*, 2003; Grace, 1991). For instance in the NAc, the two firing modes of DA neurons differentially modulate limbic and PFC input to the NAc such that PFC input is attenuated by tonic D2R activation, whereas the limbic input is increased by phasic D1R activation. Thus, changes in tonic and phasic dopamine transmission would shift the information flow between PFC inputs and limbic inputs thereby enabling behavior flexibility (Goto & Grace, 2005; Grace *et al.*, 2007).

---

<sup>2</sup>The “reward prediction error” is the difference between the predicted and obtained reward.

Interestingly, the diminished ability to recruit the PFC in drug users has been correlated with impulsivity resulting in a loss of control over drug use, a core feature of addiction (Volkow & Fowler, 2000).

In contrast, DA neurons in mesencephalic brain slice preparations only show tonic pacemaker activity or – in a very few cases – no activity (see chapter 3.3.1; Grace & Onn, 1989; Lacey *et al.* , 1989). *In vivo* data suggests that DA neurons are constantly receiving a strong GABAergic input mainly originating in the ventral pallidum holding half of the mesencephalic DA neurons in a hyperpolarized non-firing state (Floresco *et al.* , 2003; Grace & Bunney, 1985). On the other hand, burst firing *in vivo* is dependent on a combination of glutamatergic input from i.e. the PFC, pedunclopontine tegmentum (PPTg), the subthalamic nucleus (STN), the lateral preoptic-rostral hypothalamic area (Geisler *et al.* , 2007; Smith & Grace, 1992), and cholinergic input from the latero-dorsal tegmentum (LDTg; Lodge & Grace, 2006). *In vitro* electrophysiological recordings from slice preparations supports the aforementioned data since bursting activity can be induced in slice preparations by application of a combination of N-Methyl-D-aspartate (NMDA) and acetylcholine (ACh) or the bee venom apamin (Kitai *et al.* , 1999).

### 1.4.3 The role of the dopaminergic system in food reward

Food and water intake are among the most fundamental needs a living organism has on a daily basis, and everyone experiences the rewarding aspects of food. In fact, many behavioral studies on learning and memory are conducted using food reward paradigms. Food and food-related stimuli have been shown to increase dopamine levels in the NAc (Hernandez & Hoebel, 1988). Increases in dopamine transmission initiates changes in synaptic plasticity leading to long-term potentiation (LTP) or long-term depression (LTD), the major cellular mechanisms in learning and memory formation. These learning processes will “consolidate (a) liking the rewarding goal, (b) learning cues that predict its availability and actions that permit its consumption, and (c) assigning value and motivational status to the reward so that the organism can select among numerous behavioral options and determine what level of resources to put to-

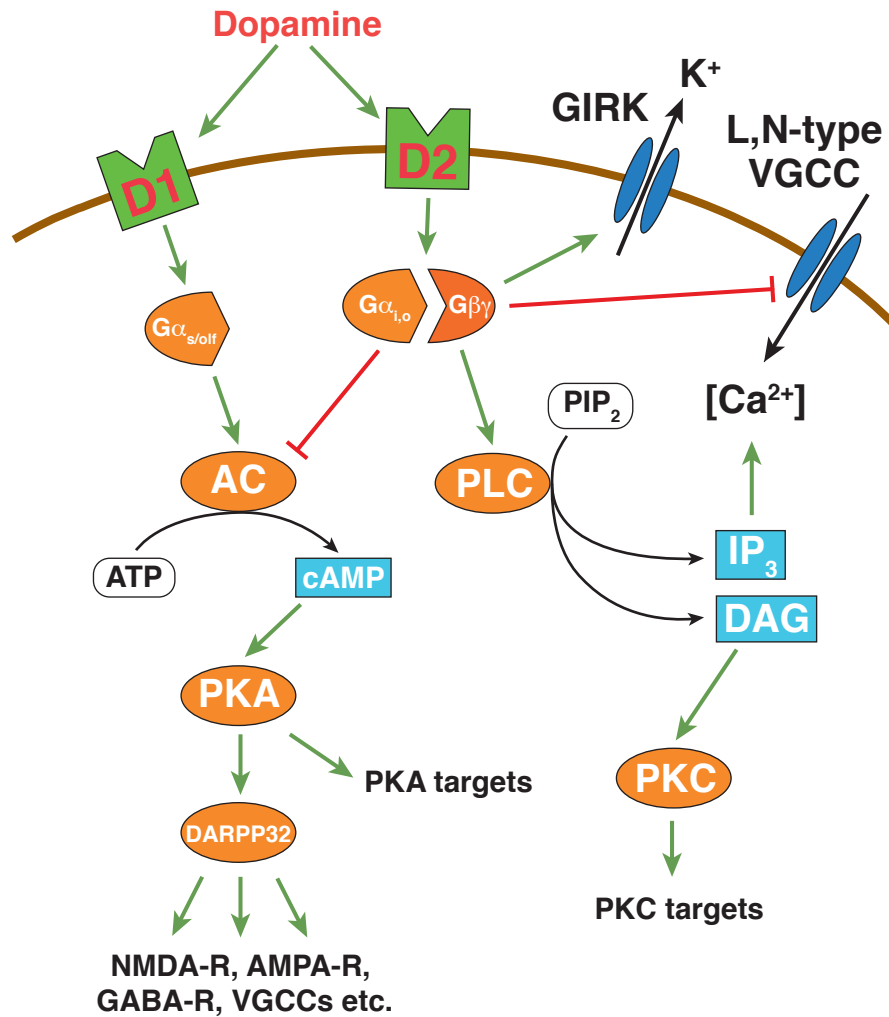


**Figure 1.4:** Overview of D1R and D2R signaling pathways (modified from Beaulieu & Gainetdinov, 2011; Greengard, 2001). *Green arrows* signify activation, *red arrows* inhibition; AC, adenylyl cyclase; cAMP, cyclic adenosine monophosphate; ATP, adenosine triphosphate; DAG, diacylglycerine; DARPP32, 32 kD dopamine and cAMP-regulated phosphoprotein; GIRK, G-protein activated inwardly rectifying potassium channel; IP<sub>3</sub>, inositoltrisphosphate; PIP<sub>2</sub>, Phosphatidylinositol-4,5-bisphosphate; PKA, protein kinase A; PKC, protein kinase C; PLC, phospholipase C, VGCC, voltage-gated calcium channel.

ward obtaining a specific goal” (in this case: acquisition of food; Hyman *et al.* , 2006). Furthermore, changes of the motivational state by food restriction leads to the augmentation of the rewarding effects of drugs of abuse (i.e. cocaine) suggesting that food and drug reward is mediated by the same pathways (Carr, 2002). A study by Johnson & Kenny (2010) suggests that overfeeding in mice leads to a decrease in responsiveness in brain reward circuits that were comparable to changes occurring after cocaine and heroin exposure.

Initial experiments nearly four decades ago have shown that ablation of DA neurons

projecting to the CPu along the nigrostriatal pathway resulted in starvation, further underlining the importance of dopamine transmission for feeding (Ungerstedt, 1971). In another set of experiments where dopamine deficiency was caused by DA neuron specific TH deletion, food intake was attenuated in a similar manner and daily injections of L-DOPA restored feeding in these mice (Szczyepka *et al.* , 1999; Zhou & Palmiter, 1995). Interestingly, adeno-associated virus (AAV)-mediated restoration of TH expression in the CPu resulted in normalization of feeding behavior whereas TH restoration in the NAc did not (Szczyepka *et al.* , 2001). Furthermore, blocking of D1Rs and D2Rs in the NAc did not prevent feeding but did attenuate the motivation of treated rats to work for food rewards in a lever pressing/feeding task (Nowend *et al.* , 2001). On the cellular level, electrophysiological studies demonstrated that food and food-predicting cues promote phasic firing in DA neurons which is associated with reward and reward-prediction thereby shaping future behavior towards the acquisition of food (Schultz *et al.* , 1997).

Taken together, these results indicate that dopamine signaling plays a pivotal role for food intake and that feeding seems to be rather associated with dopamine release by DA neurons projecting along the nigrostriatal pathway than those projecting along the mesolimbic pathway.

During the last several years, evidence has emerged linking the hypothalamic system in control of energy homeostasis with the DA reward system. This led to the hypothesis that the ARC ‘funnels’ information from fuel-sensing signals like insulin and leptin in order to modulate the activity of the DA system via direct and indirect pathways (Gao & Horvath, 2007). For example, it has been shown that orexinergic neurons of the LH project to the VTA (Fadel & Deutch, 2002) and that Orexin A potentiates NMDA receptor mediated currents of VTA DA neurons while Orexin A & B increase the firing rate of VTA DA and GABAergic neurons (Borgland *et al.* , 2006; Korotkova *et al.* , 2003).

On the other hand, there is accumulating evidence that the mesencephalon is directly affected by fuel sensing signals since the presence of IRs, LepRs and ghrelin receptors (GRs) were detected in the VTA as well as the SN. This suggests a more prominent role

of the DA system in feeding-related issues (Abizaid *et al.* , 2006; Elmquist *et al.* , 1998a; Figlewicz *et al.* , 2003; Havrankova *et al.* , 1978).

In fact, IRs as well as LepRs are functional in mesencephalic neurons since the downstream targets of insulin and leptin signaling are activated upon insulin/leptin application (Figlewicz *et al.* , 2007; Hommel *et al.* , 2006). It has been shown that insulin signaling targets the DAT in DA neurons since i.c.v. injection of insulin leads to increased mRNA levels and functional activity of DAT (Figlewicz *et al.* , 1994). Higher DAT levels might then increase dopamine clearance thereby reducing the dopamine concentration in the target regions of DA signaling. Similarly, leptin is also thought to inhibit DA transmission because i.c.v. injection of leptin results in reduced dopamine content in the NAc and a reduction in food intake (Hommel *et al.* , 2006; Krügel *et al.* , 2003). Electrophysiological studies have shown that the *in vivo* firing rate of DA neurons decreased following intravenous leptin infusion and during acute leptin application in brain slices (Hommel *et al.* , 2006); however, it should be noted that the latter finding could not be verified in another study (Korotkova *et al.* , 2006). In the case of insulin, electrophysiological evidence for an insulin effect in DA neurons is still lacking. Leptin, as well as insulin also reduce certain rewarding aspects of food which is shown by reduced sucrose self-administration and suppressed conditioned place preference (CPP) for sucrose and reversed CPP for high-fat diet (Figlewicz *et al.* , 2001, 2004, 2006). In contrast, ghrelin increased the firing rate of DA VTA neurons depending on the glutamatergic input and increased the number of excitatory inputs while decreasing inhibitory inputs. Ghrelin injection into the VTA promotes food intake which can be blocked by a ghrelin receptor antagonist (Abizaid *et al.* , 2006). However, ghrelin signaling seems to be at least in part dependent on hypothalamus-derived peptides like orexin, NPY and AgrP, since peripherally applied ghrelin failed to elicit feeding in the absence of either of the peptides (Chen *et al.* , 2004; Toshinai *et al.* , 2003).

Taken together, a large body of evidence suggests that the DA system itself is subject to direct modulation by fuel-sensing peripheral signals which could alter feeding behavior and the reward quality of food. Moreover, it has been hypothesized that the DA system is not just another downstream target of hypothalamic neuronal populations

maintaining energy balance ('funnel' hypothesis), but that the DA system has the potential to override the homeostatic system of the hypothalamus which could lead to the development of obesity (Palmiter, 2007).

## 1.5 The fat mass and obesity-associated protein (*Fto*)

The dysregulation of feeding-related circuits in the brain can seriously affect energy homeostasis and at worst, lead to the development of obesity and obesity-associated co-morbidities. Besides, variations in certain genetic factors might also predispose an individual to obesity.

Among those variations, single nucleotide polymorphisms (SNPs) within the first intron of the *FTO* gene showed one of the most robust associations with an increase in body mass index of children and adults (Dina *et al.* , 2007; Frayling *et al.* , 2007). The *Fto* gene is present in vertebrate evolution for at least 450 million years and is only detected in two species of algae which could be explained by horizontal gene transfer. Neither land plants nor invertebrates are carriers of the *Fto* gene. Studies on *Fto* expression revealed its presence in peripheral tissues and the brain. Detailed analysis in mouse brains showed abundant expression in feeding-related areas and that *Fto* is regulated by feeding and fasting (i.e. ARC, PVN, VMH; Fredriksson *et al.* , 2008; Gerken *et al.* , 2007).

Functional analysis of the *Fto* gene revealed that the *Fto* gene product shares similarities with Fe(II)- and 2-oxoglutarate-dependent oxygenases which are implicated in DNA repair and fatty acid metabolism (Clifton *et al.* , 2006). Accordingly, *in vitro* experiments showed that *Fto* localizes to the nucleus and catalyzes the demethylation of 3-methylthymine in single-stranded DNA and RNA (Gerken *et al.* , 2007; Jia *et al.* , 2008).

The involvement of the *Fto* gene on energy homeostasis was further confirmed in an *in vivo* study with *Fto* knockout mice (Fischer *et al.* , 2009). Homozygous deletion of the *Fto* gene resulted in a variety of effects such as a lean body phenotype, increased energy expenditure, a reduced amount of adipose tissue and relative hyperphagia. Overexpression of the *Fto* gene in mice led to a dose-dependent increase in body weight and fat

mass. According to the study, increased body weight is not caused by reduced energy expenditure but by increased food consumption (hyperphagia; Church *et al.*, 2010).

## 1.6 Technical aspects

### 1.6.1 The perforated patch clamp technique

Since its development almost three decades ago by Hamill *et al.* (1981), the patch-clamp technique has been proven to be an enormously powerful tool for studying the electrophysiological properties of virtually every cell type.

Among the four configurations of the patch-clamp technique (whole cell, cell attached, inside-out, outside-out), the whole cell configuration is the one most widely used. It has replaced the intracellular recording technique with sharp microelectrodes in many electrophysiological studies for certain reasons: i) It can be used on very small cells; ii) The signal-to-noise ratio is improved, because the leak between the cell interior and the bath is very small; iii) The access resistance of the patch pipette is very low, a prerequisite for the study of macroscopic ('whole cell') ionic currents; iv) It is possible to gain complete control over the cytosolic composition of the cell. The much larger pipette volume rapidly dialyzes the interior of the cell. This makes it possible to freely determine the ionic composition of the cytosol which facilitates the recording of ionic currents, e.g. GABA<sub>A</sub> receptor mediated currents (see 2.3.2).

However, the two latter advantages of the whole cell configuration can directly be linked to a major drawback. By exchanging the cytosol with the pipette solution cytoplasmic components are washed out. Such components can constitute second-messenger pathways or modulate ion channel function (voltage-dependent as well as ligand-operated). As a result the properties of the investigated cell will be altered. This renders it almost impossible to use the whole cell configuration for certain studies in which second-messenger pathways are involved (for more examples see Akaike & Harata (1994); Horn & Marty (1988)).

The perforated-patch configuration was developed to overcome this disadvantage of the whole cell configuration. Instead of rupturing the membrane which leads to the

exchange of the cytosol with the pipette solution, pore-forming substances (ionophores) are used to gain electrical access to the cell's interior without destroying the integrity of its cytoplasmic components.

Thus, the perforated-patch configuration combines the major advantages of the whole cell configuration without the disadvantage of washing-out of second messenger systems.

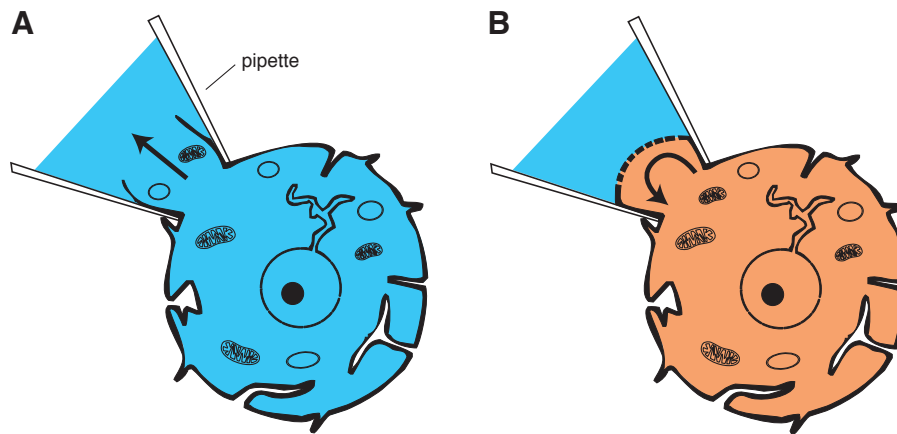


**Figure 1.5:** Schematic drawings of the whole cell and perforated-patch configuration. (A) Whole cell configuration. The cell membrane has been ruptured allowing the dialysis of the interior of the cell. (B) Perforated-patch configuration. The cell membrane under the patch pipette has been permeabilized by pore-forming agents. The integrity of the cell interior is retained (modified from Lindau & Fernandez, 1986).

### 1.6.2 Pore-forming agents

In the past a variety of pore-forming agents have been used in order to establish perforated-patch recordings.

#### ATP

In 1986, Lindau & Fernandez discovered that elevated concentrations of ATP ( $\sim 400 \mu\text{M}$ ) in the patch pipette made it possible to gain electrical access to the interior of mast cells without dialyzing the cytoplasm. Initially, they found that mast cells lost their ability to degranulate upon antigenic stimulation when recorded in the whole cell configuration. They suggested that the loss of degranulation is linked to the washout of “essential cytoplasmic components” during whole cell recordings. Application of the

new recording technique made it possible to record from these cells while preserving their ability to degranulate.

Unfortunately, the method can only be used with cells which express ATP-receptors on their cell membrane. This means that the new method is only applicable to a few cell types. Further, the access resistance which could be achieved by this method was in the range of 200 – 5,000 M $\Omega$  which is 40 – 250-fold higher than in the whole cell configuration which renders the recordings of ionic currents almost impossible.

Nonetheless, Lindau & Fernandez were among the first who successfully combined the patch-clamp technique with the use of a permeabilizing agent (in this case ATP) thereby laying the foundation for the further improvement of the perforated- patch configuration during the following years (i.e. Horn & Marty, 1988).

### **Nystatin and amphotericin B**

Based on the aforementioned findings, Horn & Marty (1988) further improved the technique by using nystatin instead of ATP. Nystatin has two major advantages over ATP. First, the access resistances achieved with nystatin are in the range of conventional whole cell recordings. Second, no specific receptors are required for permeabilization of the membrane. Thus, the technique can be applied to a greater range of cell types.

The same applies to amphotericin B, a compound which is structurally very closely related to nystatin (Rae *et al.* , 1991). Both molecules belong to the family of polyene antibiotics which have been isolated from *Streptomyces* sp. They consist of a large lactone ring with conjugated double bonds (figure 1.6 A). A single nystatin/amphotericin B molecule comprises a hydrophilic chain containing multiple hydroxyl groups and a hydrophobic heptaene chain. Both chains are aligned as parallel rods with a highly hydrophilic mycosamine residue at one end and an isolated hydroxyl group at the opposite end. Thus, the nystatin/amphotericin B molecule possesses amphipathic characteristics similar to a membrane phospholipid so that it is sometimes referred to as 'counterfeit phospholipid' (figure 1.6B; Andreoli (1973)). There is evidence that the presence of cholesterol is absolutely necessary for the incorporation of these molecules into the cell membrane where it interacts with the  $\beta$ 3-OH group of the cholesterol (figure 1.6 C ;An-

dreoli, 1973; de Kruijff *et al.*, 1974; Dennis *et al.*, 1970). Nystatin and amphotericin B have a very high affinity for ergosterol. Thus, very low concentrations of both antibiotics are needed to permeabilize ergosterol-containing membranes which are present in fungi and yeast cells and do not occur in animal or bacteria cells. Therefore, nystatin and amphotericin B can also be used for the treatment of internal fungal infections.

In order to form a functional channel, 8 to 10 nystatin/amphotericin B monomers make up a cylindrical structure, with the hydrophilic groups lining the pore and the heptaene backbone facing the hydrophobic interior of the cell membrane (Finkelstein & Holz, 1973; Kleinberg & Finkelstein, 1984). The channel has a diameter of  $\sim 0.4 - 0.8$  nm (Andreoli, 1973; de Kruijff *et al.*, 1974; Horn & Marty, 1988; Kleinberg & Finkelstein, 1984). It is only permeable for monovalent cations ( $\text{Rb}^+ > \text{K}^+ > \text{Na}^+ > \text{Li}^+$ ; de Kruijff *et al.*, 1974), slightly permeable for  $\text{Cl}^-$  (Russell *et al.*, 1977) and has no voltage-dependence. Multivalent ions are impermeant. The pores are also permeant to smaller non-electrolytes, i.e. urea and glycerol. While nystatin pores are impermeable to glucose and sucrose, both molecules slowly permeate through amphotericin B pores suggesting a slightly larger diameter for amphotericin B pores (de Kruijff *et al.*, 1974). This means that the molecular cut-off for sugar molecules is at  $\sim 200$  Da (Horn & Marty, 1988). Neither lateral diffusion in the cell membrane nor diffusion into the cytoplasm could be detected during experiments with nystatin/amphotericin B (Horn & Marty, 1988).

### **Gramicidin**

Gramicidin is a linear polypeptide antibiotic which was first isolated in 1940 from *Bacillus brevis* by René Dubos (1941) and the first antibiotic to be used clinically, paving the way for the practical application of other antibiotic drugs such as penicillin (Epps, 2006). Similar to nystatin/amphotericin B, gramicidin exerts its antibiotic effect by forming ion channels in the cell membrane and is also widely used as an ionophore in perforated-patch experiments. Gramicidin is one of the best studied ionophores because it has served as a prototypical model for ion channels in general for many years now. In fact, it is the most thoroughly studied "ion channel in terms of its electrical properties,

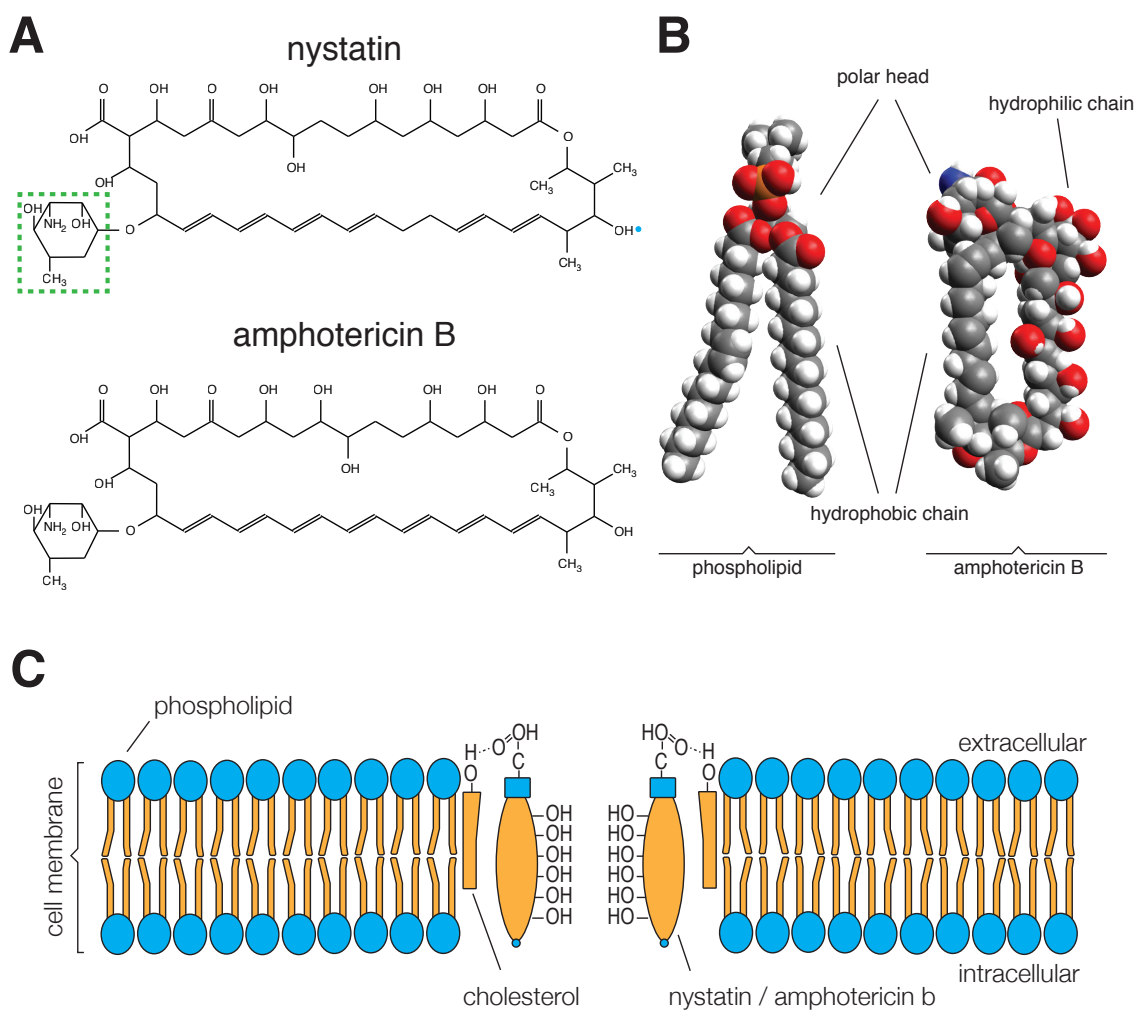


**Figure 1.6:** Molecular properties of nystatin and amphotericin B. **(A)** Chemical structures of nystatin (*top*) and amphotericin B (*bottom*). *Green dotted rectangle:* mycosamine residue; *blue circle:* isolated hydroxyl group. **(B)** Space-filling models of a phospholipid (*left*) and amphotericin B (*right*). Color code: hydrogen, *white*; carbon, *grey*; oxygen, *red*; nitrogen, *blue* (made using Avogadro [Ver. 1.0.1, <http://avogadro.openmolecules.net>]). **(C)** Partial model for nystatin/amphotericin B pores (modified from Andreoli, 1973; Kleinberg & Finkelstein, 1984).

the relationships between its chemical structure and conductance properties, and the details of its three-dimensional structure” (Wallace, 1990).

Gramicidin is able to adopt a large variety of conformations from which two major folding motifs have been identified: (a) The single-stranded helical dimer ( $\beta$ -helix; Urry (1971)) and (b) The double-stranded intertwined helix (figure 1.7 B; Veatch *et al.* (1974)). The single-stranded helix is the only form which is able to function as an ion channel and has been designated the ‘channel’ form in contrast to the ‘non-channel’ form (Andersen *et al.*, 1999; Urry *et al.*, 1983). The conformation of gramicidin seems to be dependent on its solvent history. In solvents such as chloroform/methanol, gramicidin adopts the

non-channel conformation and upon sonification and heating the non-channel conformation can be converted into the channel conformation (Killian *et al.*, 1988; LoGrasso *et al.*, 1988). However, there are also pieces of evidence which doubt that gramicidin has a 'solvent memory'. Instead solvents themselves alter the properties of gramicidin by getting incorporated in the membrane as well (Sawyer *et al.*, 1990). Interestingly, gramicidin contains alternating L- and D- amino acids in contrast to most proteins which only contain the L- form (Mitchell & Smith, 2003; Sarges & Witkop, 1965). Due to the alternating L- and D- amino acid residues, all side chains are located at the outside of the helix. The interior of the helix is made up by the polar peptide backbone thereby forming the channel pore (figure 1.7 C). The channel form is further stabilized by the tryptophan residues which are clustered at the C-terminus of the peptide chain. Due to its amphipathic character, tryptophan 'anchors' the two gramicidin monomers at the membrane interface, providing the proper orientation of both monomers to form a functional channel (see figure 1.7C; Yau *et al.*, 1998). The pore of gramicidin A has a diameter of 0.4 nm (Urry *et al.*, 1971) which is comparable to the pores formed by nystatin/amphotericin B. Therefore, the molecular weight cut-off for gramicidin channel pores is < 200 Da. Similar to nystatin/amphotericin B, gramicidin does not laterally diffuse in the membrane (Kyrozis & Reichling, 1995). It is selectively permeant for monovalent cations ( $\text{Cs}^+ > \text{Rb}^+ > \text{K}^+ > \text{Na}^+ > \text{Li}^+$ ) and has no voltage-dependence. Divalent ions do not pass the channel (Myers & Haydon, 1972).

In contrast to nystatin/amphotericin B pores, it has been reported that gramicidin channel pores are also impermeable to  $\text{Cl}^-$  (Myers & Haydon, 1972; Tajima *et al.*, 1996). Intracellular  $\text{Cl}^-$  plays an important role in many cellular processes, for instance the regulation of the cell volume and pH or the activity of specific receptors ( $\text{GABA}_A$  or glycine). Disruption of the intracellular  $\text{Cl}^-$  homeostasis could lead to the distortion of neuronal responses. An asymmetrical  $\text{Cl}^-$ -concentration between the pipette solution and the interior of the cell could produce a 'Donnan equilibrium' because  $\text{Cl}^-$ -ions were able to freely move across the membrane patch while larger negatively charged cellular components (proteins) were blocked. The subsequent movement of water and ions could damage the cell (i.e. by swelling/shrinking). Further, the build-up of a Donnan

equilibrium might result in liquid junction potentials in the range of several millivolts hindering the voltage-clamp analysis of ion channels (Akaike & Harata, 1994; Horn & Marty, 1988).

Thus, the gramicidin perforated patch technique provides a way of circumventing Cl<sup>-</sup> related issues, especially when studying Cl<sup>-</sup>-dependent responses, i.e. characterization of glycine receptors in early development.

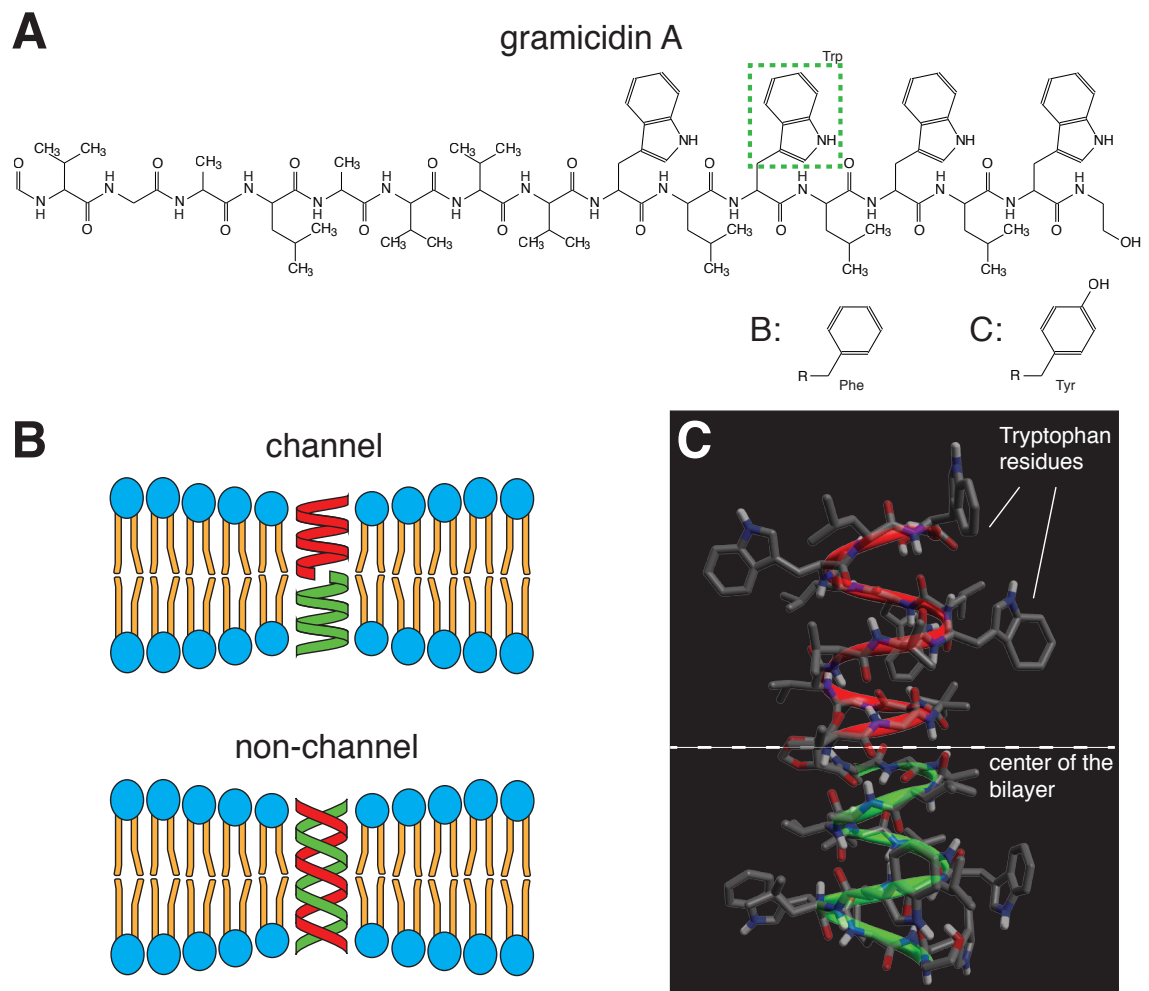


**Figure 1.7:** Molecular properties of gramicidin. (A) Chemical structure of gramicidin A. *Green dotted rectangle:* Tryptophan residue at position 11 which is exchanged by phenylalanin (gramicidin B, inset) or tyrosine (gramicidin C, inset). (B) Schematic diagrams of gramicidin in the 'channel' (*top*) and 'non-channel' confirmation (*bottom*; modified from Wallace, 1990). (C) Combined stick and ribbon model of a gramicidin single-stranded helical dimer (channel-form; made using Avogadro, PDB coordinates from Crouzy *et al.*, 1994).

**$\beta$ -Escin**

$\beta$ -escin is the active compound of escin (or aescin), a mixture of saponins from *Aesculus hippocastanum*, the horse chestnut tree (Sirtori, 2001). Although saponins are not structurally related to antibiotics their mode of action is similar as saponins interact with cholesterol to form channel pores in lipid bilayers (Bangham *et al.* , 1962). Initially,  $\beta$ -escin was used as a 'whole cell' permeabilization agent in studies of smooth muscle cells (e.g. Akagi *et al.* , 1999; Kobayashi *et al.* , 1989; Satoh *et al.* , 1994). In order to circumvent inconveniences (i.e. long perforation times) of antibiotic pore-forming agents,  $\beta$ -escin was used as an ionophore for perforated-patch recordings. It has been demonstrated that  $\beta$ -escin allows low access resistance recordings of voltage-activated  $\text{Ca}^{2+}$ -channels without  $\text{Ca}^{2+}$ -current rundown comparable to the three antibiotic ionophores (Fan & Palade, 1998). Compared to amphotericin B, the perforation times with  $\beta$ -escin are much faster ( $\sim 8$  min.) and the compound is water soluble and stable for 8 – 10h. Further, it does not interfere with giga-ohm formation leading to higher success rates in perforated patch formation (59%  $\beta$ -escin vs. 27% amphotericin B; Sarantopoulos *et al.* , 2004).

However,  $\beta$ -escin allows the diffusion of large molecules in a concentration-dependent manner. Konishi & Watanabe (1995) reported that concentrations up to 50  $\mu\text{M}$   $\beta$ -escin allow the diffusion of molecules ranging from 0.5 kDa (ATP) to 18 kDa (cytoplasmic proteins) molecular weight. It is also permeant for divalent ions (e.g.  $\text{Ca}^{2+}$ ). Thus, it is a matter of debate why the  $\text{Ca}^{2+}$ -current rundown is prevented in  $\beta$ -escin perforated patch recordings. Fan & Palade (1998) state "that a patch even with  $\beta$ -escin pores still represents more of a diffusion barrier to macromolecules than a ruptured patch". Further, it is not clear if  $\beta$ -escin diffuses laterally through the membrane and/or into the cytoplasm during the time-course of experiments. Relatively high rates of leaky cells with  $\beta$ -escin hint into that direction (Sarantopoulos *et al.* , 2004)

Therefore,  $\beta$ -escin should be used with great caution for perforated patch recordings until the compound has thoroughly been characterized.

**Table 1.1:** Properties of pore-forming compounds

Compound	Order No. [Sigma]	Cation permeability	Cl <sup>-</sup> permeability	Pore diameter (nm)	M.W. cut-off (Da)
ATP	A8937	??	??	??	??
Nystatin Amphotericin B	N6261 A4888	Rb <sup>+</sup> >K <sup>+</sup> >Na <sup>+</sup> >Li <sup>+</sup> , impermeant for divalent ions	slightly permeable	0.4 – 0.8	~ 200
Gramicidin	G5002	Cs <sup>+</sup> >Rb <sup>+</sup> >K <sup>+</sup> >Na <sup>+</sup> >Li <sup>+</sup> , impermeant for divalent ions	impermeable	0.4	≤ 200
β-Escin	E1378	permeable for Ca <sup>2+</sup>	??	??	~ 18,000

## 1.7 Objectives

Although major advances in understanding the role of neuronal circuits in control of energy homeostasis and how they interact with each other have been made, many questions remain open.

Nowadays we understand the microcircuit consisting of POMC neurons and AgRP neurons in a very great detail. However, the exact wiring of the whole hypothalamic network remains still unclear. Both, AgRP/NPY as well as POMC/CART neurons, are believed to project to the same “second-order neurons” downstream to the ARC which integrate information on energy status. Until now, the exact location of these second-order neurons could not be determined. However, the VMH has been speculated to be one possible location of the “second-order neurons”.

In addition to the hypothalamus, there is also evidence that the DA system is directly affected by fuel-sensing hormones. Thus, peripheral hormones such as insulin could directly adjust the DA reward system according to the current energy/fuel state. Several studies were able to show that insulin, leptin and ghrelin signaling in the mesencephalon alters feeding, pointing towards a role for the DA system in control of energy homeostasis. However, there are still many uncharted territories to be explored. For in-

stance in the case of insulin, convincing electrophysiological data demonstrating a direct effect on DA neurons is still lacking until now.

Furthermore, recent studies suggest that genetic factors like the *Fto* gene can affect food intake and energy expenditure. Since several factors in control of energy homeostasis such as insulin and leptin regulate the activity of the DA system, it has been hypothesized that genetic factors like *Fto* might also play a role in the DA system and alter the activity and properties of mesencephalic DA neurons. Hence, the main objectives of this thesis were:

1. To evaluate two different patch clamp recording techniques (whole cell and perforated-patch configuration) and to determine of the best suitable method for the experimental setup of the thesis.
2. To investigate the VMH and its role in the control of energy homeostasis:  
to elucidate the effect of insulin signaling on SF-1 neurons residing within the VMH and to determine if the SF-1 neurons are the long sought 'second-order' neurons downstream to the melanocortin system or if the VMH rather shapes the response towards feeding-related signals.
3. To determine the effect of insulin on the electrophysiological properties of mesencephalic DA neurons on a cellular and network level by employing cell-specific genetic modifications (IR deletion) of DA neurons in order to ultimately understand how insulin signaling in the DA system affects energy homeostasis.
4. To understand the role of the *Fto* gene in the DA reward system and how alterations of *Fto* expression affects the cellular properties of mesencephalic DA neurons.

The electrophysiological data which were acquired during the course of the thesis were also published in several publications which are listed under TEILPUBLIKATIONEN. Therefore, to present the electrophysiological data in the context of the individual projects, data from coworkers which contributed to the publications is also shown. All experimental data which were not acquired by myself are indicated as follows:

Additional data in chapter 3.2 *ff.* was provided by Tim Klöckener, B. F. Belgardt, L. Paeger, L. A. W. Verhagen, A. Husch, J. W. Sohn, B. Hampel, H. Dhillon, J. Zigman, B. B. Lowell, K. W. Williams and is referred to as Klöckener *et al.* (2011) in the text.

Additional data in chapter 3.3 *ff.* was provided by A. Christine Könnner, S. Tovar, A. Mesaros, C. Sánchez-Lasheras, N. Evers, L. A.W. Verhagen, H. S. Brönneke, A. Kleinriders, B. Hampel and is referred to as Könnner *et al.* (2011) in the text.

Additional data in chapter 3.4 *ff.* was provided by my brother Martin Heß and H. S. Brönnecke, L. A. W. Verhagen, M. O. Dietrich, S. D. Jordan, B. F. Belgardt, T. Franz, B. Hampel and is referred to as Hess *et al.* (2011) in the text.

## 2 Materials and Methods

### 2.1 Animal care

Care of all animals was within institutional animal care committee guidelines. All animal procedures were approved by local government authorities (Bezirksregierung Köln, Cologne, Germany) and were in accordance with NIH guidelines. Mice were housed in groups of 3 – 5 at a temperature of 22 – 24°C with a 12 h light/12 h dark cycle. After weaning (P21), mice were either fed regular chow food (NCD; Teklad Global Rodent 2918; Harlan) containing 53.5 % carbohydrates, 18.5 % protein, and 5.5 % fat (12 % of calories from fat) or a high-fat diet (HFD; C1057; Altromin) containing 32.7 % carbohydrates, 20 % protein, and 35.5 % fat (55.2 % of calories from fat). All animals had access to water and chow *ad libitum*. The different mouse strains used for this study were kindly provided by Martin Heß, Tim Klöckener and Christine Könner. An overview of is given in *table 2.1*.

### 2.2 Brain slice preparation

The animals were anesthetized with halothane (B4388; Sigma-Aldrich, Taufkirchen, Germany) and subsequently decapitated. The brain was rapidly removed and a block of tissue containing the hypothalamus or the midbrain was immediately cut out. Coronal slices (250 – 300  $\mu\text{m}$ ) were cut with a vibration microtome (HM-650 V; Thermo Scientific, Walldorf, Germany) under cold (4 °C), carbogenated (95% O<sub>2</sub> and 5% CO<sub>2</sub>), glycerol-based modified artificial cerebrospinal fluid (GaCSF; Ye *et al.* 2006) to enhance the viability of neurons. GaCSF contained (in mM): 250 Glycerol, 2.5 KCl, 2 MgCl<sub>2</sub>, 2 CaCl<sub>2</sub>, 1.2 NaH<sub>2</sub>PO<sub>4</sub>, 10 HEPES, 21 NaHCO<sub>3</sub>, 5 Glucose and was adjusted to pH 7.2 with NaOH resulting in an osmolarity of  $\sim$ 310 mOsm. Brain slices were transferred into carbogenated artificial cerebrospinal fluid (aCSF). First, they were kept for 20 min. in a 35 °C 'recovery bath' and then stored at room temperature (24 °C) for at least 30

**Table 2.1:** Mouse strains used for the thesis

Brain region	Mouse genotype	Diet	Sex	Age (d)
Hypothalamus	SF-1 <sup>GFP</sup>	NCD	male	21 – 28
	SF-1 <sup>GFP:ΔIR</sup>	NCD	male	21 – 28
	POMC <sup>GFP</sup> ;SF-1 <sup>ΔIR</sup>	HFD	male	105 – 140
	POMC <sup>GFP</sup>	HFD	male	105 – 140
Midbrain	C57BL/6J	NCD	male	28 – 56
	Th <sup>ΔIR</sup>	NCD	male/female	28 – 35
	IR <sup>fl/fl</sup>	NCD	male/female	28 – 35
	Fto <sup>+/+</sup>	NCD	male/female	28 – 56
	Fto <sup>-/-</sup>	NCD	male/female	28 – 56
	DAT <sup>ΔFto</sup>	NCD	male/female	28 – 56
	Fto <sup>fl/fl</sup>	NCD	male/female	28 – 56

min prior to recording. For the recordings, slices were transferred to a Sylgard-coated (Dow Corning Corp., Midland, MI, USA) recording chamber ( $\sim 3$  ml volume) and, if not mentioned otherwise, continuously superfused with carbogenated aCSF at a flow rate of  $\sim 2$  ml  $\cdot$  min<sup>-1</sup>. aCSF contained (in mM): 125 NaCl, 2.5 KCl, 2 MgCl<sub>2</sub>, 2 CaCl<sub>2</sub>, 1.2 NaH<sub>2</sub>PO<sub>4</sub>, 21 NaHCO<sub>3</sub>, 10 HEPES, and 5 Glucose and was adjusted to pH 7.2 with NaOH resulting in an osmolarity of  $\sim 310$  mOsm.

### 2.3 Patch-clamp recordings

Current- and voltage-clamp recordings in neurons of the hypothalamus and the midbrain were performed in either the whole cell or perforated patch-clamp configuration. In the hypothalamus, neurons which express proopiomelanocortin (POMC) or steroidogenic factor 1 (SF-1) were investigated. In the midbrain, dopaminergic (DA) neurons in the ventral tegmental area (VTA) and substantia nigra *pars compacta* (SNpc) were investigated.

Neurons were visualized with a fixed stage upright microscope (BX51WI, Olympus,

Hamburg, Germany) using 40 $\times$  and 60 $\times$  water-immersion objectives (LUMplan FI/IR 40 $\times$ , 0.9 numerical aperture (NA), 2 mm working distance (WD); LUMplan FI/IR 60 $\times$ , ?? NA, 2 mm WD, Olympus) with infrared differential interference contrast optics (Dodt & Zieglgänsberger, 1990) and fluorescence optics.

Putative DA SNpc and DA VTA neurons were identified by their anatomical location in the SNpc or VTA and by their characteristic electrophysiological signature (i.e. slow and regular firing and the presence of a large  $I_h$ -dependent "sag"-potential (Hommel *et al.*, 2006; Lacey *et al.*, 1989; Richards *et al.*, 1997; Ungless *et al.*, 2001)). POMC and SF-1 neurons were also identified by their anatomical location in the arcuate nucleus (ARC) or ventromedial hypothalamus (VMH) and by their GFP fluorescence that was visualized with an X-Cite 120 illumination system (EXFO Photonic Solutions, Ontario, Canada) in combination with a Chroma 41001 filter set (EX: HQ480/40 $\times$ , BS: Q505LP, EM: HQ535/50m, Chroma, Rockingham, VT, USA). Electrodes with tip resistances between 3 and 5 M $\Omega$  were fashioned from borosilicate glass (0.86 mm inner diameter [ID]; 1.5 mm outer diameter [OD]; GB150-8P; Science Products) with a vertical pipette puller (PP-830; Narishige, London, UK). Recordings in the ARC and VMH were made at room temperature. Recordings of DA midbrain neurons were made at  $\sim 31^\circ\text{C}$  using an inline solution heater (SH27B; Warner Instruments, Hamden, CT, USA) operated by a temperature controller (TC-324B; Warner Instruments). All recordings were performed with an EPC10 patch-clamp amplifier (HEKA, Lambrecht, Germany) controlled by the program PatchMaster (version 2.32; HEKA) running under Windows. Data were sampled at intervals of 100  $\mu\text{s}$  (10 kHz) and low-pass filtered at 2 kHz with a four-pole Bessel filter. Whole cell capacitance was determined by using the capacitance compensation (C-slow) of the EPC10. Cell input resistances ( $R_M$ ) were calculated from voltage responses to hyperpolarizing current pulses. The calculated liquid junction potential between intracellular and extracellular solution was also compensated (calculated with Patcher's Power Tools plug-in from <http://www.mpibpc.mpg.de/groups/neher/index.php?page=software> for Igor Pro 6 [Wavemetrics, Lake Oswego, OR, USA]).

### 2.3.1 Whole cell recordings

Whole cell recordings were performed following the methods of Hamill *et al.* (1981). Normal aCSF was used as extracellular solution (see 2.2). The pipette solution contained (in mM): 135 K-gluconate, 10 KCl, 10 HEPES, 0.1 EGTA, 2 MgCl<sub>2</sub>, 3 K-ATP, 0.3 Na-GTP adjusted with KOH to pH 7.2 resulting in an osmolarity of ~300 mOsm. The liquid junction potential (+14.6 mV) was also compensated.

### 2.3.2 Measurements of postsynaptic currents

Postsynaptic currents (PSCs) were measured in the whole cell configuration. Patch pipettes were filled with (in mM): 140 KCl, 10 HEPES, 0.1 EGTA, 5 MgCl<sub>2</sub>, 5 K-ATP, 0.3 Na-GTP adjusted to pH 7.3 with KOH resulting in an osmolarity of ~300 mOsm. Additionally, in DA neurons the intracellular sodium channel blocker QX-314 (2 mM; Q-150, Alomone, Jerusalem, Israel) was added to the intracellular solution to avoid contaminations with sodium currents. The high intracellular chloride concentration in the recording pipettes shifted the chloride equilibrium potential to a more depolarized potential, which reversed the polarity of GABA<sub>A</sub> receptor mediated currents from outward to inward, and made their detection easier by increasing the driving force on the chloride ions. Cells were voltage clamped at -60 mV and data were sampled at a frequency of 10 kHz. The liquid junction potential (+3.6 mV) was also compensated. The contribution of excitatory and inhibitory PSCs (EPSCs, IPSCs) to the synaptic input was determined in three steps. First, the overall frequency of PSCs was measured. Second, glutamatergic EPSCs were blocked with DL-2-Amino-5-phosphonopentanoic acid (D-AP5; 50 μM; A5282, Sigma) and 6-Cyano-7-nitroquinoxaline-2,3-dione (CNQX; 10 μM; C127, Sigma) to isolate the IPSCs, which were identified as GABAergic (inhibitory) PSCs by their sensitivity to picrotoxin (PTX; 100 μM; P1675, Sigma). The overall PSC frequency was determined after the recording had stabilized (>10 minutes after break in) for a 2 minutes interval. The IPSC frequency was measured after 10 – 15 minutes D-AP5/CNQX application for a 2 minutes interval. The EPSC frequency was determined by subtracting the IPSC frequency from the overall frequency. To calculate EPSC and IPSC frequency, the PSC recordings were analyzed off line. The data were digitally filtered and the DC

component was removed using the smooth (10 ms time period) and the DC remove (10 ms time period) functions provided in the Spike2 software (Cambridge Electronics [CED], Cambridge, UK). PSCs were automatically detected when the signal crossed a threshold that was set and adjusted manually depending on the noise level of the signal. This semi-automated detection procedure was verified by visual inspection.

### 2.3.3 Perforated-patch clamp recordings

Perforated-patch experiments were conducted using protocols modified from Horn & Marty (1988) and Akaike & Harata (1994). Recordings were performed with ATP and GTP free pipette solution containing (in mM): 128 K-gluconate, 10 KCl, 10 HEPES, 0.1 EGTA, 2 MgCl<sub>2</sub> adjusted to pH 7.3 with KOH resulting in an osmolarity of ~300 mOsm. ATP and GTP were omitted from the intracellular solution to prevent uncontrolled permeabilization of the cell membrane (Lindau & Fernandez, 1986). The patch pipette was tip filled with internal solution and back filled with 0.02% tetraethylrhodamine-dextran (D3308, Invitrogen, Eugene, OR, USA) and ionophore-containing internal solution to achieve perforated patch recordings.

Nystatin (N6261; Sigma) was dissolved in methanol according to the instructions of Akaike & Harata (1994). The final methanol concentration (2%) had no obvious effect on the investigated neurons.

Amphotericin B (A4888; Sigma) and Gramicidin (G5002; Sigma) were dissolved in dimethyl sulfoxide (DMSO; D8418, Sigma) following the protocols of Rae *et al.* (1991) and Kyrozis & Reichling (1995). The used DMSO concentration (0.1 – 0.3 %) had no obvious effect on the investigated neurons. All ionophores were added to the modified pipette solution shortly before use. The final concentration of nystatin and amphotericin B was ~200  $\mu\text{g} \cdot \text{ml}^{-1}$ , the final concentration of gramicidin was ~10 – 75  $\mu\text{g} \cdot \text{ml}^{-1}$ .

### 2.3.4 Single cell labeling

To label single cells, 1% biocytin (B4261; Sigma-Aldrich) was added to the pipette solution. Upon completion of the electrophysiological experiments, perforated-patch recordings were converted to the whole cell configuration and biocytin was allowed to diffuse

into the cell for at least 5 min. The brain slices were fixed in Roti-Histofix (Po873; Carl Roth, Karlsruhe, Germany) overnight at 4°C and rinsed in 0.1 M Tris-HCl-buffered solution (pH 7.2; three times for 20 min each time; RT; TBS). Afterwards, the slices were incubated in TBS containing 1% Triton X-100 (39795.01, Serva, Heidelberg, Germany) and 10% normal goat serum (30 min; RT; S-1000; Vector Labs, Burlingame, CA, USA). Brain slices were washed in TBS (three times for 10 min each time) and subsequently incubated in Alexa Fluor 633 (Alexa 633)-conjugated streptavidin (1:600; 2 days; 4°C; S21375; Invitrogen, Karlsruhe, Germany) that was dissolved in TBS containing 10% normal goat serum. Brain slices were rinsed in TBS (2 days with three solution changes; 4°C), dehydrated, and then cleared and mounted in Permount (SP15B-500; Fisher Scientific, Nepean, Ontario, Canada). The fluorescence images were captured with a confocal microscope (LSM 510, Carl Zeiss, Göttingen, Germany) equipped with Plan-Neofluar 10× (0.3 NA) and Plan-Apochromat 20× (0.75 NA) objectives. Streptavidin-Alexa 633 was excited with a HeNe laser at 633 nm. Emission of Alexa 633 was collected through a 650 nm LP filter. Scaling, noise reduction and z-projections were done using ImageJ v1.35d with the WCIF plugin bundle ([www.uhnresearch.ca/facilities/wcif/](http://www.uhnresearch.ca/facilities/wcif/)). For the 3D-reconstruction of neurons, AMIRA (Visage Imaging GmbH, Berlin, Germany) was used. The final figures were prepared with Photoshop and Illustrator CS5 (Adobe Systems Incorporated, San Jose, CA, USA).

### 2.3.5 Drugs

Insulin (100 – 200 nM; I9278, Sigma), cocaine hydrochloride (10 μM, C5776, Sigma), the D<sub>2</sub>-receptor agonist (-) quinpirole (1 – 1000 nM, Q102, Sigma) and the GIRK channel antagonist tertiapin-Q (500 nM, STT-170, Alomone, Jerusalem, Israel) were added to the normal aCSF. The K<sub>ATP</sub> channel blocker tolbutamide (200 μM, To891, Sigma), the K<sub>ATP</sub> opener diazoxide (200 μM, D9035, Sigma), the D<sub>2</sub>-receptor antagonist (-) sulpiride (1 – 10 μM, BG0325, Biotrend, Cologne, Germany) and the PI3K inhibitor wortmannin (1 μM, W1628, Sigma) were dissolved in dimethyl sulfoxide (DMSO, D8418, Sigma) and added to the normal aCSF with a final DMSO concentration of 0.1 – 0.25%.

For PSC measurements D-AP5 (50 μM), CNQX (10 μM) and PTX (100 μM) were bath-

applied in the given concentrations at a flow rate of  $\sim 2 \text{ ml} \cdot \text{min}^{-1}$ . CNQX was dissolved in DMSO and added to the normal aCSF with a final DMSO concentration of 0.04%.

The DMSO concentrations had no obvious effect on the investigated neurons. QX-314 (2 mM) was added to the intracellular solution. All solutions were bath-applied at a flow rate of  $\sim 2 \text{ ml} \cdot \text{min}^{-1}$ . All drug containing solutions were freshly prepared at the day of the experiments. Insulin was added to the normal aCSF shortly before the experiments.

### 2.3.6 Data analysis

Data analysis was performed with Spike2 (version 6; Cambridge Electronic Design Ltd., Cambridge, UK), Igor Pro 6 (Wavemetrics, Portland, OR, USA) and Graphpad Prism (version 5.0b; Graphpad Software Inc., La Jolla, CA, USA). Numerical values in the text are given as mean  $\pm$  standard error. Because the insulin responsiveness of DA midbrain and SF-1 neurons was not homogenous we used the '3 times standard deviation (SD) criterion' (Dhillon *et al.*, 2006; Kloppenburg *et al.*, 2007). For each neuron, the firing rate averaged from 15 sec intervals was taken as one data point. To determine the mean firing rate with SD 8 to 10 data points at stable firing rates were averaged. A neuron was considered insulin responsive if the change in firing induced by insulin was 3 times larger than the SD. Coefficients of variation (CVs) were obtained according to Wolfart *et al.* (2001).

To determine differences in means of basic electrophysiological properties between the different genotypes, unpaired *t* tests were used. To determine differences between treated and untreated states paired *t* tests or one-way ANOVA was performed; post hoc pairwise comparisons were performed using *t* tests with the Newman-Keuls method for p value adjustment. Unpaired *t* tests were performed to determine differences in the PSC frequency between control neurons and neurons lacking the insulin receptor.

A significance level of 0.05 was accepted for all tests. The '+' signs in the box plots show the mean, the horizontal line the median of the data. The whiskers were calculated according to the 'Tukey' method.

## 3 Results

### 3.1 The perforated patch technique

Most of the following experiments involved the investigation of second messenger dependent processes. Second messenger pathways are very sensitive towards wash out of cytoplasmic components so that the application of the whole cell configuration might lead to ambiguous results (Akaike & Harata, 1994). Therefore, the perforated patch configuration was employed for the majority of experiments owing to the fact that recordings can be obtained in a non-invasive manner. Here, I compared recordings in the perforated-patch configuration with recordings in the whole cell configuration in terms of basic electrophysiological properties.

#### 3.1.1 Whole cell vs. perforated-patch clamp

Patch clamp recordings were performed from hypothalamic SF-1 neurons and mesencephalic dopaminergic (DA) neurons in the whole cell and the perforated-patch clamp configuration with amphotericin B as pore-forming agent.

Initially, the basic electrophysiological parameters of DA neurons (action potential [AP] frequency, membrane resistance [ $R_{mem}$ ]) did not differ between neurons recorded in the the perforated patch configuration or neurons recorded in the whole cell configuration immediately after breakthrough (see table 3.1). However, during the first 15 minutes of a whole cell recording a strong decrease in AP frequency could be observed in SF-1 neurons (figure 3.1 A, *left panel*) as well as DA neurons (figure 3.1 B, *left panel*) while perforated patch recordings remained stable in both neuron types (figure 3.1A,B, *right panels*). In numerous cases the ‘whole cell induced’ hyperpolarization could be reversed by tolbutamide, a selective blocker of ATP-dependent potassium channels ( $K_{ATP}$ ). This finding suggests the whole cell configuration modifies  $K_{ATP}$  channel properties which

are mostly dependent on intracellular components (i.e. ATP, phospholipids; Nichols, 2006; Tarasov *et al.*, 2004).

Further analysis revealed that in whole cell recordings of DA neurons the AP frequency decreased over the 15 min. period by  $\sim 70\%$  from  $2.11 \pm 0.29$  Hz to  $0.75 \pm 0.35$  Hz ( $p < 0.01$ ;  $n = 7$ ; figure 3.1). Only 1 neuron out of 7 (14%) did not change its AP frequency during the 15 min. time period. In contrast, the AP frequency did not change in perforated patch recordings during the 15 min. time period (figure 3.1 C; 0 min.:  $2.36 \pm 0.19$  Hz, 15 min.:  $2.33 \pm 0.22$  Hz,  $p > 0.05$ ;  $n = 8$ ). In addition,  $R_{mem}$  dropped during the first 15 minutes of whole cell recordings whereas  $R_{mem}$  remained stable in perforated patch recordings (whole-cell:  $80.1 \pm 5.5\%$ ,  $n = 7$ ; perforated:  $103.0 \pm 3.0\%$ ,  $n = 3$ ).

Next, several spike-related parameters were analyzed for whole cell and perforated-patch recordings over the 15 min. time period. The relative amplitude of the spike afterhyperpolarization (AHP) decreased during the first 15 min of whole cell recordings while the AHP amplitude recorded with perforated patch configuration remained stable (figure 3.2A,B,C; whole-cell:  $88.6 \pm 4.8\%$ ,  $n = 8$ ; perforated:  $101.3 \pm 0.8\%$ ,  $n = 8$ ). The size of the AHP largely depends on small conductance  $Ca^{2+}$ -dependent potassium channels ('SK channels'; Bean, 2007), suggesting that recordings in the whole cell configuration are likely affecting the  $Ca^{2+}$  homeostasis. While there were no significant differences in spike amplitude, threshold and width, the variance of these parameters greatly increased after 15 minutes of whole cell recording compared to perforated-patch recordings.

**Table 3.1:** Comparison of initial values of basic electrophysiological parameters of mesencephalic DA neurons recorded in the perforated and whole cell configuration.

	Whole cell configuration	Perforated patch configuration
<b>AP frequency (Hz)</b>	$2.1 \pm 0.3$ ( $n = 7$ )	$2.4 \pm 0.2$ ( $n = 8$ )
<b>Membrane resistance (M<math>\Omega</math>)</b>	$449.1 \pm 51.1$ ( $n = 8$ )	$416.4 \pm 48.9$ ( $n = 8$ )
<b>Spike amplitude (mV)</b>	$99.4 \pm 3.7$ ( $n = 8$ )	$98.0 \pm 1.1$ ( $n = 7$ )
<b>Firing Threshold (mV)</b>	$-40.4 \pm 0.9$ ( $n = 8$ )	$-41.5 \pm 1.1$ ( $n = 6$ )
<b>AHP amplitude (mV)</b>	$35.0 \pm 2.3$ ( $n = 8$ )	$32.3 \pm 1.2$ ( $n = 9$ )
<b>Spike width (ms)</b>	$1.4 \pm 0.1$ ( $n = 8$ )	$1.3 \pm 0.1$ ( $n = 6$ )

Data are given as mean  $\pm$  S.E.M. AP, action potential; AHP, afterhyperpolarization. Initial values were obtained in whole cell recordings immediately after break in and in perforated patch recordings after the access resistance ( $R_a$ ) and the action potential (AP) amplitude were stable.

None of the investigated parameters differed significantly between neurons recorded in the whole cell and perforated patch configuration.

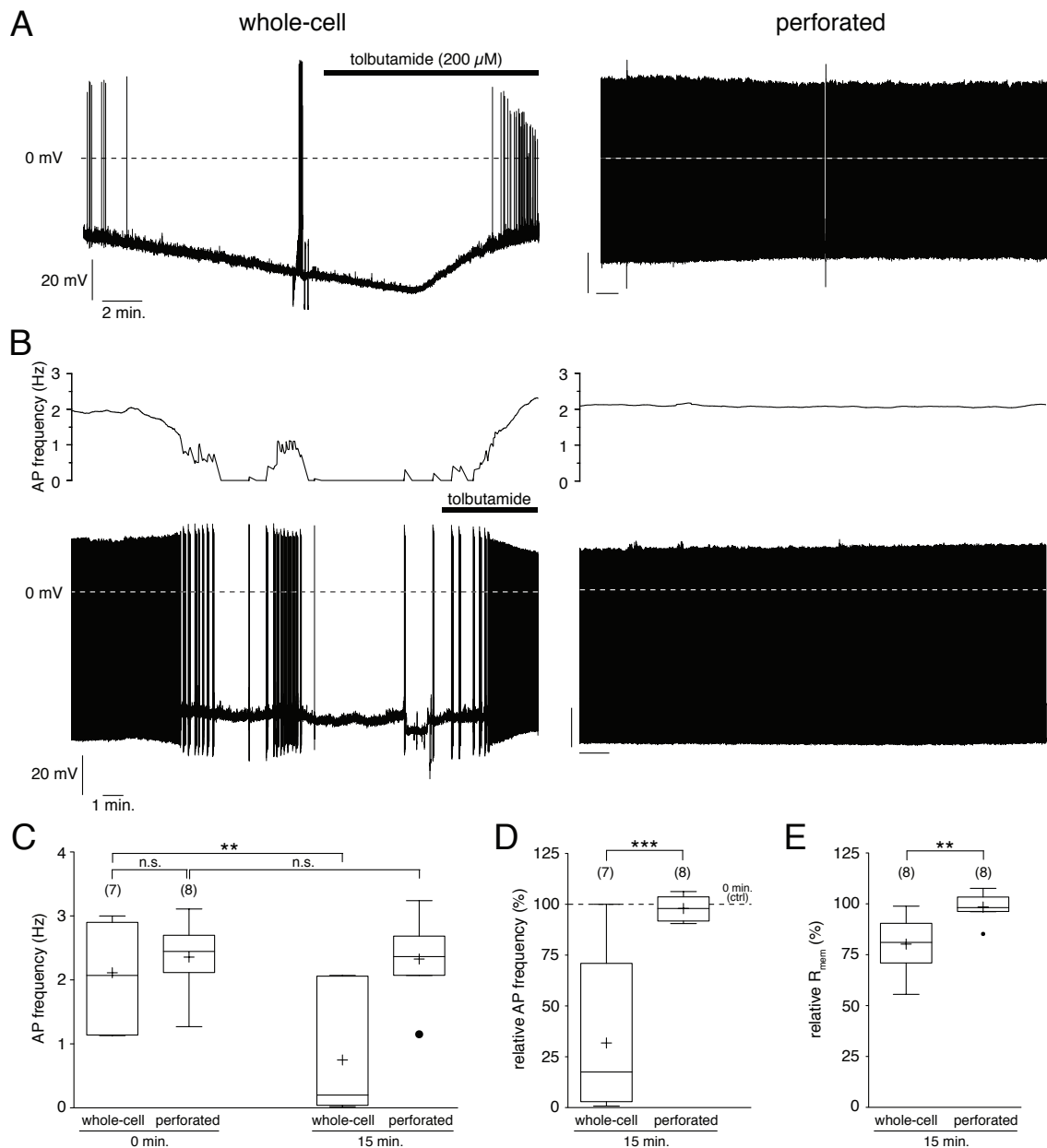


**Figure 3.1:** Comparison of whole-cell and perforated patch recordings of hypothalamic SF-1 and mesencephalic dopaminergic (DA) neurons. *(A) Left* Current-clamp recording of a SF-1 neuron in whole cell configuration. The washout leads to the activation of  $K_{ATP}$  channels resulting in the hyperpolarization of the cell. Addition of tolbutamide reversed the hyperpolarization. *Right* Recording of a SF-1 neuron in perforated patch configuration. No rundown/hyperpolarization could be detected. *(B)* Recordings of DA neurons in whole cell configuration (*left*) and perforated patch configuration (*right*) and corresponding AP frequency over time plots (*upper panels*). In whole-cell mode,  $K_{ATP}$  activation leads to hyperpolarization of the neuron and addition of tolbutamide leads to recovery of spontaneous activity. In contrast, the perforated-patch recording remains stable over the whole time period. *(C)* Absolute AP frequency of DA neurons during whole cell and perforated-patch recordings at the beginning of the recording (0 min.) and after 15 min. *(D)* Relative AP frequency of DA neurons recorded in the whole cell and the perforated-patch configuration after 15 min. recording time. Data are normalized to the respective initial values (0 min.). *(E)* Relative input resistance of DA neurons recorded in whole-cell and perforated patch mode after 15 min. Data are normalized to the respective initial values (0 min.). For details on box plots see Materials and Methods. \*:  $p \leq 0.05$ , \*\*:  $p \leq 0.01$ , \*\*\*:  $p < 0.001$ . AP, action potential; DA, dopaminergic;  $K_{ATP}$ , ATP-dependent potassium channel; SF-1, steroidogenic factor 1.

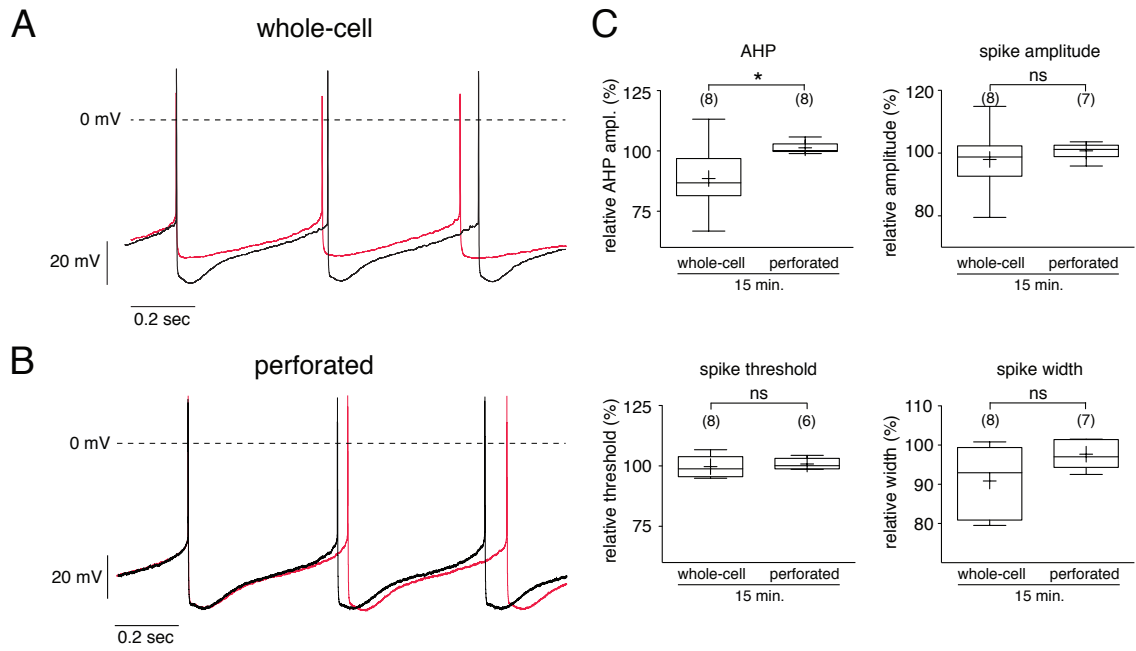


**Figure 3.2:** Comparison of spike-related parameters during whole cell and perforated-patch recordings. (A) Overlay of current clamp traces of a whole cell recording at the beginning of the experiment (*black*) and after a period of 15 min. (*red*). Note the decrease in AHP amplitude after 15 min. (B) Overlay of current clamp traces of a perforated-patch recording at the beginning (*black*) and after a period of 15 min. (*red*). No changes in spike form were observed during the time period. (C) Comparison of spike parameters of whole cell and perforated recordings after 15 min. recording time. Data are normalized to initial control values (0 min.). For details on box plots see Materials and Methods. \*:  $p \leq 0.05$ . AHP, afterhyperpolarization.

### 3.1.2 Technical considerations

Since the aforementioned results clearly showed that the whole cell configuration did not produce reliable results, the perforated-patch configuration was used on a daily basis for the majority of experiments. Despite the technical similarities of both configurations, there are a few peculiarities which should be taken into account when using the perforated-patch configuration. After formation of a giga-seal, on-cell spikes could be observed. Due to the incorporation of ionophores into the membrane patch the recording situation gradually changed from on-cell to the perforated-patch configuration which was reflected in a decrease in series resistance and an increase in spike amplitude (figure 3.3A). A perforated-patch recording was regarded as stable when no further change in spike amplitude and membrane potential occurred (figure 3.3A *right arrow*). When a perforated-patch recording changed to the whole cell configuration, an abrupt increase in spike amplitude became evident (figure 3.3B *arrow*). Since the pipette solution did not contain ATP, the spontaneous disruption of the membrane patch was also often followed by a hyperpolarization of the neuron (due to  $K_{ATP}$ -channel activation).

Conversion from perforated-patch to the whole cell configuration might not always be reflected in obvious changes of the aforementioned electrophysiological parameters. Strauss *et al.* (2001) showed that a fluorescent dye in the pipette solution improves the control of the perforated-patch recordings. Therefore, pipettes were backfilled with a tetraethylrhodamine-dextran-containing solution allowing to visually check the integrity of the membrane patch. Due to its molecular weight of 3000 Da, tetraethylrhodamine-dextran can neither permeate through the cell membrane nor the pores made by the ionophores. The *upper panel* of figure 3.3C shows an intact membrane (*white arrow-head*) during a perforated-patch recording. After spontaneous rupture of the membrane the neuron is immediately filled with the fluorescent dye (figure 3.3C *lower panel*). Taken together, the combination of electrophysiological and visual criteria makes it possible to reliably use the perforated-patch technique.

### 3.1.3 Ionophores

Three antibiotic ionophores (nystatin, amphotericin B, gramicidin) were tested for their performance on a daily basis. Due to a more elaborate preparation process for nystatin-containing intracellular solutions which involves the use of methanol as solvent and several adjustments of the pH of the nystatin-containing solution, nystatin was discarded as an ionophore for further experiments.

Eventually, amphotericin B and gramicidin were chosen as pore-forming agents. As

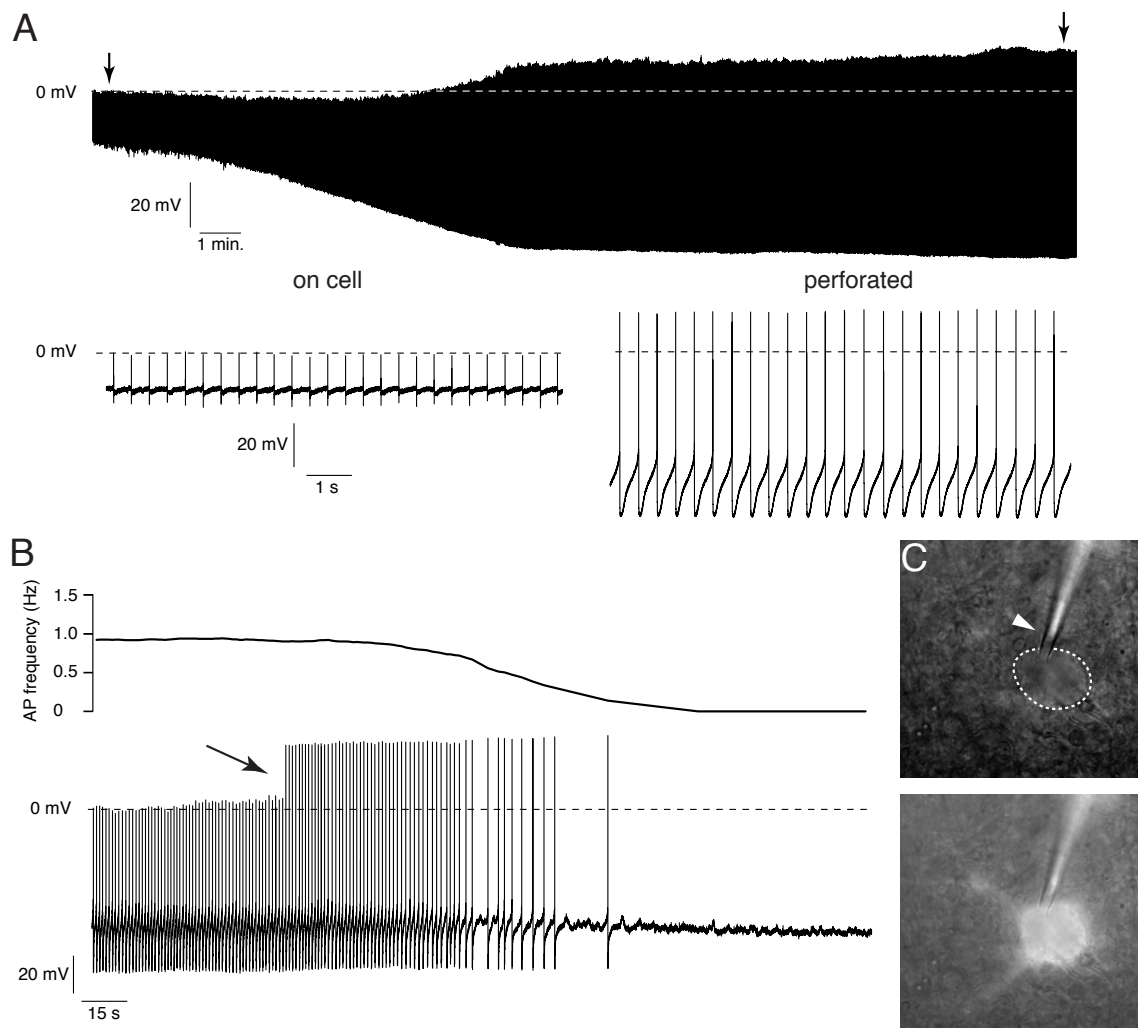


**Figure 3.3:** Overview of the perforated-patch configuration. **(A)** Representative trace showing the transition from 'on-cell' to the 'perforated-patch' configuration in a dopaminergic midbrain neuron. The arrows correspond to the sections displayed below. **(B)** Example of the spontaneous conversion from perforated-patch to the whole cell configuration. The arrow marks the jump in spike amplitude due to break-through of the membrane patch. **(C)** Tetraethylrhodamin-dextran signal showing the integrity of the membrane patch (*upper panel*) and after break-through (*lower panel*)

**Table 3.2:** Comparison of the effects of amphotericin B and gramicidin on spike parameters of mesencephalic DA neurons

	<b>Amphotericin B</b>	<b>Gramicidin</b>
<b>Firing Rate (Hz)</b>	$2.2 \pm 0.3$ ( $n = 13$ )	$2.5 \pm 0.2$ ( $n = 8$ )
<b>Input resistance (M<math>\Omega</math>)</b>	$354.1 \pm 55.1$ ( $n = 8$ )	$318.7 \pm 37.4$ ( $n = 6$ )
<b>Firing Threshold (mV)</b>	$-42.2 \pm 1.0$ ( $n = 8$ )	$-42.5 \pm 1.5$ ( $n = 6$ )
<b>AHP amplitude (mV)</b>	$31.5 \pm 2.1$ ( $n = 8$ )	$28.9 \pm 1.4$ ( $n = 6$ )

Data are given as mean  $\pm$  S.E.M. AHP, afterhyperpolarization. none of the investigated parameters differed significantly between neurons recorded with amphotericin B and gramicidin.

already described in section 1.6.2, amphotericin B and gramicidin are very similar regarding their biophysical properties except for the chloride permeability. While amphotericin B possesses a slight permeability for Cl<sup>-</sup>-ions, gramicidin pores are impermeable for Cl<sup>-</sup>-ions. The analysis of AP frequency, membrane resistance, AHP amplitude, firing threshold showed no obvious differences between recordings with amphotericin B or gramicidin (see table 3.2). Additionally, neither cell shrinking nor swelling could be observed during perforated patch recordings with amphotericin B further suggesting that the chloride concentration which was used for the intracellular solution was in the same range as the physiological chloride concentration.

## 3.2 Regulation of SF-1 neurons in the ventromedial hypothalamus by fuel sensing signals

The effect of the adiposity signal insulin was determined in SF-1 neurons which are a subpopulation of VMH neurons (figure 3.4A). As reported previously, mice lacking SF-1 neurons develop massive obesity resulting from both hyperphagia and reduced energy expenditure, demonstrating the importance of SF-1 neurons in control of energy homeostasis (Majdic *et al.* , 2002).

The role of insulin signaling in SF-1 neurons in control of energy homeostasis was investigated using mice with a cell-specific ablation of the insulin receptor (IR) in SF-1 neurons (SF-1<sup>ΔIR</sup>). On a normal chow diet (NCD), energy homeostasis related parameters like body weight and glucose homeostasis did not change in SF-1<sup>ΔIR</sup> mice in comparison to control animals. However, SF-1<sup>ΔIR</sup> mice on a high-fat diet (HFD) are protected against diet-induced leptin resistance, weight gain, adiposity and impaired glucose tolerance (Klöckener *et al.* , 2011).

Here, the role of insulin in SF-1 neurons was investigated in greater detail on a cell-specific and network level.

### 3.2.1 Properties of SF-1 neurons

VMH neurons are a heterogeneous neuron population which can be distinguished based on their electrophysiological properties (Miki *et al.* , 2001). SF-1 neurons were identified by their GFP fluorescence and recorded in the perforated-patch configuration. Subsequent analysis of basic electrophysiological properties revealed a large variability (see table 3.3).

Based on their response to hyperpolarizing current injections, SF-1 neurons could be divided into four groups (type A – D; see figure 3.4B). In type A neurons the firing frequency before and after a 1 s hyperpolarizing current injection remained largely unchanged, whereas type B neurons showed a phasic increase in firing frequency (rebound). In type C neurons the membrane potential repolarized with a delay after the 1 sec. hyperpolarization. Type D neurons had a slightly more hyperpolarized resting membrane potential and produced low-threshold spikes upon membrane hyperpolar-

**Table 3.3:** Functional properties of SF-1 neurons (SF-1<sup>GFP</sup>)

	Capacitance (pF)	AP frequency (Hz)	Membrane potential (mV)	Input resistance (GΩ)
<b>mean ± SEM</b>	12.5 ± 3.8	3.5 ± 1.8	−46.8 ± 3.7	1.24 ± 0.44
<b>minimum</b>	6	0.8	−51.6	0.52
<b>maximum</b>	20.5	7.3	−39.2	2.11
<i>n</i>	14	13	14	14

ization. Except for type D, all neuron phenotypes have been previously described in unidentified VMH neurons (Miki *et al.* , 2001).

An example for the morphology of SF-1 neurons is given in figure 3.4C. Biocytin-staining and subsequent reconstruction revealed that SF-1 neurons project to the ARC as well as the DMH. Moreover, SF-1 neurons have arborizations in the area between ARC and VMH, a region which had previously been described as the potential site of interaction between VMH neurons ARC neurons (Sternson *et al.* , 2005; van den Pol & Cassidy, 1982).

To summarize, SF-1 neurons are a heterogeneous subpopulation of VMH neurons which connect the VMH to the ARC. Additionally, SF-1 neurons project to regions of the hypothalamus which are believed to contain second order neurons of the melanocortin system.

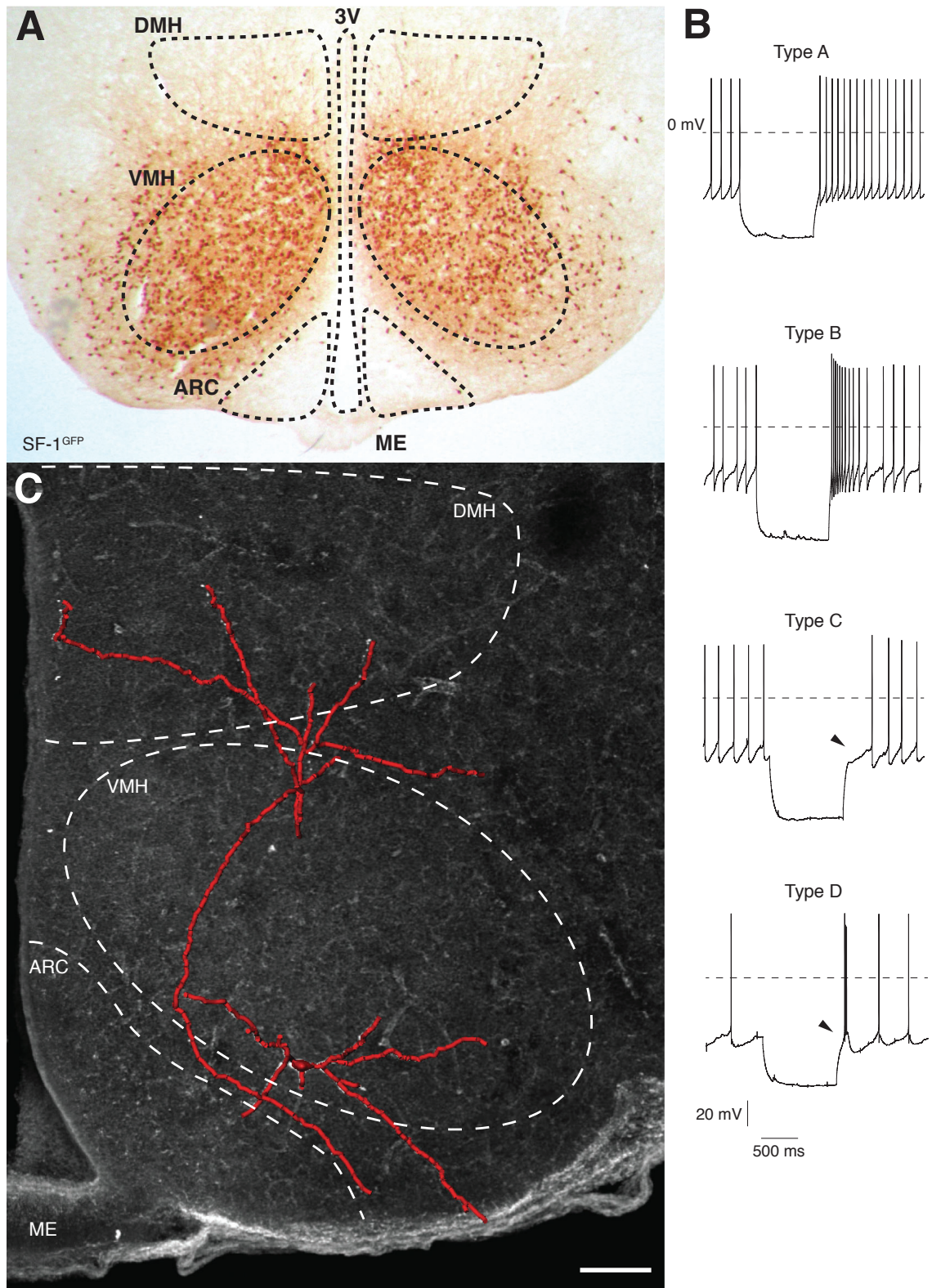


**Figure 3.4:** Electrophysiological properties and morphology of SF-1 neurons. (A) Immunohistochemistry for GFP which labels SF-1 neurons in the VMH of SF-1<sup>GFP</sup> mice (modified from Klöckener *et al.*, 2011; 3V, third ventricle; ARC, arcuate nucleus; DMH, dorsomedial hypothalamus; ME, median eminence; VMH, ventromedial hypothalamus). (B) Four different types of SF-1 neurons were identified based on the membrane voltage response to 1 s current injection to hyperpolarize the cell to  $\sim -90$  mV. Type C arrowhead: repolarization delay; type D arrowhead: low-threshold spike. (C) Amira<sup>®</sup> reconstruction of a biocytin-filled SF-1 neuron (red). Note the projections to the ARC and DMH. (scale: 100  $\mu$ m).

### 3.2.2 Insulin hyperpolarizes and decreases the firing rate of SF-1 neurons

The effect of insulin on SF-1 neurons was investigated in wildtype SF-1 neurons (SF-1<sup>GFP</sup>, SF-1<sup>LacZ</sup>) and SF-1 neurons lacking the insulin receptor (IR; SF-1<sup>GFP:ΔIR</sup>, SF-1<sup>LacZ:ΔIR</sup>). Insulin is known to activate the PI3K pathway which leads to the production of PIP<sub>3</sub> (see section 1.2). Immunohistochemical analysis for PIP<sub>3</sub> was performed in mice which selectively express  $\beta$ -galactosidase (LacZ) in SF-1 neurons. Mice were intravenously injected with insulin. 20 min after insulin stimulation, a strong PIP<sub>3</sub> immunoreactivity could be detected in  $\sim$ 40% of SF-1 neurons of SF-1<sup>LacZ</sup> mice suggesting that PIP<sub>3</sub> formation was robustly activated. Thus, insulin leads to cell-autonomous formation of PIP<sub>3</sub> in SF-1 neurons following the activation of the PI3K pathway. In contrast, insulin failed to induce PIP<sub>3</sub> formation in SF-1 neurons of SF-1<sup>LacZ:ΔIR</sup> mice (Klöckener *et al.*, 2011; see figure 5.2 (Appendix)).

Perforated-patch recordings were performed in mice which selectively expressed GFP in SF-1 neurons (figure 3.4A; SF-1<sup>GFP</sup>, SF-1<sup>GFP:ΔIR</sup>). In both genotypes the basic biophysical properties such as whole cell capacitance, membrane potential, firing rate and input resistance were similar (table 3.4). Insulin inhibited approximately  $\sim$ 40% of the SF-1<sup>GFP</sup> neurons (figure 3.5A,C) when recordings were performed in the mediobasal VMH where most of the insulin-stimulated PIP<sub>3</sub>-formation was detectable (personal communication Tim Klöckener). The percentage of insulin responsive SF-1 neurons corresponds well to the percentage of SF-1 neurons which exhibited a strong PIP<sub>3</sub> immunoreactivity. This finding suggests that a strong activation of the PI3-kinase pathway is necessary to elicit an immediate electrophysiological response to insulin in SF-1 neurons. Upon insulin application, insulin-responsive neurons the membrane potential hyperpolarized from  $-48.2 \pm 0.7$  mV to  $-54.1 \pm 1.7$  mV ( $n = 6$ ;  $p < 0.05$ ; figure 3.5D (left)) and the firing rate decreased from  $2.2 \pm 0.5$  Hz to  $0.7 \pm 0.5$  Hz ( $n = 5$ ;  $p < 0.05$ ; figure 3.5D (right)). However, the responsiveness to insulin could not be correlated with the neuron types described in section 3.2.1 (data not shown). Co-application of tolbutamide, a specific  $K_{ATP}$ -channel antagonist, along with insulin reversed the membrane potential and firing rate to control values (figure 3.5A,D). None of the SF-1<sup>GFP:ΔIR</sup> neurons were

**Table 3.4:** Comparison of functional properties of SF-1<sup>GFP</sup> and SF-1<sup>GFP:ΔIR</sup> neurons.

Genotype	Capacitance (pF)	AP frequency (Hz)	Membrane potential (mV)	Input resistance (GΩ)
SF-1 <sup>GFP</sup>	12.5 ± 3.8 (n = 14)	3.5 ± 1.8 (n = 13)	-46.8 ± 3.7 (n = 14)	1.24 ± 0.44 (n = 14)
SF-1 <sup>GFP:ΔIR</sup>	16.4 ± 6.6 (n = 11)	2.9 ± 1.6 (n = 9)	-48.5 ± 6.1 (n = 12)	1.51 ± 0.78 (n = 11)
<i>t</i> - test	ns 0.08	ns 0.41	ns 0.39	ns 0.29

inhibited by insulin (0 of 12; figure 3.5B, C, E). Note that insulin induced excitation in one of the SF-1<sup>GFP</sup> neurons and two of the SF-1<sup>GFP:ΔIR</sup> neurons.

Taken together, the results indicate that insulin activates the PI3K pathway in SF-1 neurons and that insulin hyperpolarizes the membrane potential and decreases the firing rate of a subset of SF-1 neurons by opening  $K_{ATP}$ -channels. Therefore, insulin signaling in SF-1 neurons is likely to act by the same mechanism as described for POMC neurons of the ARC (Plum *et al.*, 2006a) or pancreatic  $\beta$ -cells (Khan *et al.*, 2001).

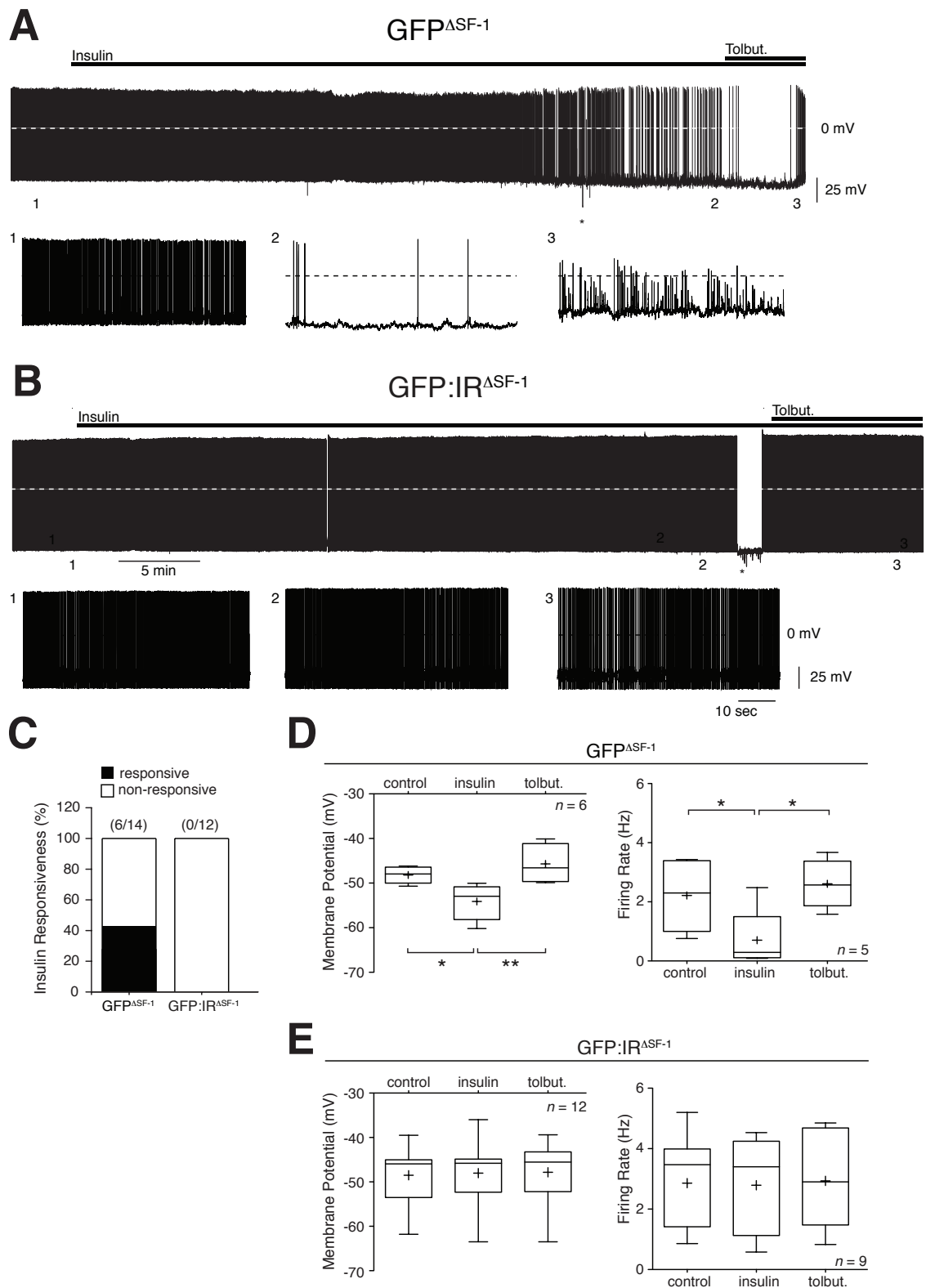


**Figure 3.5:** Insulin effect on SF-1 neurons. (**A,B**) Representative recordings of identified insulin responsive SF-1-positive neurons of a SF-1<sup>GFP</sup> mouse (**A**) and a SF-1<sup>GFP:ΔIR</sup> mouse (**B**) before and during addition of 200 nM insulin, followed by application of 200 μM tolbutamide. (**C**) Percentage of insulin-responsive SF-1 neurons from SF-1<sup>GFP</sup> mice and SF-1<sup>GFP:ΔIR</sup> mice. (**D**) Membrane potential (left) and firing (right) of identified SF-1 neurons from SF-1<sup>GFP</sup> mice before and during application of 200 nM insulin, followed by addition of 200 μM tolbutamide. (**E**) Membrane potential (left) and firing (right) of identified SF-1 neurons from SF-1<sup>GFP:ΔIR</sup> mice before and during application of 200 nM insulin, followed by addition of 200 μM tolbutamide. For details on box plots see Materials and Methods. \*:  $p \leq 0.05$ ; \*\*:  $p \leq 0.01$ .

### 3.2.3 Ablation of insulin receptors in SF-1 neurons alters synaptic connectivity in HFD mice

Unidentified VMH neurons have been reported to provide glutamatergic input on POMC neurons of the ARC (Sternson *et al.*, 2005). Biocytin-stainings of individual SF-1 neurons revealed that SF-1 neurons also innervate the area between the VMH and ARC which is thought to function as a 'relay' between VMH and ARC neurons (for an example see figure 3.4C), suggesting that SF-1 neurons might provide synaptic input to POMC neurons. To elucidate the nature of the microcircuit of SF-1 and POMC neurons and to investigate the impact of insulin signaling on the network level, measurements of postsynaptic currents in POMC neurons were performed. Because insulin signaling dependent alterations in several energy homeostasis related parameters become evident when mice are given a high-fat diet (HFD; see section 3.2), measurements were performed using POMC<sup>GFP</sup> and POMC<sup>GFP</sup>;SF-1<sup>ΔIR</sup> HFD mice.

In HFD mice in which the insulin receptor (IR) was inactivated in SF-1 neurons the IPSC frequency measured in POMC neurons was lower than in control HFD animals (POMC<sup>GFP</sup>:  $2.3 \pm 0.4$  Hz;  $p < 0.05$ ; POMC<sup>GFP</sup>;SF-1<sup>ΔIR</sup>:  $1.1 \pm 0.3$  Hz; figure 3.6C). The EPSC frequency did not differ between POMC neurons of POMC<sup>GFP</sup> and POMC<sup>GFP</sup>;SF-1<sup>ΔIR</sup> mice (POMC<sup>GFP</sup>:  $0.7 \pm 0.2$  Hz; POMC<sup>GFP</sup>;SF-1<sup>ΔIR</sup>:  $1.2 \pm 0.4$  Hz; figure 3.6C).

Comparison of absolute frequencies might lead to misinterpretations in terms of the actual ratio between inhibitory and excitatory input for individual neurons. The ratio of the IPSC to EPSC frequency was calculated for every investigated neuron, revealing that the relative contribution of the excitatory input is significantly increased in POMC neurons of POMC<sup>GFP</sup>;SF-1<sup>ΔIR</sup> mice. (POMC<sup>GFP</sup>:  $0.29 \pm 0.05$ ; POMC<sup>GFP</sup>;SF-1<sup>ΔIR</sup>:  $0.51 \pm 0.09$ ;  $p < 0.05$ ; figure 3.6D).

Thus, cell-specific ablation of the IR in SF-1 neurons promotes the increase of excitatory drive on POMC neurons of the ARC.

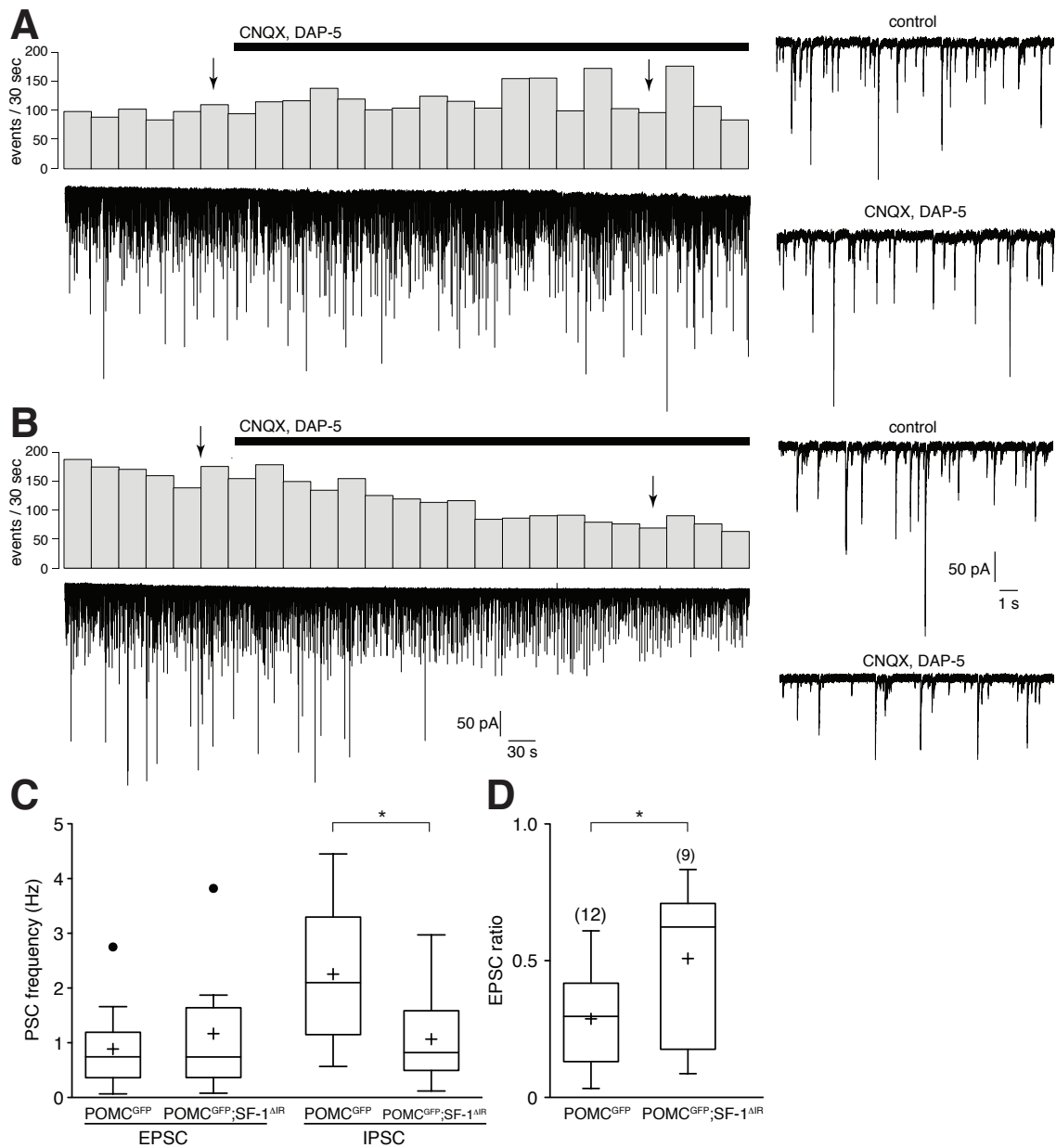


**Figure 3.6:** Alterations in synaptic connectivity in POMC neurons of POMC<sup>GFP</sup>;SF-1<sup>DeltaIR</sup> on a high-fat-diet. **(A, B)** Representative traces of postsynaptic currents of POMC neurons in POMC<sup>GFP</sup> **(A)** and POMC<sup>GFP</sup>;SF-1<sup>ΔIR</sup> HFD mice **(B)**. Arrowheads mark the position of the current sections in the right panel. **(C)** Absolute excitatory and inhibitory frequencies of POMC neurons in POMC<sup>GFP</sup> and POMC<sup>GFP</sup>;SF-1<sup>ΔIR</sup> HFD mice. **(D)** Contribution of excitatory synaptic input relative to the total synaptic input on POMC neurons. For details on box plots see Materials and Methods. \*:  $p \leq 0.05$ .

### 3.3 Regulation of mesencephalic dopaminergic midbrain neurons by fuel sensing signals

In the previous chapters the role of insulin signaling in SF-1 neurons, a subpopulation of hypothalamic neurons in control of energy homeostasis, was thoroughly investigated. Only recently, evidence has emerged that fuel sensing signals such as the peripheral hormones leptin, insulin and ghrelin might also exert direct effects on other neural circuits, such as the dopaminergic (DA) system which is implicated in mediating reward behavior and motivational aspects of feeding behavior (Figlewicz & Benoit, 2009).

To investigate the role of insulin signaling in mesencephalic DA neurons located in the substantia nigra *pars compacta* (SNpc) as well as the ventral tegmental area (VTA), mice with a cell-specific deletion of the IR in tyrosine hydroxylase (Th) expressing neurons (Th<sup>ΔIR</sup>) were generated. Ablation of the IR in Th-positive neurons results in increased body weight, increased fat mass, and hyperphagia. Moreover, under food-restricted conditions the response to the motor-activating effects of cocaine is altered in Th<sup>ΔIR</sup> mice compared to wildtype mice (Könner *et al.* , 2011). Taken together, these findings suggest an important role for insulin signaling in the DA circuitry as a potential link between the control of food intake and the reward circuitry.

To understand how these phenotypic alterations are mediated by insulin signaling, the effect of insulin on mesencephalic DA neurons was investigated in detail on the single cell level and the network level.

#### 3.3.1 Properties of mesencephalic dopaminergic neurons

For control measurements, a total amount of 60 neurons was recorded. Of these cells, the majority was located in the SNpc (88%). The remainder was recorded in the adjacent VTA (12 %). The electrophysiological data of SNpc and VTA neurons were pooled since they were not significantly different on the level of analysis used here (data not shown).

Putative DA neurons were identified using electrophysiological criteria which have been established in DA neurons in the SNpc (Grace & Onn, 1989; Lacey *et al.* , 1989; Liss *et al.* , 1999; Richards *et al.* , 1997; Uchida *et al.* , 2000; Yung *et al.* , 1991). The

main criteria which were used to identify DA neurons are: 1.) large cell bodies with bipolar and multipolar somata shapes (figure 3.7B), 2.) spontaneous, low frequency ( $\sim 2 - 4$  Hz) pacemaker-like activity (figure 3.7A), 3.) broad action potentials (APs) with large afterhyperpolarizations (AHPs), 4.) a large hyperpolarization-activated current ( $I_h$ ; figure 3.7C) and 5.) inhibition by dopamine which is caused by the activation of a  $D_2$ -autoreceptor ( $D_2R$ ) linked G-protein activated potassium conductance (GIRK; figure 3.7D).

However, it has been reported that the aforementioned criteria do not reliably predict DA neurons in the VTA (Margolis *et al.*, 2006). Since there is a general agreement that GABAergic (non-DA) neurons do not have an  $I_h$  (Cameron *et al.*, 1997; Jones & Kauer, 1999) and only a small number of VTA neurons were used in this study the contribution of TH-negative (non-DA) neurons to the observed effects presented in the thesis is likely to be very small and therefore not regarded as problematic.

DA neurons which were identified using the aforementioned criteria had large cell bodies (membrane capacitance:  $49.8 \pm 0.9$  pF,  $n=45$ ) and exhibited a membrane conductance density of  $58.5 \pm 2.7$  pS/pF ( $n=36$ ). 85% were spontaneously active ( $2.3 \pm 0.1$  Hz,  $n=51$ ) and fired in a regular pacemaker-like manner. The precision of the pacemaker was estimated by calculating the coefficient of variation (CV; see Materials and Methods) which was only  $12.0 \pm 1.0\%$  ( $n=31$ ) of the mean interspike interval (ISI), which is in line with previous studies (Wolfart *et al.*, 2001). The spike-related parameters were also in the previously reported range for mesencephalic DA neurons (spike threshold:  $-42.7 \pm 0.5$  mV,  $n=31$ ; spike width:  $2.0 \pm 0.1$  ms,  $n=21$ ; AHP amplitude:  $32.0 \pm 0.9$  mV,  $n=31$ ; Richards *et al.*, 1997; Yung *et al.*, 1991).

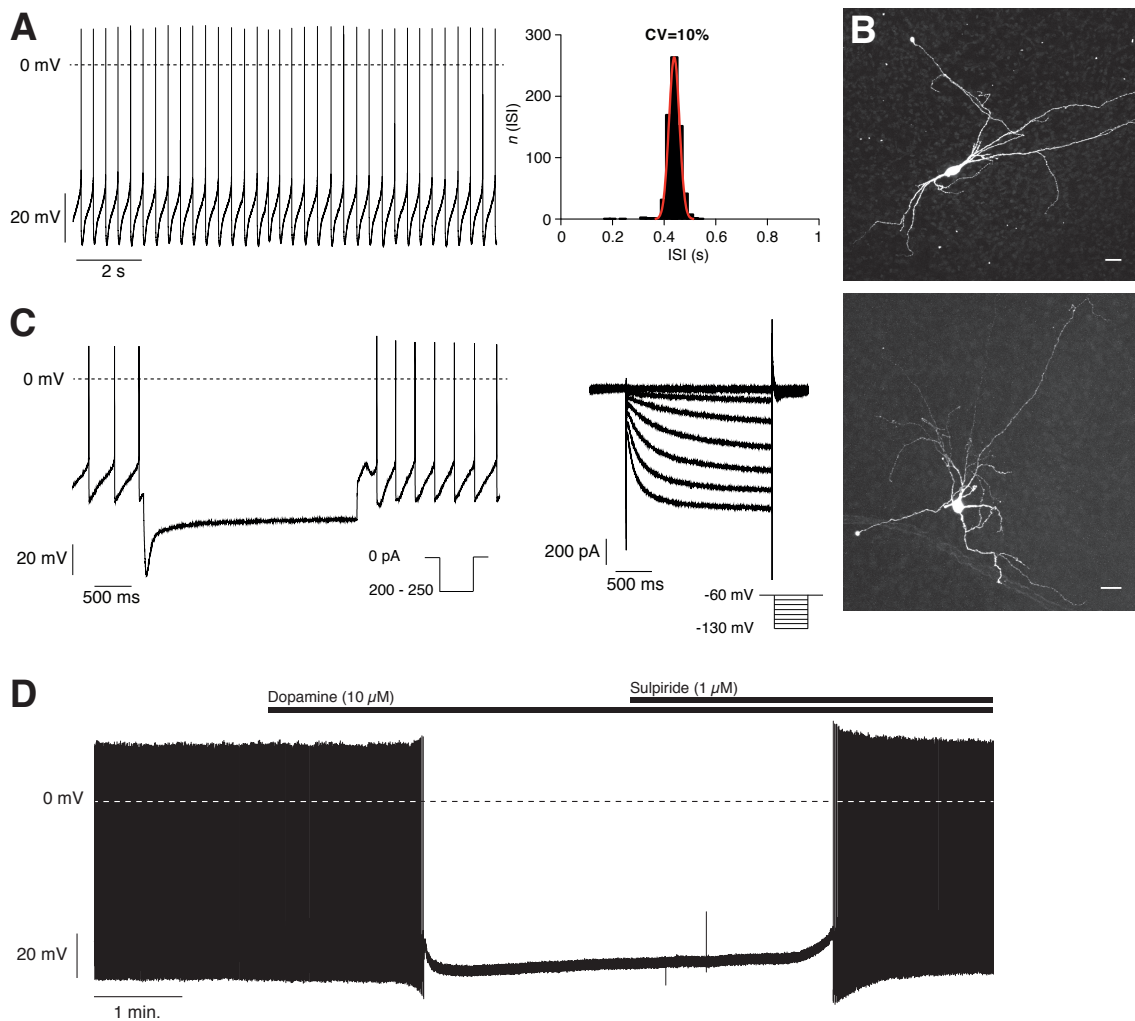


**Figure 3.7:** Electrophysiological properties and morphology of mesencephalic DA neurons. (A) *Left panel*, Representative current-clamp recording of a DA neuron and the corresponding ISI histogram (*right panel*). The ISI frequency distribution was fit with a single Gaussian function (*red line*) which was used to calculate the coefficient of variation (CV). (B) *Upper and lower panel* Biocytin-stainings of two DA neurons showing different projection patterns. scale bar 20  $\mu\text{m}$ . (C) *Left panel* Membrane voltage response to 3s current injection to initially hyperpolarize the cell to  $\sim -120$  mV revealing a large 'sag' component which is mediated by the activation of  $I_h$ . *Right panel* Voltage-clamp recording demonstrating the large  $I_h$  in DA neurons.  $I_h$  was evoked with voltage steps from -60 mV to -130 mV. (D) Current-clamp recording of a DA neuron before and during application of dopamine (10  $\mu\text{M}$ ) demonstrating the inhibitive effect of dopamine on DA neurons. Subsequent application of the D2R-specific antagonist (-)-sulpiride (1  $\mu\text{M}$ ) leads to a complete recovery of membrane potential and firing frequency. CV, coefficient of variation; D2R, D<sub>2</sub> receptor; DA, dopamine;  $I_h$ , hyperpolarization-activated current; ISI, interspike interval.

### 3.3.2 Insulin activates the PI3-kinase pathway and increases the activity of mesencephalic dopaminergic neurons

The impact of insulin signaling on DA mesencephalic neurons was analyzed in mice lacking the IR specifically in TH-expressing cells ( $\text{Th}^{\text{LacZ}:\Delta\text{IR}}$ ,  $\text{Th}^{\Delta\text{IR}}$ ) and their wildtype littermates ( $\text{Th}^{\text{LacZ}}$ ,  $\text{Th}^{\text{fl/fl}}$ ).

First, the number of Th-positive neurons in the SNpc and the VTA was compared between control and  $\text{Th}^{\Delta\text{IR}}$  mice to address whether ablation of the IR has an influence on the development and/or maintenance of mesencephalic DA neurons. Ablation of the IR does not change the number of Th-positive neurons (figure 3.8A,B; Könnner *et al.* , 2011). Previous studies have shown that insulin activates the PI3K pathway in a variety of brain regions, i.e. the ventromedial hypothalamus or the nucleus arcuatus (Klöckener *et al.* , 2011; Plum *et al.* , 2006a). Since activation of the PI3K pathway could also be observed in the VTA (Figlewicz *et al.* , 2007), the effect of TH-neuron specific IR-deficiency was investigated in mice which selectively express  $\beta$ -galactosidase (LacZ) in TH-expressing neurons ( $\text{Th}^{\text{LacZ}:\Delta\text{IR}}$ ,  $\text{Th}^{\text{LacZ}}$ ). Immunohistochemical analysis for  $\text{PIP}_3$  revealed that  $\text{PIP}_3$  formation was strongly activated in  $\sim 50\%$  of mesencephalic DA neurons of control mice 10 min after intravenous insulin stimulation (figure 3.8C,D *upper panels*; Könnner *et al.* , 2011). In contrast, insulin failed to induce  $\text{PIP}_3$  formation in Th-positive neurons of  $\text{Th}^{\Delta\text{IR}}$  mice whereas  $\text{PIP}_3$  formation in Th-negative neurons remained unaltered (figure 3.8 C,D *lower panels*; Könnner *et al.* , 2011).

Taken together, these data show that insulin is able to efficiently activate the PI3K signal cascade in mesencephalic DA neurons of control mice and that insulin signaling is specifically inactivated in IR-deficient midbrain DA neurons.

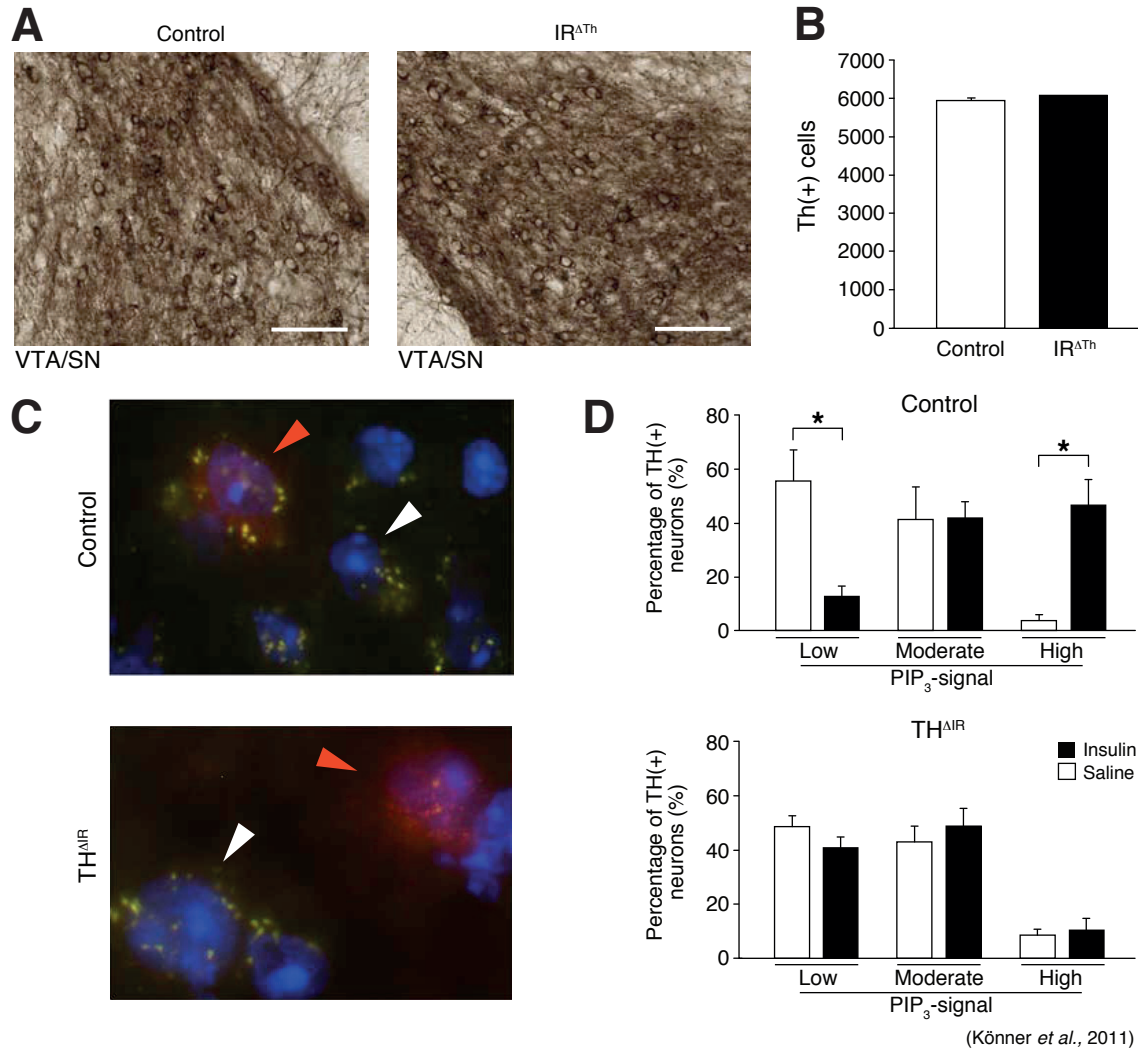


**Figure 3.8:** Immunohistochemical characterization of Th-positive neurons of Th<sup>ΔIR</sup> and control mice. (A) Representative sections from control and Th<sup>ΔIR</sup> animals. Scale bar: 50 μm. (B) Quantification of the total numbers of Th-expressing neurons in control and Th<sup>ΔIR</sup> animals. (C) Double immunohistochemistry for lacZ and PIP<sub>3</sub> in neurons of Th<sup>LacZ</sup> and Th<sup>LacZ:ΔIR</sup> reporter mice. A representative section is shown. Blue (DAPI), DNA; red, β-gal (Th-expressing neurons); green, PIP<sub>3</sub>. Red arrowhead, Th-expressing neuron; white arrowhead, Th-negative neuron. (D) Quantification of PIP<sub>3</sub> immunoreactivity of Th-expressing neurons in Th<sup>LacZ</sup> (upper panel) and Th<sup>LacZ:ΔIR</sup> (lower panel) reporter mice after saline or insulin stimulation for 10 min. (Modified from Könner *et al.*, 2011).

Perforated-patch recordings were performed in IR-deficient Th<sup>ΔIR</sup> mice and control littermates. The spontaneous spike frequency was not different between control and Th<sup>ΔIR</sup> DA neurons (controls:  $2.1 \pm 0.2$  Hz,  $n=25$ ; IR<sup>ΔTh</sup>:  $1.8 \pm 0.2$  Hz,  $n=27$ ;  $p > 0.05$ ; data not shown). In  $\sim 59\%$  (10 out of 17) of control midbrain DA neurons insulin (200 nM) significantly increased the spike frequency from  $2.1 \pm 0.4$  Hz to  $2.9 \pm 0.5$  Hz ( $p < 0.01$ ; figure 3.9A,B). The percentage of insulin-responsive neurons is in the same range as the percentage of DA neurons which have exhibited a strong PIP<sub>3</sub> immunoreactivity suggesting that a strong activation of the PI3K pathway mediates the immediate electrophysiological response to insulin in DA neurons. In contrast, in DA neurons of IR<sup>ΔTh</sup> mice the spike frequency did not change significantly (control:  $1.9 \pm 0.4$  Hz; insulin:  $1.9 \pm 0.4$  Hz,  $n=10$ ,  $p > 0.05$ ; figure 3.9A,C) and only one neuron out of ten responded to insulin (figure 3.9C,D).

Analysis of synaptic input revealed decreased excitatory postsynaptic currents (EPSC) frequency in IR<sup>ΔTh</sup> DA neurons as compared to control DA neurons (controls:  $2.2 \pm 0.2$  Hz,  $n=6$ ; IR<sup>ΔTh</sup>:  $1.0 \pm 0.3$  Hz,  $n=6$ ;  $p < 0.01$ ; figure 3.9E) while the frequency of the inhibitory postsynaptic currents (IPSCs) was unaltered (controls:  $3.2 \pm 0.5$  Hz,  $n=6$ ; IR<sup>ΔTh</sup>:  $3.3 \pm 0.5$  Hz,  $n=6$ ;  $p > 0.05$ ; data not shown). Furthermore, the ratio of the EPSC frequency relative to the total PSC frequency was calculated for every investigated neuron. The relative contribution of the excitatory input is also significantly decreased in DA neurons of Th<sup>ΔIR</sup> mice compared to DA neurons of control animals (control:  $41.6 \pm 1.6\%$ ,  $n=6$ ; Th<sup>ΔIR</sup>:  $22.3 \pm 7.1\%$ ,  $n=6$ ;  $p < 0.05$ ).

Taken together the results show that insulin modulates the intrinsic firing properties in a subset of midbrain DA neurons. Furthermore, the IR pathway is involved in the establishment or maintenance of excitatory synaptic connections in midbrain DA neurons or in increasing the activity of excitatory presynaptic neurons.

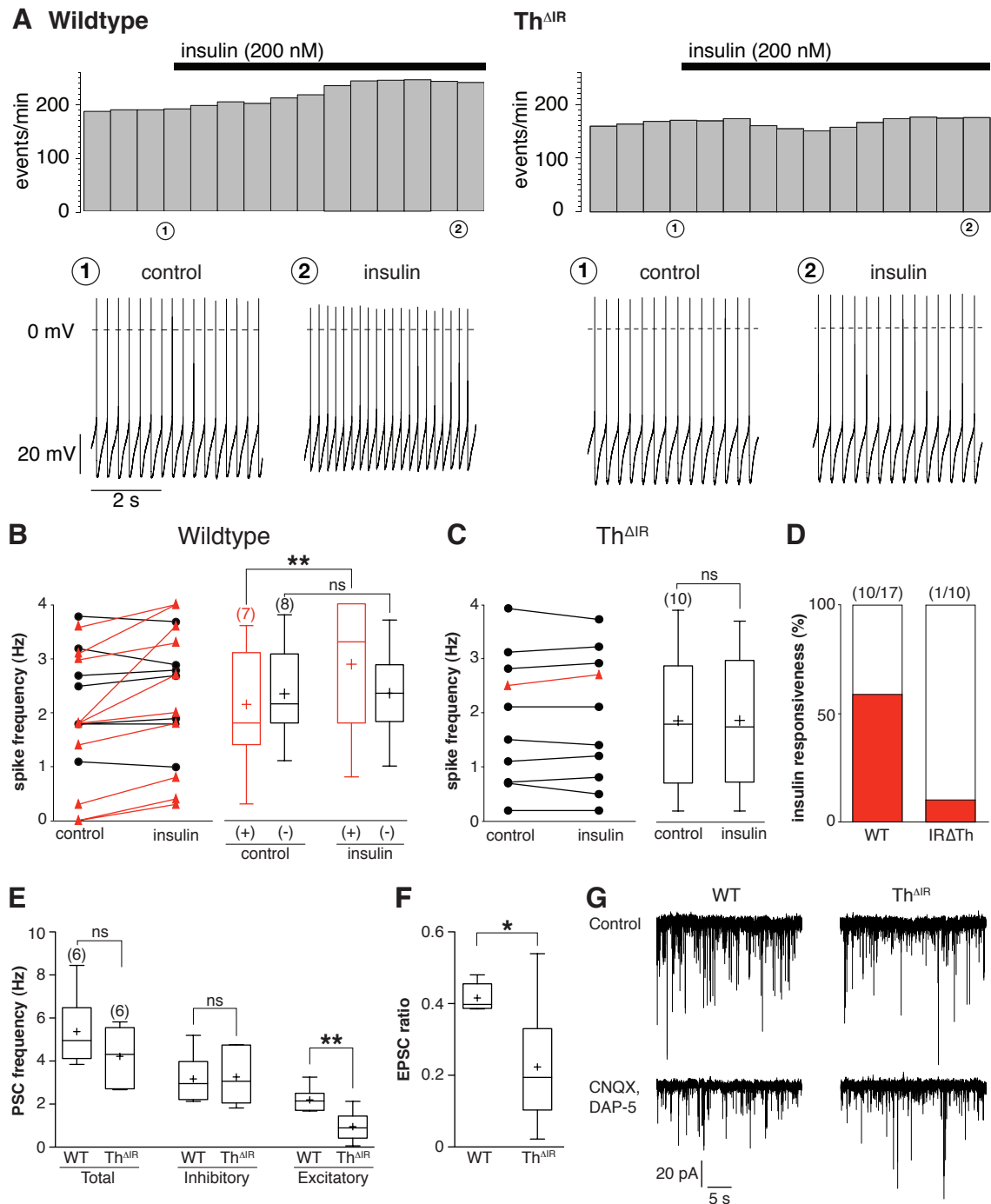


**Figure 3.9:** Insulin increases the activity of mesencephalic DA neurons. **(A) Top:** Peristimulus time histogram (bin width: 60 sec) of recordings from a control (*left*) and an Th<sup>ΔIR</sup> neuron (*right*) during insulin (200 nM) application. **Bottom:** original traces from the recordings shown above at two different time points (indicated by numbers). **(B,C)** Effect of insulin on the spike frequency of mesencephalic DA neurons from control mice **(B)** and Th<sup>ΔIR</sup> mice **(C)**. *Left panels:* Dots and triangles indicate the change in firing frequency of the individual neurons (control:  $n=17$ ; Th<sup>ΔIR</sup>:  $n=10$ ). Red triangles, insulin-responsive cells according to the 3 times SD criterion (see Materials and Methods); black dots, non-responsive cells. *Right panels:* Change in absolute firing frequency in control and Th<sup>ΔIR</sup> animals. **(D)** Percentage of control (10/17) and Th<sup>ΔIR</sup> (1/10) neurons that responded to bath application with a significant increase in firing frequency. **(E)** Absolute frequencies of postsynaptic currents (PSCs) of DA neurons of control ( $n=6$ ) and Th<sup>ΔIR</sup> ( $n=6$ ) mice. **(F)** Contribution of excitatory synaptic input relative to the total synaptic input on DA neurons in control and Th<sup>ΔIR</sup> mice. **(G)** Representative traces of PSCs of DA neurons in control and Th<sup>ΔIR</sup> mice. For details on box plots see Materials and Methods. \*:  $p<0.05$ ; \*\*:  $p<0.01$ . DA, dopaminergic; SD, standard deviation.

### 3.3.3 The excitatory effect of insulin on mesencephalic dopaminergic neurons is cell-intrinsic

To rule out the possibility that the observed excitatory effect of insulin on mesencephalic DA neurons is indirectly caused by presynaptic effects, additional experiments were conducted under conditions where synaptic transmission was blocked. DA neurons were synaptically isolated by application of CNQX, DAP-5 (block of excitatory synaptic input) and picrotoxin (block of inhibitory synaptic input). These conditions lead to an increase in firing frequency, indicating that the net synaptic input on DA neurons is inhibitory (control:  $1.9 \pm 0.4$  Hz; synaptic blockers:  $2.2 \pm 0.4$  Hz;  $n=8$ ;  $p < 0.05$ ; data not shown). Subsequent application of insulin (200 nM) increased the firing frequency comparable to the experiments performed without blockers (control:  $2.3 \pm 0.4$  Hz; insulin:  $2.8 \pm 0.4$  Hz;  $n=6$ ;  $p < 0.001$ ). Moreover, the membrane conductance density decreased from  $53.0 \pm 6.4$  pS/pF (control) to  $42.3 \pm 3.9$  pS/pF during insulin application (200 nM;  $p < 0.05$ ;  $n=5$ ; figure 3.10A,B).

The analysis of the AP waveform before and during insulin application showed that there is a significant change in spike amplitude (control:  $87.1 \pm 4.0$  mV, insulin:  $81.3 \pm 3.8$  mV,  $n=5$ ,  $p < 0.01$ ), AHP amplitude (AHP; control:  $30.9 \pm 2.3$  mV, insulin:  $28.6 \pm 2.7$ ,  $n=5$ ,  $p < 0.05$ ) and AHP membrane potential (control:  $-71.4 \pm 2.6$  mV, insulin:  $-68.3 \pm 2.9$ ,  $n=5$ ,  $p < 0.01$ ; see table 3.5).

**Table 3.5:** Spike properties of mesencephalic DA neurons before and after insulin application

	Control	Insulin (200 nM)
<b>Threshold</b> (mV)	$-40.2 \pm 1.5$	$-39.0 \pm 2.1$
<b>Amplitude</b> (mV)	$87.1 \pm 4.0$	$81.3 \pm 3.8^{**}$
<b>Width</b> (ms)	$1.4 \pm 0.1$	$1.4 \pm 0.1$
<b>AHP Amplitude</b> (mV)	$30.9 \pm 2.3$	$28.6 \pm 2.7^*$
<b>E<sub>M</sub> of AHP</b> (mV)	$-71.4 \pm 2.6$	$-68.3 \pm 2.9^{**}$

Data are given as mean  $\pm$  S.E.M. AHP, afterhyperpolarization; E<sub>M</sub>, membrane potential.  
\*  $p < 0.05$ , \*\*  $p < 0.01$  – significantly different from control.

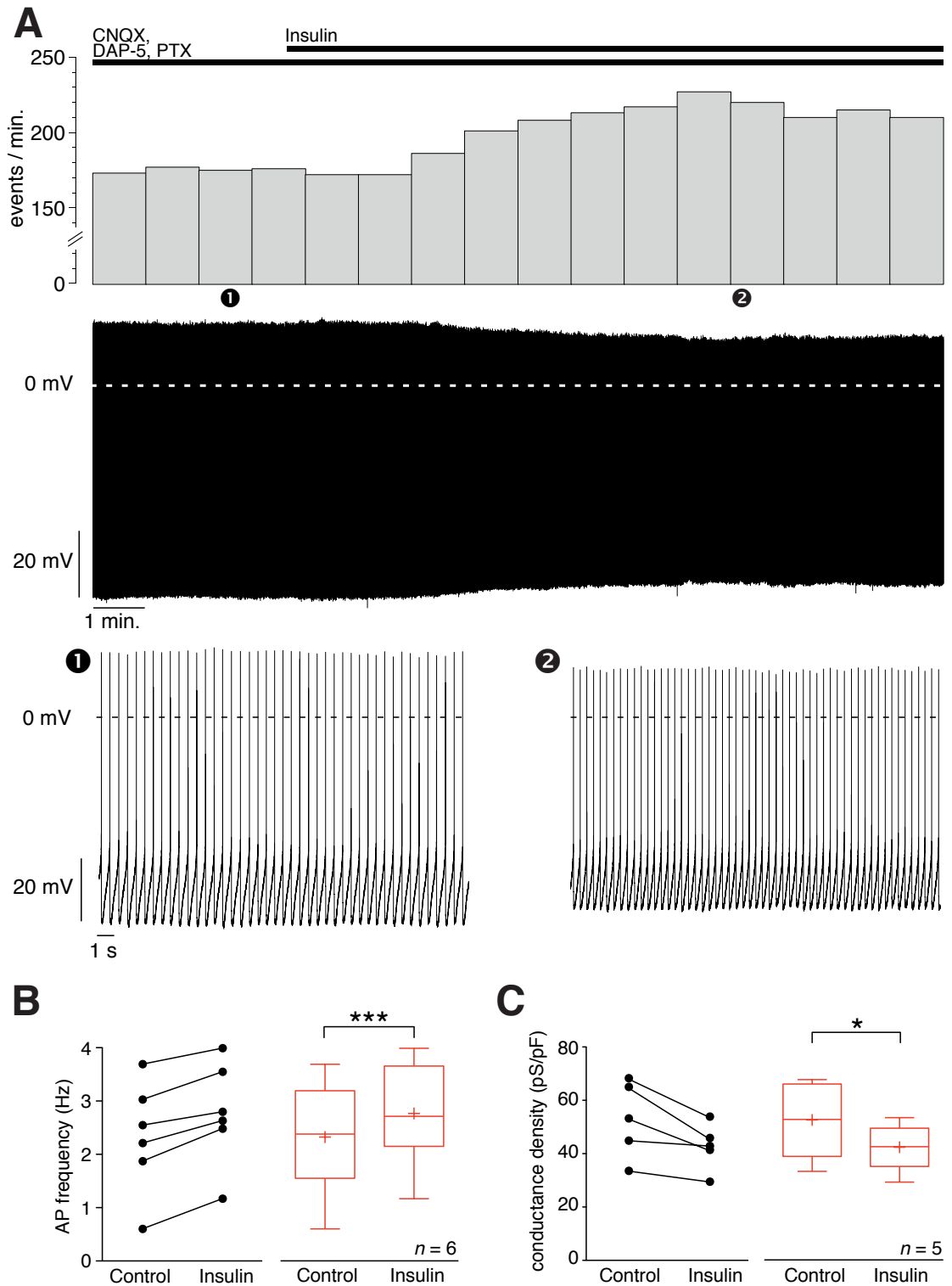


**Figure 3.10:** The insulin effect on mesencephalic DA neurons is cell-intrinsic. (A) Perforated-patch recording of a SNpc DA neuron which was isolated from synaptic input before and during insulin (200 nM) application. *Top:* Peristimulus histogram (bin width: 60s) of the perforated patch recording depicted in the *middle panel*. *Bottom:* Excerpts of the recording (*middle*) at two different time points indicated by numbers. (B,C) Effect of insulin (200 nM) on the spike frequency (B,  $n=6$ ) and conductance density (C,  $n=5$ ) of synaptically isolated SNpc DA neurons. For details on box plots see Materials and Methods. \*\*\*:  $p < 0.001$ , \*\*:  $p < 0.01$ , \*:  $p < 0.05$ , n.s.:  $p \geq 0.05$ . DA, dopaminergic; SNpc, substantia nigra pars compacta.

### 3.3.4 Wortmannin reverses the excitatory effect of insulin

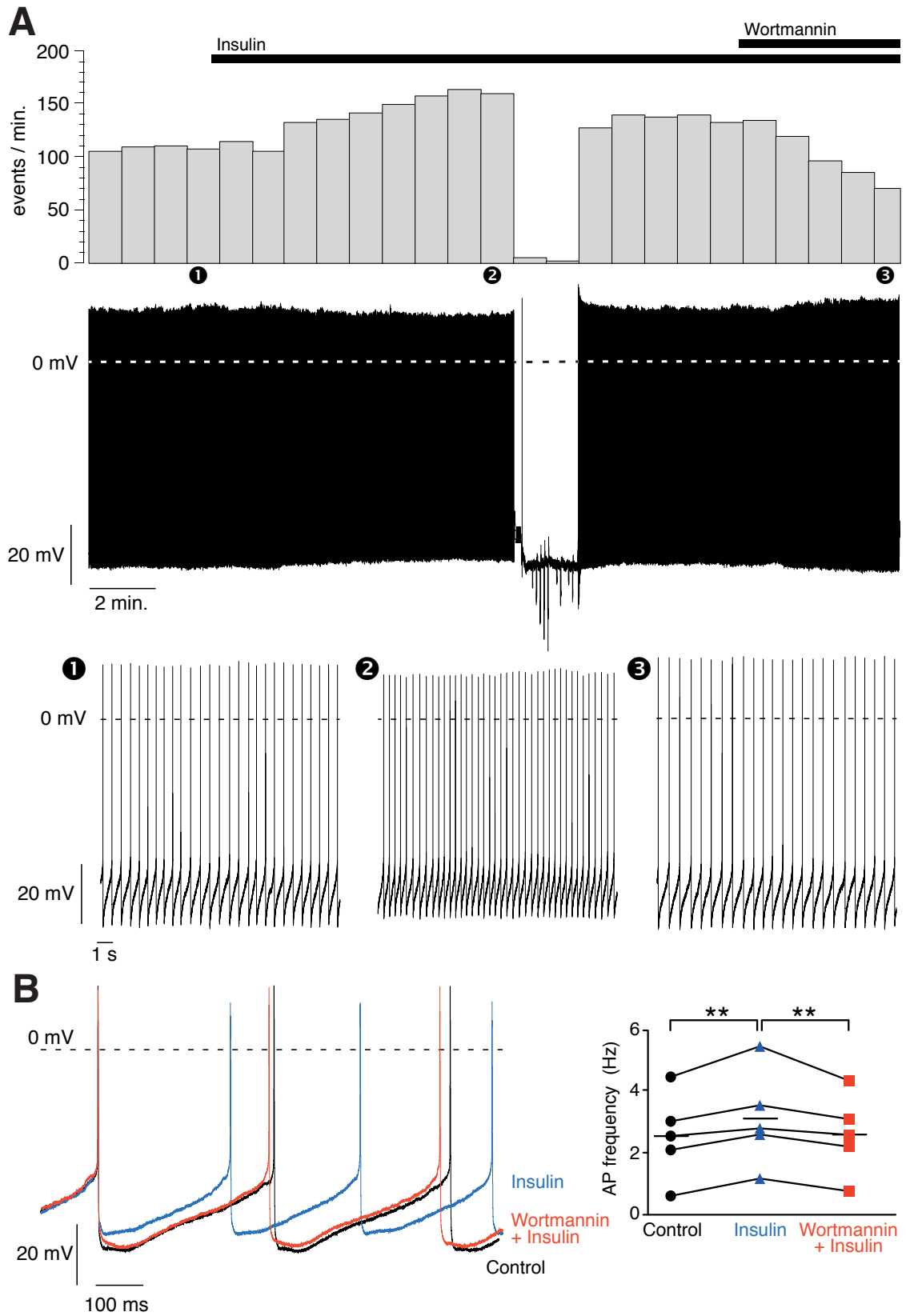
Immunohistochemical analysis revealed that insulin activates the PI3K pathway in DA neurons resulting in the formation of PIP<sub>3</sub> (figure 3.8B; Könnner *et al.* , 2011). To determine if the observed effect of insulin on the activity of DA neurons is mediated by the PI3K pathway, experiments with wortmannin (1  $\mu$ M), a specific inhibitor of PI3K, were conducted. Application of wortmannin along with insulin reversed the excitatory effect of insulin (control:  $2.6 \pm 0.6$  Hz, insulin:  $3.1 \pm 0.7$  Hz, wortmannin:  $2.6 \pm 0.6$  Hz,  $n=5$ ,  $p < 0.01$  [control vs. insulin, insulin vs. wortmannin]; figure 3.11C).

These results indicate that the activation of the PI3K pathway mediates the modulation of electrophysiological properties induced by insulin.

---

**Figure 3.11 (following page):** Wortmannin reverses the excitatory effect of insulin on mesencephalic DA neurons. (A) Perforated-patch recording of a SNpc DA neuron before, during insulin (200 nM) application and further addition of wortmannin (1  $\mu$ M). *Top:* Peristimulus histogram (bin width: 60s) of the perforated-patch recording depicted in the *middle panel*. *Bottom:* Excerpts of the recording (*middle*) at three different time points indicated by numbers. (B) *left:* Overlay of spike traces of a perforated-patch recording of a SNpc DA neuron before (*black*), during insulin application (*blue*) and further addition of wortmannin (*red*). *Right:* Absolute frequencies of SNpc DA neurons before, during insulin (200 nM) application and further addition of wortmannin (1  $\mu$ M;  $n=5$ ). horizontal lines, mean; \*\*:  $p < 0.01$ . DA, dopaminergic; SNpc, substantia nigra *pars compacta*.

---



### 3.4 Regulation of mesencephalic dopaminergic midbrain neurons by the obesity-associated *Fto* gene

In the previous chapter, it has been demonstrated that the DA circuitry can be modulated by hormones such as insulin suggesting that DA signaling might also be involved in the regulation of energy homeostasis. Besides the dysregulation of fuel-related signals, variation of certain genetic factors (e.g. *Fto*) are associated with the development of obesity (O’Rahilly, 2009).

To investigate the role of *Fto* in the function of the dopaminergic midbrain circuitry perforated-patch clamp recordings were performed in mice which lack *Fto* in every cell of the body (*Fto*<sup>-/-</sup>) and in mice in which *Fto* is specifically deleted in cells which express the dopamine transporter (DAT), one of the main characteristics of mesencephalic DA neurons (DAT<sup>Δ*Fto*</sup>). Control measurements were conducted in the respective littermates, *Fto*<sup>+/+</sup> and *Fto*<sup>fl/fl</sup>.

#### 3.4.1 *Fto* alters cocaine-induced responses of mesencephalic dopaminergic neurons

To analyse the functionality of the DA circuitry in control (*Fto*<sup>+/+</sup>) and *Fto*-deficient (*Fto*<sup>-/-</sup>) mice cocaine was used as a pharmacological tool. Cocaine has been demonstrated to exert numerous of its behavioral effects via modulation of different sites of the DA circuitry (ventral tegmental area [VTA], substantia nigra [SN], caudate putamen [CPu], nucleus accumbens [NAc]; Chiara & Imperato, 1988; Ungless *et al.*, 2001).

Ablation of the *Fto* gene does not change the number of Th-positive neurons (figure 3.12A; courtesy of M. Heß) suggesting that the *Fto* gene does not influence the development and/or maintenance of mesencephalic DA neurons. The ability of cocaine to modulate the activity of the DA circuitry was assessed by comparing cocaine-induced *c-fos* expression both in the midbrain (SN/VTA), the CPu and the NAc of *Fto*<sup>+/+</sup> and *Fto*<sup>-/-</sup> mice, respectively (figure 3.12B; M. Heß). While cocaine application resulted in a robust stimulation of *c-fos* expression in *Fto*<sup>+/+</sup> mice, cocaine did not induce *c-fos* expression in the SN/VTA as well as in the CPu was abolished in *Fto*<sup>-/-</sup> mice.

To investigate potential alterations of mesencephalic DA neurons in the absence of

Fto expression on a single cell level, electrophysiological properties of DA neurons of Fto<sup>+/+</sup> and Fto<sup>-/-</sup> mice and the response towards cocaine were compared.

The firing rate and the precision of pacemaker firing expressed as coefficient of variation (CV) are not significantly different between SNpc DA neurons of Fto<sup>+/+</sup> and Fto<sup>-/-</sup> mice (see table 3.6). However, analysis of basic biophysical properties and spike parameters revealed that Fto<sup>-/-</sup> neurons differed significantly from control neurons in terms of input resistance (Fto<sup>+/+</sup>:  $356.0 \pm 18.2 \text{ M}\Omega$ ,  $n=24$ ; Fto<sup>-/-</sup>:  $461.0 \pm 29.4 \text{ M}\Omega$ ,  $n=29$ ;  $p < 0.01$ ), conductance density (Fto<sup>+/+</sup>:  $58.2 \pm 3.1 \text{ pS/pF}$ ,  $n=21$ ; Fto<sup>-/-</sup>:  $47.7 \pm 2.8 \text{ pS/pF}$ ,  $n=26$ ;  $p < 0.05$ ) and spike threshold (Fto<sup>+/+</sup>:  $-42.6 \pm 0.7 \text{ mV}$ ,  $n=17$ ; Fto<sup>-/-</sup>:  $-45.2 \pm 0.6 \text{ mV}$ ,  $n=21$ ;  $p < 0.01$ ; see table 3.6) under basal conditions.

Bath application of cocaine (10  $\mu\text{M}$  for 10 min) reduced the firing frequency of DA neurons of Fto<sup>+/+</sup> mice on average by 80% (figure 3.12C,D). During a wash with saline the firing rate reversed and even rebounded to levels 69% above the control (figure 3.12C,D; 5.4). A second cocaine application during the rebound also reduced the firing significantly. A consecutive wash increased the firing rate to levels of the rebound after the first cocaine application. In contrast, cocaine reduced the firing rate by approximately 46% in DA neurons of Fto<sup>-/-</sup> mice which is significantly less than its effect on control neurons. A wash reversed the firing to control levels without causing a rebound (figure 3.12C,D). A second application of cocaine with a consecutive wash had the same effect as the first application (figure 3.12C,D).

Thus, disruption of Fto expression clearly altered the response of DA neurons to cocaine.

**Table 3.6:** Electrophysiological parameters of  $Fto^{+/+}$  and  $Fto^{-/-}$  SNpc DA neurons

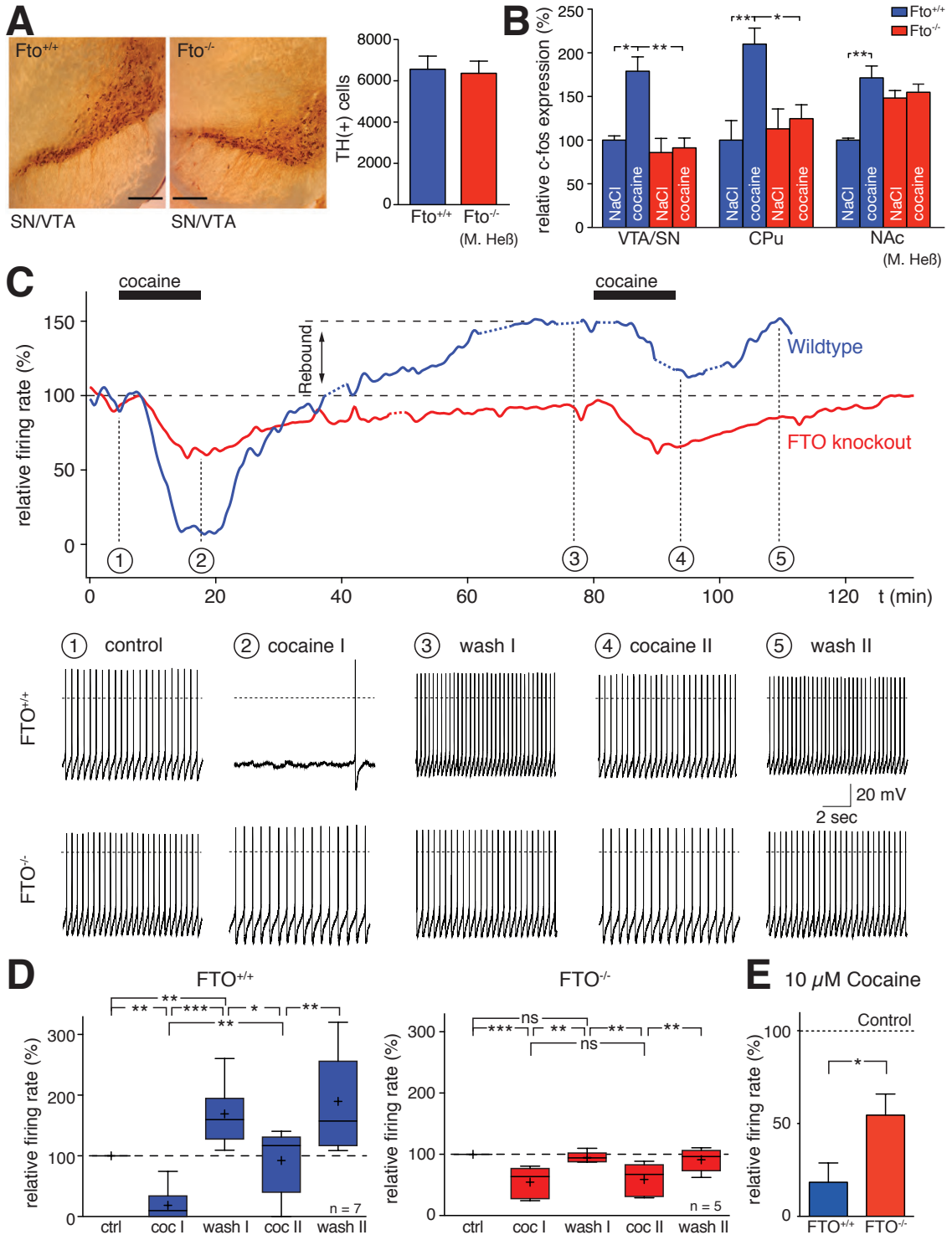
	$Fto^{+/+}$ (Control)	$Fto^{-/-}$
<b>Whole-cell capacitance</b> (pF)	$50.7 \pm 1.4$ ( $n = 22$ )	$49.9 \pm 1.8$ ( $n = 27$ )
<b>Firing Rate</b> (Hz) <sup>†</sup>	$2.1 \pm 0.1$ ( $n = 24$ )	$1.9 \pm 0.2$ ( $n = 24$ )
<b>Coefficient of variation [CV]</b> (%) <sup>†</sup>	$11.5 \pm 1.2$ ( $n = 23$ )	$10.6 \pm 1.1$ ( $n = 16$ )
<b>Membrane Potential</b> (mV)	$-59.0 \pm 0.7$ ( $n = 20$ )	$-58.8 \pm 0.7$ ( $n = 25$ )
<b>Input resistance</b> (M $\Omega$ )	$356.0 \pm 18.2$ ( $n = 24$ )	$461.0 \pm 29.4^{**}$ ( $n = 29$ )
<b>Conductance density</b> (pS/pF)	$58.2 \pm 3.1$ ( $n = 21$ )	$47.7 \pm 2.8^*$ ( $n = 26$ )
<b>Firing Threshold</b> (mV)	$-42.6 \pm 0.7$ ( $n = 17$ )	$-45.2 \pm 0.6^{**}$ ( $n = 21$ )
<b>Spike width</b> (ms)	$2.0 \pm 0.1$ ( $n = 17$ )	$2.1 \pm 0.1$ ( $n = 21$ )
<b>AHP amplitude</b> (mV)	$33.0 \pm 1.2$ ( $n = 17$ )	$30.3 \pm 1.2$ ( $n = 21$ )

Data are given as mean  $\pm$  S.E.M. AHP, afterhyperpolarization.

<sup>†</sup> only spontaneously active neurons were analyzed.

\*:  $p < 0.05$ , \*\*:  $p < 0.01$  – significantly different from control.

**Figure 3.12 (following page):** Modified cocaine responsiveness in SNpc DA neurons of  $Fto^{-/-}$  mice. **(A)** Quantification of the total numbers of Th-expressing neurons in  $Fto^{+/+}$  and  $Fto^{-/-}$  animals. Immunohistochemistry for TH was performed in SN/VTA sections from  $Fto^{+/+}$  and  $Fto^{-/-}$  animals. Total number of TH-positive cells in  $Fto^{+/+}$  and  $Fto^{-/-}$ -mice are given as mean  $\pm$  SEM ( $n=3$  for each genotype; modified from M. Heß). **(B)** Quantitative real-time PCR analysis of cocaine-induced c-Fos expression of the SN/VTA, CPu and NAc in  $Fto^{+/+}$  vs.  $Fto^{-/-}$  mice. Results are expressed as relative c-Fos expression  $\pm$  SEM ( $Fto^{+/+}$ :  $n=7$  [NaCl=3, cocaine=4];  $Fto^{-/-}$ :  $n=7$  [NaCl=3, cocaine=4]; modified from M. Heß). **(C)** Recordings of SNpc DA neurons from a  $Fto^{+/+}$  and a  $Fto^{-/-}$  mouse before, during and after two consecutive applications of cocaine (10  $\mu$ M). The upper traces represent the firing rates during the entire experiments, the lower traces show sections of the original recordings at times as indicated in the upper traces. For details on box plots see Materials and Methods. **(D)** Relative changes in SNpc DA neuron firing rate induced by cocaine in  $Fto^{+/+}$  ( $n=7$ ) and  $Fto^{-/-}$  mice ( $n=5$ ). Data are given as mean  $\pm$  SEM. \*\*\*:  $p < 0.001$ , \*\*:  $p < 0.01$ , \*:  $p < 0.05$ , n.s.:  $p \geq 0.05$ . CPu, caudate putamen; DA, dopaminergic; NAc, nucleus accumbens; SNpc, substantia nigra pars compacta; VTA, ventral tegmental area.



### 3.4.2 Fto regulates D<sub>2</sub>-receptor-dependent control of firing in mesencephalic DA neurons in a cell-autonomous manner

Cocaine indirectly affects the activity of mesencephalic DA neurons by blocking the DAT. As a result, the dopamine concentration increases which in turn results in an elevated activation of dopamine receptors. Mesencephalic DA neurons express D2Rs which inhibit firing of SN/VTA neurons upon activation by dopamine (figure 3.7D; Lacey *et al.* , 1989; Uchida *et al.* , 2000).

To directly address the role of Fto in controlling D2R-mediated signaling, the ability of the selective D2R agonist (-)quinpirole to alter the electrophysiological properties of DA neurons in Fto<sup>+/+</sup> and Fto<sup>-/-</sup> mice was investigated. While quinpirole (10 nM) inhibited firing in DA neurons of Fto<sup>+/+</sup> mice almost completely, the effect of quinpirole on DA neurons of Fto<sup>-/-</sup> mice was significantly attenuated (figure 3.13A; Fto<sup>+/+</sup>: 23.4 ± 8.8 %, n=8; Fto<sup>-/-</sup>: 50.6 ± 11.4 %, n=5; *p* < 0.05; relative values are normalized to control firing before (-)quinpirole [10 nM] application). Similarly, the density of the quinpirole induced conductance (D2R mediated) in dopaminergic neurons was largely attenuated in cells from Fto<sup>-/-</sup> compared to those from Fto<sup>+/+</sup> mice (figure 3.13B; Fto<sup>+/+</sup>: 88.5 ± 11.4 pS/pF, n=12; Fto<sup>-/-</sup>: 58.7 ± 9.9 pS/pF, n=9; *p* < 0.05).

In summary, these experiments clearly demonstrate that Fto modulates the activity of DA neurons via a D2R-dependent mechanism on an electrophysiological level. To further substantiate the previously described finding, realtime PCR analyses were performed which confirmed a significant reduction of D2R in the SN/VTA of Fto<sup>-/-</sup> mice compared to Fto<sup>+/+</sup> mice. Moreover, mRNAs for the dopamine transporter (DAT) as well as tyrosine hydroxylase (TH) are also downregulated in Fto<sup>-/-</sup> mice (figure 3.13D; M. Heß).

To address whether Fto controls D2R-activation in a DA neurons in a cell-autonomous manner, the cocaine response was investigated in mice where the Fto gene was specifically inactivated in DA neurons (DAT<sup>ΔFto</sup>) and their respective control littermates (Fto<sup>fl/fl</sup>). DA neurons of control mice showed a cocaine response which was similar to the cocaine-induced reduction in firing rate of DA neurons of Fto<sup>+/+</sup> mice. The cocaine response of DA neurons of DAT<sup>ΔFto</sup> was significantly attenuated compared

to DA neurons of control mice (figure 3.13E; control:  $23.4 \pm 9.6$  %,  $n=10$ ;  $\text{DAT}^{\Delta\text{Fto}}$ :  $49.9 \pm 9.7$  %,  $n=7$ ;  $p < 0.05$ ) and thus in line with the findings in DA neurons of the whole body Fto knockout ( $\text{Fto}^{-/-}$ ).

Taken together, these experiments clearly suggest that Fto regulates D2R-dependent control of firing in dopaminergic midbrain neurons and that this Fto-dependent effect on D2R-signaling occurs on a cell-intrinsic level. The profound changes on a cellular level are further reflected on the behavioral level, since Fto inactivation (cell-specific as well as body wide) attenuates cocaine-induced behavioral responses.

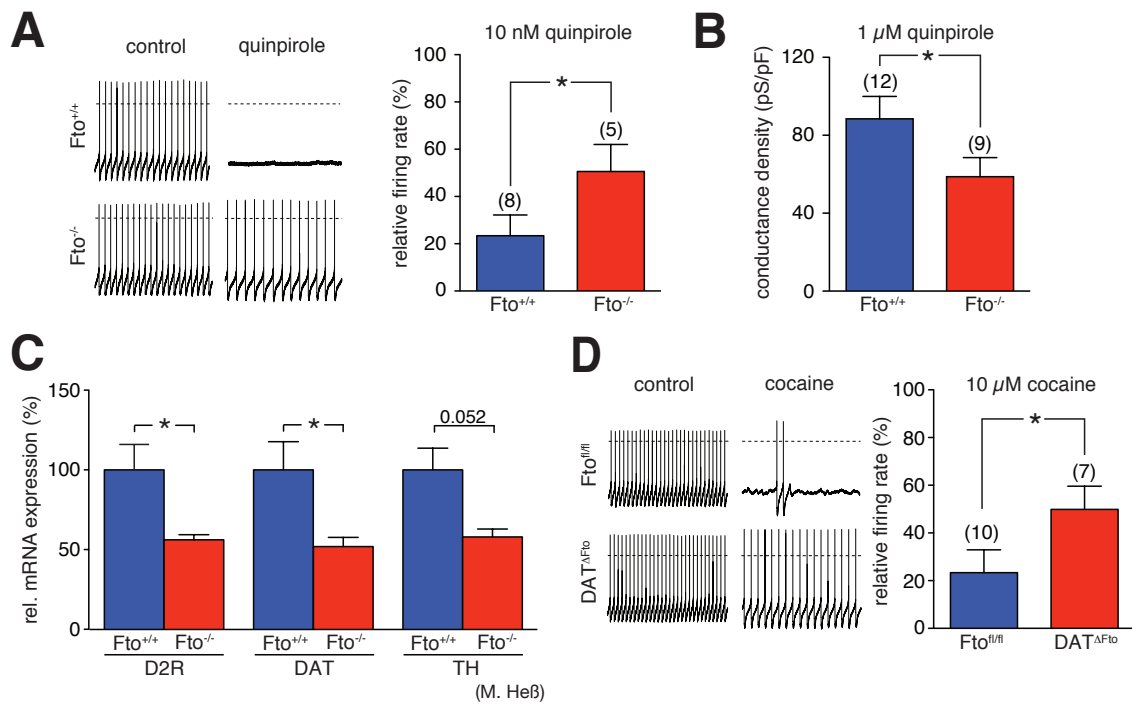


**Figure 3.13:** Fto regulates the activity of DA neurons via a D2R-dependent mechanism. (A) *left panel:* Perforated-patch recordings of SNpc DA neurons of  $\text{Fto}^{+/+}$  and  $\text{Fto}^{-/-}$  mice before and during application of 10 nM quinpirole. *right panel:* Relative changes in SNpc DA neuron firing rate induced by quinpirole in  $\text{Fto}^{+/+}$  ( $n=8$ ) and  $\text{Fto}^{-/-}$  mice ( $n=5$ ). (B) D2R-dependent net conductance density elicited by 1  $\mu\text{M}$  quinpirole in SNpc DA neurons of  $\text{Fto}^{+/+}$  and  $\text{Fto}^{-/-}$  mice. (C) Quantitative real-time PCR analysis of midbrain tissue to assess type 2 dopamine receptor (D2R), DAT and TH expression in  $\text{Fto}^{+/+}$  and  $\text{Fto}^{-/-}$  mice ( $n=7$  per genotype; modified from M. Heß). (D) *left panel:* Perforated patch recordings of SNpc DA neurons of  $\text{Fto}^{\text{fl/fl}}$  and  $\text{DAT}^{\Delta\text{Fto}}$  mice before and during application of 10  $\mu\text{M}$  cocaine. *right panel:* Relative changes in SNpc DA neuron firing rate induced by cocaine in  $\text{Fto}^{\text{fl/fl}}$  ( $n=10$ ) and  $\text{Fto}^{\Delta\text{Fto}}$  mice ( $n=7$ ). Data are given as mean  $\pm$  SEM. \*:  $p < 0.05$ , n.s.:  $p \geq 0.05$ . CPu, caudate putamen; D2R, dopamine type 2 receptor; DA, dopaminergic; DAT, dopamine transporter; GIRK, G-Protein activated inwardly rectifying potassium channel; NAc, nucleus accumbens; SNpc, substantia nigra *pars compacta*; TH, tyrosine hydroxylase; VTA, ventral tegmental area.

### 3.4.3 D2R-signaling is necessary for cocaine-induced 'rebound'

In DA neurons of control littermates ( $Fto^{+/+}$ ), the initial response to cocaine is a hyperpolarization which is caused by D2R-dependent activation of G-protein coupled inwardly rectifying potassium channels (GIRK; figure 3.12C,D). During the washout of cocaine an  $\sim 1.5$ -fold increase in firing rate ('rebound') could be observed in DA neurons of  $Fto^{+/+}$  mice. In contrast, DA neurons of mice with a full body  $Fto$  knockout ( $Fto^{-/-}$ ) which were treated the same way lack the rebound (figure 3.12C,D).

Since previous experiments have already demonstrated that  $Fto$  regulates D2R-signaling, the role of D2R-signaling for the occurrence of rebound excitation in DA neurons was further investigated in  $Fto^{+/+}$  mice. In order to abolish D2R-signaling in DA neurons, (-)sulpiride ( $1 \mu\text{M}$ ), a specific D2R antagonist, was used. Application of sulpiride resulted in a slight but not significant increase in firing rate and conductance density indicating a low activation state of D2Rs and downstream targets (GIRKs) under control conditions which is in accordance with previous studies (Lacey *et al.*, 1990; firing rate, control:  $2.9 \pm 0.2$  Hz, sulpiride:  $3.1 \pm 0.2$  Hz,  $n=8$ ,  $p \geq 0.05$ ; conductance density, control:  $45.1 \pm 8.0$  pS/pF, sulpiride:  $46.3 \pm 7.6$  pS/pF,  $n=6$ ,  $p \geq 0.05$ ; data not shown). Additional application of  $10 \mu\text{M}$  cocaine had no effect on DA neurons, since cocaine-dependent inhibition of DA neurons relies on D2R-dependent signaling. Also the rebound excitation during cocaine washout was completely abolished in the presence of sulpiride (figure 3.14A,C).

These results clearly demonstrate that D2R-dependent signaling is mandatory for the occurrence of cocaine-induced rebound excitation.

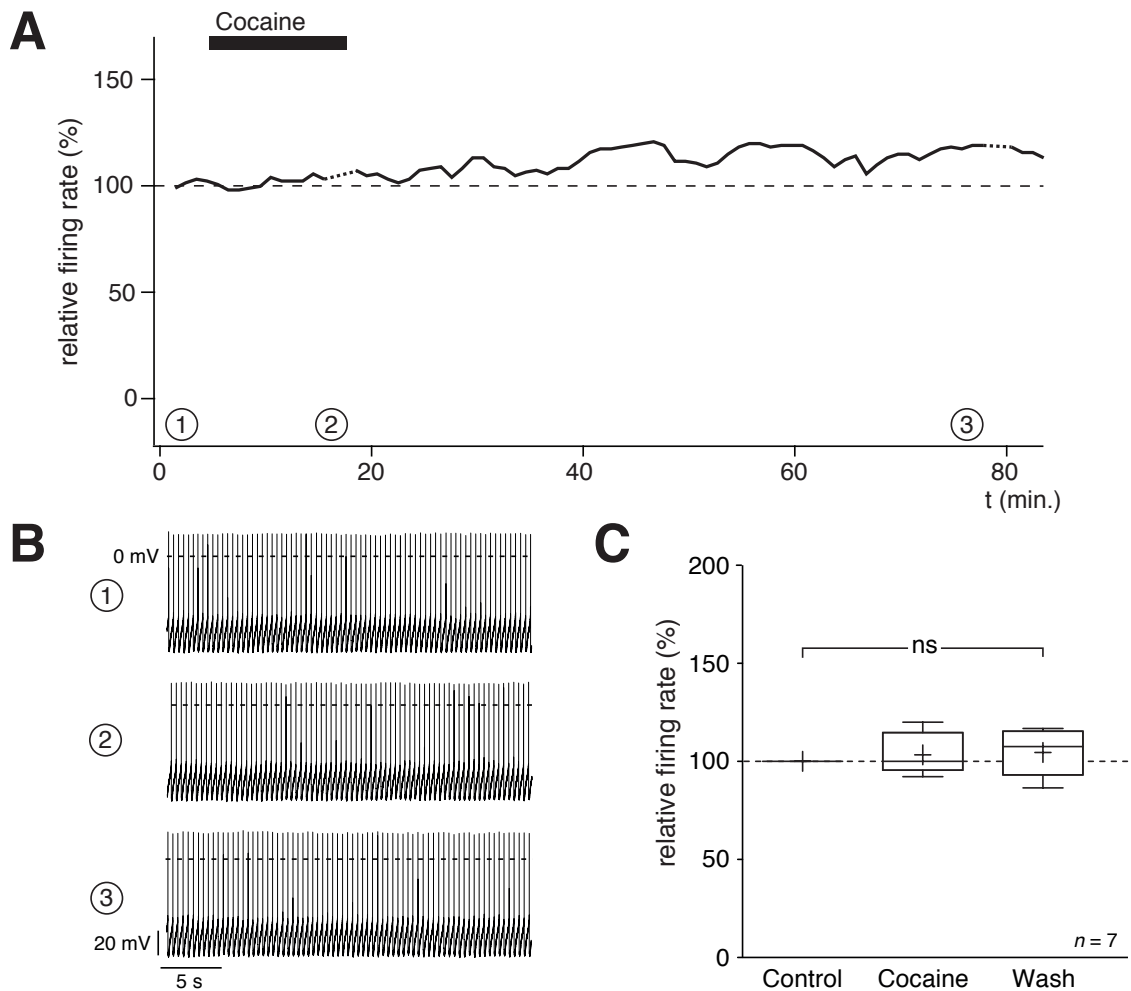


**Figure 3.14:** D2R-signaling is necessary for cocaine-induced rebound excitation in DA neurons of control mice. (A) Peristimulus histogram (PSTH) of the perforated patch recordings of SNpc DA neurons from control mice ( $Fto^{+/+}$ ) before, during and after application of cocaine ( $10 \mu\text{M}$ ) in the presence of (-)-sulpiride ( $1 \mu\text{M}$ ), a specific D2R antagonist. (B) Original recordings at times as indicated in the PSTH. (C) Relative changes in SNpc DA neuron firing rate before, during and after cocaine treatment in DA neurons of  $Fto^{+/+}$  ( $n=7$ ) mice under conditions where D2R-signaling is blocked. n.s.:  $p \geq 0.05$ . D2R, dopamine type 2 receptor; DA, dopaminergic; PSTH, peristimulus histogram; SNpc, substantia nigra *pars compacta*.

### 3.4.4 Fto affects the pacemaker efficacy in mesencephalic dopaminergic neurons of cocaine-sensitized animals

In the previous chapters it has been demonstrated that mesencephalic DA neurons of Fto-deficient (Fto<sup>-/-</sup>) and control (Fto<sup>+/+</sup>) mice respond differently towards acute cocaine stimulation which is also reflected in different behavioral responses towards cocaine between Fto<sup>-/-</sup> and control mice. A single injection of cocaine significantly increased locomotor activity by ~3.7-fold in control mice (figure 3.15A; M. Heß), but did not significantly induce locomotor activity in Fto<sup>-/-</sup> mice beyond the degree of saline-treated animals (figure 3.15A; M. Heß). Moreover, while repeated daily cocaine injections over 5 days caused a sensitization for the ability of cocaine to activate locomotor activity in control mice, even repeated cocaine injections failed to significantly activate locomotor activity in Fto<sup>-/-</sup> mice.

To further investigate the differences between Fto<sup>+/+</sup> and Fto<sup>-/-</sup> mice upon repeated cocaine exposure on a cellular level, perforated-patch recordings of SNpc DA neurons were performed in Fto<sup>+/+</sup> and Fto<sup>-/-</sup> mice which had never been treated with cocaine (naïve) and animals which had received intraperitoneal cocaine injections for 5 consecutive days (sensitized).

Analysis of basic electrophysiological parameters revealed that SNpc DA neurons of cocaine-sensitized animals are significantly smaller which is reflected in a decreased whole cell capacitance compared to the respective naïve controls (see table 3.7; Fto<sup>+/+</sup>: naïve  $49.9 \pm 1.8$  pS/pF,  $n=27$ , sensitized  $40.7 \pm 1.7$  pS/pF,  $n=7$ ,  $p < 0.05$ ; Fto<sup>-/-</sup>: naïve  $50.7 \pm 1.4$  pS/pF,  $n=22$ , sensitized  $40.6 \pm 1.7$  pS/pF,  $n=13$ ,  $p < 0.001$ ). In control animals (f<sup>+/+</sup>), no significant difference in firing frequency, membrane potential and membrane conductance density could be observed between SNpc DA neurons of naïve and sensitized animals. In contrast, comparison between DA neurons of naïve and sensitized Fto-deficient mice revealed that DA neurons of sensitized Fto-deficient mice have a lower firing rate (naïve:  $1.9 \pm 0.2$  Hz,  $n=22$ ; sensitized:  $1.1 \pm 0.2$  Hz,  $n=12$ ;  $p < 0.01$ ), a higher membrane potential (naïve:  $-58.8 \pm 0.7$  mV,  $n=25$ ; sensitized:  $-55.7 \pm 1.8$  mV,  $n=9$ ;  $p < 0.05$ ) and a higher conductance density (naïve:  $47.4 \pm 2.6$  pS/pF,  $n=28$ ; sensitized:  $69.8 \pm 8.2$  pS/pF,  $n=12$ ;  $p < 0.01$ ).

**Table 3.7:** Basic electrophysiological properties of SNpc DA neurons of naïve and cocaine sensitized  $Fto^{+/+}$  and  $Fto^{-/-}$  mice

	$Fto^{+/+}$		$Fto^{-/-}$	
	Naïve	Sensitized	Naïve	Sensitized
<b>Whole-cell capacitance</b> (pF)	$49.9 \pm 1.8$ ( $n = 27$ )	$40.7 \pm 1.7^*$ ( $n = 7$ )	$50.7 \pm 1.4$ ( $n = 22$ )	$40.6 \pm 1.7^{***}$ ( $n = 13$ )
<b>Firing rate</b> (Hz) <sup>†</sup>	$2.1 \pm 0.1$ ( $n = 24$ )	$1.6 \pm 0.3$ ( $n = 7$ )	$1.9 \pm 0.2$ ( $n = 24$ )	$1.1 \pm 0.2^{**}$ ( $n = 12$ )
<b>Membrane potential</b> (mV)	$-59.0 \pm 0.7$ ( $n = 20$ )	$-59.2 \pm 1.2$ ( $n = 6$ )	$-58.8 \pm 0.7$ ( $n = 25$ )	$-55.7 \pm 1.8^*$ ( $n = 9$ )
<b>Conductance density</b> (pS/pF)	$58.2 \pm 3.1$ ( $n = 21$ )	$49.7 \pm 4.4$ ( $n = 7$ )	$47.4 \pm 2.6$ ( $n = 28$ )	$69.8 \pm 8.2^{**}$ ( $n = 12$ )

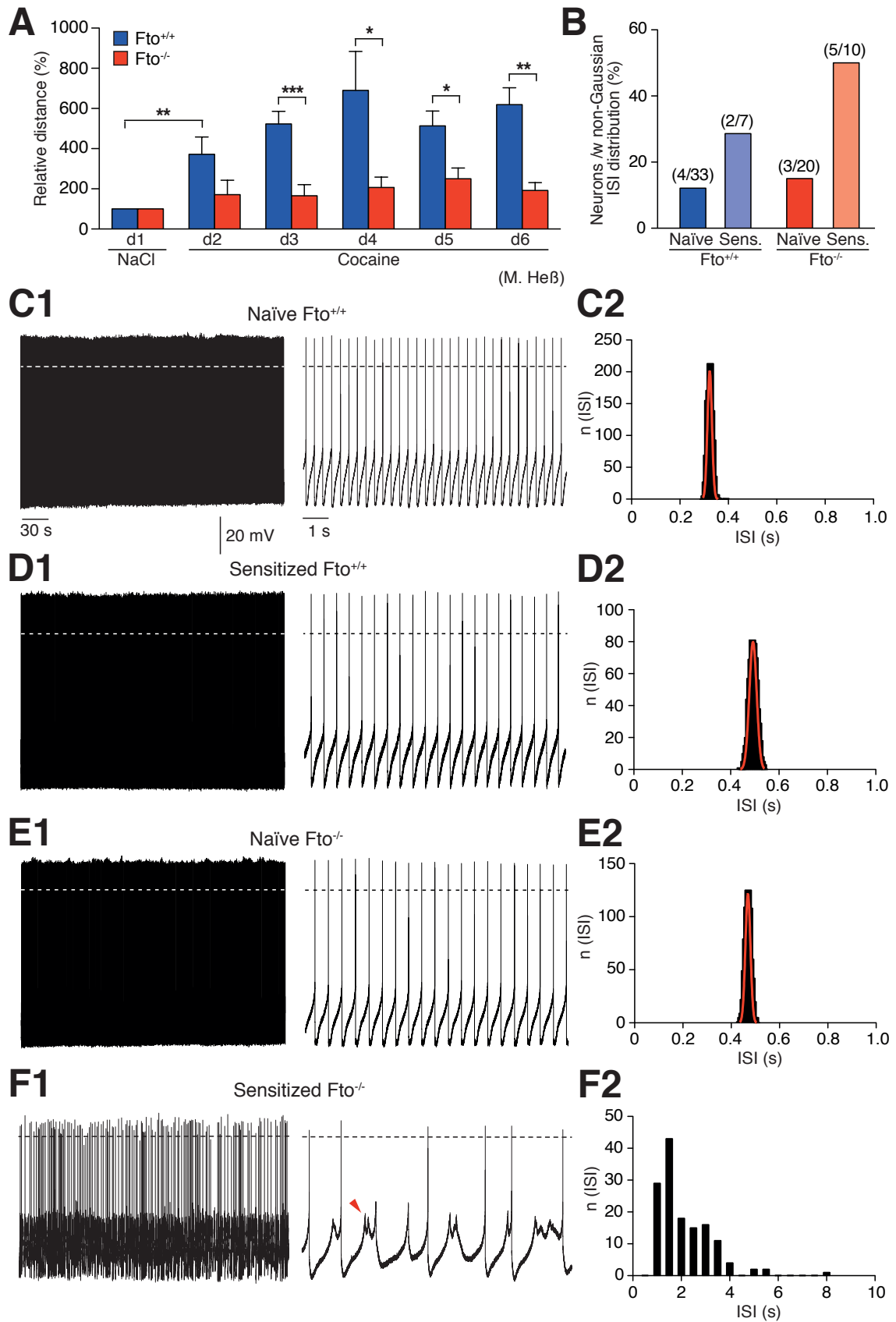
Data are given as mean  $\pm$  S.E.M.

<sup>†</sup> only spontaneously active neurons were analyzed.

\*  $p < 0.05$ , \*\*  $p < 0.01$ , \*\*\*  $p < 0.001$  – significantly different from the respective naïve control.

One of the main characteristics of mesencephalic DA neurons is the very precise pacemaker-like firing. Accordingly, interspike interval (ISI) frequency distributions of DA neurons have a narrow bell-shape which can be described with a single Gaussian function. Only in a few DA neurons of naïve control ( $Fto^{+/+}$ ;  $\sim 12\%$ ) and  $Fto$ -deficient ( $Fto^{-/-}$ ;  $\sim 15\%$ ) mice, the ISI distribution could not be described with a single Gaussian function (figure 3.15B). In cocaine-sensitized mice of both genotypes, a higher percentage of DA neurons exhibited irregular ('non-Gaussian') firing patterns compared to their respective naïve controls with by far the strongest impact on DA neurons of sensitized  $Fto^{-/-}$  mice (figure 3.15B,C,D; sensitized  $Fto^{+/+}$ :  $\sim 29\%$ ; sensitized  $Fto^{-/-}$ :  $\sim 50\%$ ).

**Figure 3.15 (following page):** *Fto* affects the pacemaker efficacy in DA neurons of cocaine-sensitized animals. **(A)** Repeated cocaine injection (20mg/kg BW) is not able to elicit locomotor activity in *Fto*-deficient mice. After the initial test day (see figure 3h), *Fto*-deficient mice were challenged for the following 4 days with an i.p. cocaine injection (20mg/kg BW). Even repeated cocaine injections were not able to cause an increase in locomotor activity in *Fto*-deficient mice, whereas control mice respond with an even more elevated activity as compared to the first cocaine injection (day 2). Distance is expressed as percent increase compared to baseline activity (NaCl i.p. injection). *Fto*<sup>+/+</sup>: n=13 (d1-4), n=5 (d5-6); *Fto*<sup>-/-</sup>: n=9 (d1-4), n=5 (d5-6; courtesy of M. Heß). **(B)** Percentage of SNpc DA neurons showing non-gaussian (non-pacemaker) gaussian ISI distributions. **(C1 – F1)** Perforated-patch recordings of a SNpc DA neurons of a naïve *Fto*<sup>+/+</sup> (C1), sensitized *Fto*<sup>+/+</sup> (D1), naïve *Fto*<sup>-/-</sup> (E1) and sensitized *Fto*<sup>+/+</sup> (F1) mice. **(C2 – F2)** Corresponding ISI histograms of the recordings in C1 – F1. The ISI frequency distribution could be described with a single Gaussian function (red line) in most of the neurons of naïve animals demonstrating a very precise pacemaker rhythm. In contrast, ISI histograms of DA neurons of sensitized *Fto*<sup>-/-</sup> mice show that pacemaker precision is heavily compromised (F2). Note the ‘spikelets’ on top of the sustained depolarizations (*red arrowhead*). \*:  $p < 0.05$ ; \*\*:  $p < 0.01$ ; \*\*\*:  $p < 0.001$ ; n.s.:  $p \geq 0.05$ . CV, coefficient of variation; DA, dopaminergic; ISI, interspike interval; SNpc, substantia nigra *pars compacta*.



## 4 Discussion

### 4.1 The Perforated-Patch Configuration revisited

Since its development, the perforated-patch configuration of the patch clamp technique has been proven to overcome certain disadvantages of the whole cell configuration. Especially when it comes to second messenger mediated effects, whole cell experiments can produce misleading results. This is mainly caused by the dialysis of the interior of the cell leading to the wash-out of cytoplasmic components critical for second messenger pathways. In contrast, the perforated-patch configuration preserves the cellular integrity of the cell. It has been proven to be advantageous in a large variety of applications, most notably in elucidating the impact of intracellular cascades on the activity of voltage-dependent and ligand-gated ion channels (for a comprehensive review see Akaike & Harata, 1994).

In the beginning of this study it became clear that the whole cell configuration was not suitable for the kind of experiments which were about to be conducted. Instead, the perforated-patch configuration was employed for most of the experiments. When recorded in the whole cell configuration the vast majority of the neurons gradually hyperpolarized and consequently stopped firing during the first 15 minutes of recording time mainly due to the activation of  $K_{ATP}$  channels. This finding is not confined to a single neuronal subpopulation since  $K_{ATP}$ -dependent hyperpolarization could be observed in hypothalamic as well as mesencephalic DA neurons. The activity of  $K_{ATP}$  channels is modulated by interactions with ATP and other intracellular components such as  $Mg^{2+}$ -bound nucleotides and PIPs (Ashcroft & Kakei, 1989; Baukowitz *et al.*, 1998; Nichols, 2006). However, saturating concentrations of ATP in the intracellular solution did not prevent  $K_{ATP}$  channel activation. One explanation for the observed effect could be that ATP is being hydrolyzed during the time course of the recording resulting in a gradual change of intracellular ATP concentration and therefore  $K_{ATP}$  channel activity.

One of the main objectives of this study was to investigate the effect of insulin sig-

naling on different neuronal populations. Insulin's action on different neuron types is thought to involve the activation of  $K_{ATP}$  channels as a downstream target (Khan *et al.* , 2001; Spanswick *et al.* , 2000). Under certain circumstances, the dialysis dependent effect on  $K_{ATP}$  channels caused by the whole cell configuration cannot be separated from the insulin signaling dependent effect on  $K_{ATP}$  channels. Thus, an observed hyperpolarization during a whole cell recording might be misleadingly regarded as an insulin effect. Furthermore, the effect of insulin might be overemphasized under whole cell conditions. Previous studies have shown that  $K_{ATP}$  peak current amplitudes in whole cell recordings are  $\sim 50\%$  larger than in perforated-patch recordings (Teramoto *et al.* , 2006). Unpublished findings in POMC neurons argue in the same vein. Therefore, it is difficult to draw any conclusions based on whole cell experiments in terms of insulin's effect on the neuronal activity and its physiological relevance.

Investigation of several spike parameters during whole cell recordings indicate the reduction of  $Ca^{2+}$ -activated small conductance potassium channels. This notion is further substantiated by direct measurements of SK currents (see figure 5.1). These findings suggest that the calcium homeostasis is also affected by the whole cell configuration. During this study, an intracellular solution with very low calcium buffering capabilities was used which would explain the observed rundown of calcium-dependent conductances. The composition of the intracellular solution was intentionally chosen according to the solutions used in a variety of studies employing whole cell recordings in order to yield comparable results (Hommel *et al.* , 2006; Plum *et al.* , 2006a; Stern, 2001; Wolfart *et al.* , 2001).

In contrast to the observed prominent rundown of neuronal activity during the first 15 minutes, perforated patch recordings remained stable up to 4 hours of recording time. None of the investigated neurons showed a time-dependent decay in firing activity during a 15 minute time frame. Investigation of spike related parameters also revealed minimal changes during the first 15 minutes of recording time. Despite its undeniable advantages compared to the whole cell configuration, practical application of the perforated patch configuration turned out to be more demanding in several aspects: 1.) Perforation times are between 15 – 25 minutes which might related to the accessibility

of the membrane patch for the pore forming agents. Thus, more time is needed before the experiment itself can be started. 2.) Often, spontaneous rupturing of the membrane patch occurs resulting in a lower number of successful perforated patch recordings compared to whole cell recordings. During this study, the original protocols were adjusted in such a way that the perforated-patch configuration routinely works with a success rate similar to whole cell recordings. 3.) Several studies reported that series resistances ( $R_S$ ) within the range of whole cell recordings can be achieved with the perforated patch configuration (3 – 25 M $\Omega$ ; Horn & Marty, 1988; Kyrozis & Reichling, 1995; Rae *et al.* , 1991) and that the geometry of the patch pipette tip plays a pivotal role for gaining low access resistances and reducing the perforation times (Rae *et al.* , 1991). However, in this study values for  $R_S$  were usually in the range from 30 – 60 M $\Omega$  making it difficult to analyze ionic conductances – for instance voltage-gated sodium and calcium currents – in voltage clamp mode.

In summary, the application of the perforated patch clamp configuration for the experiments in this study helped to circumvent dialysis-dependent issues which would have hindered the analysis of second-messenger mediated effects such as the impact of insulin signaling on neuronal activity. Adjustments of the protocols of previous studies rendered it possible to routinely use the perforated-patch configuration on a daily basis. However, future experiments are needed to further improve perforated patch recordings to unleash its full potential. Low  $R_S$  values are a prerequisite for the study of ionic currents which would be important for unambiguously identifying downstream targets of second messenger pathways.

## **4.2 The ventromedial hypothalamus in control of energy homeostasis**

Many studies over the last five decades have identified the VMH as one of the key metabolic control centers mediating anorexigenic effects (Hervey, 1959; Marshall & Mayer, 1956; Xu *et al.* , 2003).

Further evidence in favor for an important role for the VMH in metabolic control was gained by using targeted transgenesis and cell-type specific mouse models. Mice lacking

SF-1 fail to properly develop the VMH and have massive obesity (Majdic *et al.* , 2002) suggesting that SF-1 neurons within the VMH are critical for the suppression of feeding. Insights in the modulatory effect of peripheral hormones on VMH neurons came from experiments where leptin signaling was disrupted (Balthasar *et al.* , 2004; Dhillon *et al.* , 2006). Additionally, there is also electrophysiological evidence that peripheral hormones alter the activity of VMH neurons (Miki *et al.* , 2001; Spanswick *et al.* , 1997, 2000).

However, the role of insulin signaling in the VMH – especially its physiological significance – has not been thoroughly explored.

Using several complementary mouse models provided by Klöckener *et al.* (2011), the effect of insulin signaling was characterized on a single cell level in SF-1 neurons. The combination of neuron-specific gene manipulation in the VMH and electrophysiological techniques rendered it possible to directly address the role of insulin signaling in the VMH and its functional importance in controlling body weight.

#### 4.2.1 Properties of SF-1 neurons

Unidentified VMH neurons have already been described as a heterogeneous neuronal population in terms of electrophysiological properties (Miki *et al.* , 2001; Minami *et al.* , 1986). However, the electrophysiological properties of SF-1 neurons have not been investigated so far. Therefore, SF-1 neurons were characterized in terms of their basic membrane properties and by their responses to hyperpolarizing current injections. Analysis revealed that SF-1 neurons exhibit a great variability in terms of their basic electrophysiological properties which indicates that SF-1 neurons constitute a heterogeneous neuronal subpopulation within the VMH. On the basis of the current responses, SF-1 neurons can be separated into different neuron types. These neuron types largely match the ones already described in unidentified VMH neurons (Miki *et al.* , 2001). Furthermore, these experiments suggest that SF-1 neurons might express different combinations of ion channels. For instance, the generation of LTS, which indicates the presence of low threshold  $\text{Ca}^{2+}$  channels (Llinás & Yarom, 1981), were observed in only one neuron type. In addition to that, previous studies suggested that only VMH neurons responsive to changes in glucose concentration are insulin and leptin sensitive (Spanswick *et al.* , 1997,

2000). These glucose-responsive neurons could be matched to specific neuron types (Miki *et al.* , 2001). However, the sensitivity to insulin in SF-1 neurons does not correlate with the 'glucose-responsive' phenotype which is thought to be sensitive to insulin.

Biocytin/streptavidin stainings revealed that SF-1 neurons innervate the DMH as well as the area between VMH and ARC (an example is given in figure 3.4). The latter had previously been described as the potential site of interaction between VMH neurons and neurons of the ARC (van den Pol & Cassidy, 1982) and it has further been shown that VMH neurons innervating this area provide glutamatergic (excitatory) input on POMC as well as AgRP neurons (Sternson *et al.* , 2005). The innervation of the DMH by SF-1 neurons is another interesting finding, since melanocortin receptors are highly expressed in the DMH (Mountjoy *et al.* , 1994) rendering the DMH a potential target site for the melanocortin system of the ARC. DMH neurons also express LepR and receive afferent projections from median hypothalamic sites such as the VMH, LH and have arborizations primarily in the PVN. Therefore it has been hypothesized that the activity of the DMH is also directly regulated by peripheral signals and that the DMH funnels afferent input to the PVN (Berthoud, 2002).

In summary, these initial findings demonstrate that SF-1 neurons are a heterogeneous subpopulation of VMH neurons. Neuroanatomical data suggest that SF-1 neurons directly interact with neurons of the ARC and DMH meaning that SF-1 neurons are capable of shaping the activity of neurons of the melanocortin system by direct interaction or by modulating the activity of neuronal populations which are thought to be downstream of the melanocortin system.

#### **4.2.2 Insulin signaling modulates the neuronal activity of SF-1 neurons and alters the synaptic connectivity in HFD mice**

The role of insulin signaling in SF-1 neurons was investigated using mice with a cell-specific ablation of the IR in SF-1 neurons (SF-1<sup>ΔIR</sup>). One of the main findings was that the body weight phenotype of SF-1<sup>ΔIR</sup> mice compared to control animals was not different when the mice were fed a NCD. In contrast, SF-1<sup>ΔIR</sup> mice on a HFD were partially protected from HFD-induced hyperphagia, weight gain and obesity (Klößener

*et al.*, 2011). These findings indicate that insulin signaling in the VMH plays a pivotal role in control of energy homeostasis and that it can – under certain circumstances – contribute to the development of obesity.

Analysis of insulin signaling on the single cell level revealed that IRs in SF-1 neurons are fully functional since activation of IRs led to the formation of PIP<sub>3</sub> following the activation of PI3K. In contrast, insulin failed to activate PI3K in SF-1 neurons of SF-1<sup>ΔIR</sup> mice (Klößener *et al.*, 2011). Application of insulin to hypothalamic slices inhibited the activity of SF-1 neurons. The inhibitory effect was mediated by the activation of K<sub>ATP</sub> channels since insulin's ability to decrease the firing rate of SF-1 neurons was reversed by tolbutamide, a specific K<sub>ATP</sub> channel blocker. In SF-1 neurons of SF-1<sup>ΔIR</sup> mice, insulin failed to suppress neuronal activity, suggesting that the observed effect is cell-intrinsic. Thus, insulin signaling in SF-1 neurons seems to activate the same downstream pathways as in unidentified VMH neurons, POMC neurons of the ARC and peripheral cells such as pancreatic β-cells (Khan *et al.*, 2001; Plum *et al.*, 2006a; Spanswick *et al.*, 2000). Another finding in terms of insulin-responsiveness of SF-1 neurons was that only a subset of SF-1 neurons responded to insulin. The relative number of insulin-responsive SF-1 neurons corresponds well with the percentage of SF-1 neurons which have exhibited a strong PI3K activation suggesting that there is a relatively high threshold for insulin-dependent activation of K<sub>ATP</sub> channels. Notably, most of the insulin-responsive SF-1 neurons are clustered around the mediobasal VMH, an area which provides glutamatergic (excitatory) input to POMC neurons in the ARC (Sternson *et al.*, 2005). These findings are in accordance with previous studies in POMC neurons demonstrating that profound PI3K activation — achieved by insulin stimulation or ablation of PTEN — resulted in activation of K<sub>ATP</sub> channels causing inhibition of neuronal activity (Plum *et al.*, 2006a). In contrast to the ARC where HFD-induced hyperinsulinaemia causes insulin resistance leading to a complete loss of insulin-mediated PI3K signaling (Schubert *et al.*, 2004), PI3K signaling in the VMH is still functional. One explanation could be that – due to the highly permeable BBB at the base of the hypothalamus – neurons in the ARC are exposed to higher, desensitizing insulin concentrations compared to VMH neurons. Thus under HFD, these regional differences in insulin concentration causes the termina-

tion of PI3K signaling in the ARC whereas it leads to a strong increase in PIP<sub>3</sub> formation and hence PI3K activity in the VMH. This increase can be substantially attenuated by ablation of IR signaling in SF-1 neurons (Klöckener *et al.*, 2011).

Taken together, overactivation of insulin signaling under HFD conditions might result in inhibition of SF-1 neurons leading in turn to a decrease of glutamatergic drive on POMC neurons in the ARC.

The aforementioned notion could be further substantiated by measurements of synaptic input on POMC neurons in mice which were fed a HFD. When mice are exposed to HFD, ablation of IR signaling in SF-1 neurons leads to an increase of excitatory drive on POMC neurons compared to control animals. Accordingly, the spontaneous activity of POMC neurons was increased in SF-1<sup>ΔIR</sup> mice under a HFD (Klöckener *et al.*, 2011).

Insulin stimulation of SF-1 neurons enhances the production of PIP<sub>3</sub> which will subsequently bind to and activate K<sub>ATP</sub> channels leading to the hyperpolarization and silencing of SF-1 neurons. However, in POMC neurons, leptin and insulin signaling is also required for *Pomc* transcription (Belgardt & Brüning, 2010; Belgardt *et al.*, 2008). Since mice lacking the principal PIP<sub>3</sub>-activated downstream kinase (PDK1) in SF-1 neurons were not protected nor sensitive to diet-induced obesity and hyperglycemia (Klöckener *et al.*, 2011), insulin only seems to regulate the firing activity of SF-1 neurons. A strong PI3K activation as it is present under HFD conditions is necessary to evoke the observed effects on neuronal activity. Due to differential accessibility of insulin, the VMH is not subject to insulin-dependent desensitization of PI3K signaling. Therefore HFD-induced hyperinsulinaemia causes an increased insulin signaling in the VMH which in turn inhibits the activity of glutamatergic inputs on POMC neurons. This in turn leads to the silencing of anorexigenic POMC neurons thereby further promoting obesity.

Taken together, the results suggest that SF-1 neurons in the VMH are not second-order neurons downstream of the melanocortin system in the ARC but rather first-order neurons which are subjected to direct and cell-autonomous modulation by fuel sensing signals such as insulin. By providing glutamatergic inputs on anorexigenic

POMC neurons, SF-1 neurons act in concert with POMC neurons in mediating satiety signals.

### 4.2.3 Outlook

This part of the study has provided substantial evidence for the role of insulin signaling in the VMH. Here, I want to outline some future experiments that should be conducted to gain further insight into the functional neuroanatomy of the VMH:

- Biocytin/streptavidin stainings showed that SF-1 neurons have arborizations to several hypothalamic areas which are also in control of energy homeostasis. Therefore, I would suggest to characterize the morphology of SF-1 neurons in greater detail. Since different neuron subtypes of SF-1 neurons were detected during the study based on their electrophysiology, it would be interesting to see if electrophysiological characteristics of certain neuron types can be correlated to morphology.
- Since electrophysiological data of this study suggests that SF-1 neurons might differ in their ion channel expression, a detailed analysis of the different ionic currents should be performed.
- Our results suggest that leptin- and insulin-responses of SF-1 neurons are likely to be segregated, meaning that SF-1 neurons either express LepRs or IRs (Klößener *et al.*, 2011). It would be interesting to see, if the insulin- and leptin-sensitive share the same projection targets or if leptin and insulin signaling in the VMH is also segregated on a morphological level.
- The study by Dhillon *et al.* (2006) suggests that leptin signaling in SF-1 neurons increases their activity and counteracts the effects of HFD-induced obesity. However, our results suggest that the role of leptin signaling is more complex on the cellular level since SF-1 neurons have been found to be excited as well as inhibited by leptin (Klößener *et al.*, 2011). Therefore, it would be necessary to further characterize the leptin-responsive subpopulation of SF-1 neurons especially in terms of their impact on POMC neuron activity.

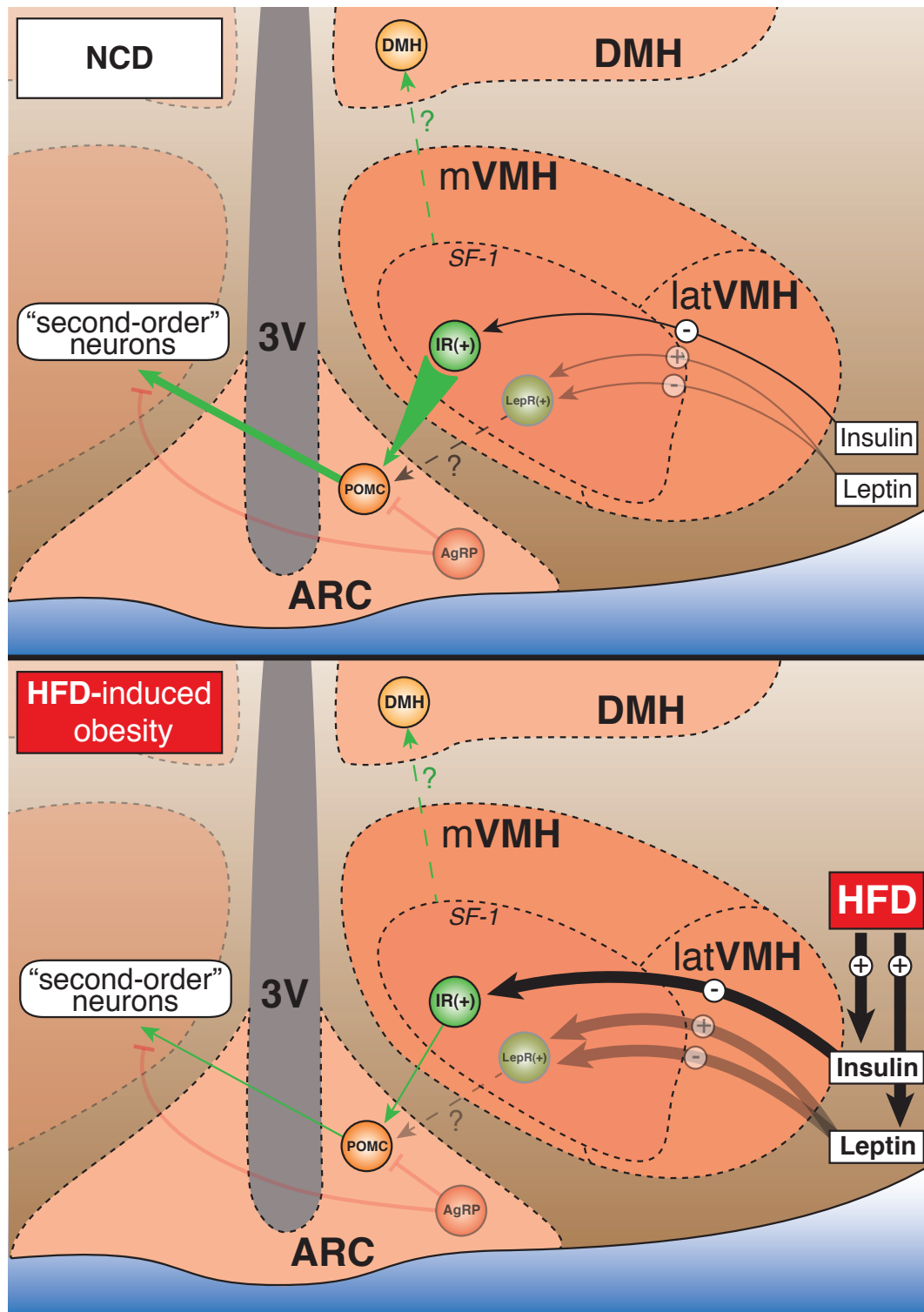


**Figure 4.1:** Proposed wiring diagram for projections of SF-1 VMH neurons to POMC neurons in the ARC (modified from Paxinos & Franklin, 2008). *Green arrows* signify activation, *red arrows* inhibition; 3V, third ventricle; AgRP, agouti-related protein; ARC, arcuate nucleus; DMH, dorso-medial hypothalamus; HFD, high-fat diet; latVMH, lateral ventromedial hypothalamus; mVMH, medial VMH; NCD, normal chow diet; POMC, proopiomelanocortin.

### 4.3 Regulation of mesencephalic dopaminergic neurons by feeding-related signals

Since a series of pioneering studies in the hypothalamus identified the pivotal role of the CNS in control of energy homeostasis (Brobeck, 1951; Brobeck & Tepperman, 1943; Hetherington, 1940, 1944), tremendous progress has been made in elucidating the mechanisms of how the interplay between different food-related signals from the periphery and hypothalamic circuits regulate feeding and energy expenditure (Gao & Horvath, 2007; Niswender & Schwartz, 2003; Schwartz *et al.*, 2000). However, under certain circumstances, homeostatic control of energy homeostasis fails to adequately regulate feeding resulting in the development of obesity at the extreme suggesting that additional neuronal circuits are involved in the regulation of energy homeostasis.

In fact, a large body of evidence suggests that the DA system which is implicated in motor control and such complex processes like reward, motivation and reinforcement also plays an important role in feeding related issues. Initial lesion studies demonstrated that ablation of DA neurons projecting to the CPu results in starvation (Ungerstedt, 1971). Similarly, DA neuron-specific deletion of Th attenuated food intake which could be restored by daily L-DOPA injections (Szczypka *et al.*, 1999; Zhou & Palmiter, 1995). Electrophysiological studies argue in the same vein, since food and food-predicting cues are able to induce phasic activity in DA neurons, an activity pattern which is closely associated with reward and reward-prediction (Schultz *et al.*, 1997).

Two scenarios have been hypothesized in which way signals related to energy stores are conveyed to the DA system: 1.) The indirect pathway: The hypothalamus funnels information from food related signals – i.e. insulin and leptin – to modulate the activity of the DA system via afferent projections from orexinergic and MCH neurons in the LH (Gao & Horvath, 2007). Thus, the DA system would act downstream of the hypothalamic system to promote feeding. 2.) The direct pathway: The DA system is directly modulated by peripheral food-related signals. Therefore, hormonal signals could directly modulate the subjective reward value of food and the motivation to eat. This hypothesis also implies that the DA system is superimposed on the hypothalamic feed-

ing related circuits and that it has the potential to override the hypothalamic system in terms of metabolic control (Palmiter, 2007).

Evidence in favor for the second hypothesis came from several studies in the past ten years that could show that insulin, leptin and ghrelin directly modulate reward seeking and drug relapse, behaviors associated with the DA system (Figlewicz *et al.* , 2001; Figlewicz & Benoit, 2009; Figlewicz *et al.* , 2004, 2006; Fulton *et al.* , 2006; Jerlhag *et al.* , 2006). Further studies which employed genetically engineered mice and AAV-mediated gene knockdown could demonstrate that leptin and ghrelin signaling in the mesencephalon influence feeding behavior. Both studies provided electrophysiological evidence that leptin and ghrelin directly modulate the activity of VTA DA neurons (Abizaid *et al.* , 2006; Hommel *et al.* , 2006). Thus, direct action of feeding-related signals in the DA system provides a potential link between the control of food intake and the reward circuitry.

However, the exact role of insulin signaling in DA neurons in the regulation of energy homeostasis has not been defined, yet. Using complementary mouse models provided by Köhner *et al.* (2011), it was possible to characterize the impact of insulin signaling on the single cell level in DA VTA and SNpc neurons. Furthermore, alterations of synaptic connectivity in DA VTA/SN neurons were also investigated using the same mouse models.

#### **4.3.1 Properties of mesencephalic dopaminergic neurons**

Mesencephalic DA neurons in the SNpc and VTA were electrophysiologically identified based on well-established criteria (Grace & Onn, 1989; Lacey *et al.* , 1989; Richards *et al.* , 1997; Uchida *et al.* , 2000; Yung *et al.* , 1991). These criteria comprise long duration APs, low pacemaker-like activity, a large  $I_h$  and D2 autoreceptor-dependent inhibition by dopamine and have been widely used to identify potential DA neurons in the VTA as well as the SNpc (Abizaid *et al.* , 2006; Hommel *et al.* , 2006; Schilström *et al.* , 2006; Wolfart *et al.* , 2001; Zolles *et al.* , 2006). In this regard it is important to note that these criteria were originally developed from recordings in the SNpc which were additionally verified by immunohistochemistry (Richards *et al.* , 1997; Yung *et al.* , 1991). In contrast, appli-

cation of these criteria to neurons in the VTA does not reliably predict that a neuron is DA-containing. Additionally, the likelihood to record from a non-DA neuron in the VTA is higher than in the SNpc since  $\sim 90\%$  of the neurons in the SNpc are TH-positive compared to only  $\sim 60\%$  in the VTA. Only the absence of an  $I_h$  reliably predicts that a VTA neuron is TH-negative and therefore non-DA (Margolis *et al.*, 2006). This means in turn that  $I_h$  negative DA neurons are excluded from analysis in the first place. For instance, a recent study has reported the existence of VTA DA neurons exclusively projecting along the mesocorticolimbic pathway which exhibit unusual properties for a DA neuron such as fast AP firing (10 – 15 Hz) and the absence of a prominent  $I_h$  and the inhibition by D2 autoreceptors (Lammel *et al.*, 2008). On the other hand, almost 50% of  $I_h$  positive VTA neurons are Th-negative, meaning that a large number of neurons recorded based on this criterion are in fact non-DA. This being the situation, many studies conducted in the VTA have to be approached with great caution.

Although VTA neurons were also identified according to the aforementioned criteria in this study, the contribution of non-DA VTA neurons to the observed effects is regarded as rather non-problematic since only a small amount of cells (12%) was recorded in the VTA. Particular attention was paid to only record from  $I_h$ -positive VTA neurons with long duration APs since DA neurons projecting to the NAc could be reliably predicted by these two features (Margolis *et al.*, 2008). Nevertheless, in future electrophysiological experiments it would be of great benefit to either use immunocytochemical identification or single-cell RT-PCR in order to unambiguously identify VTA neurons as dopaminergic. Application of either one of the techniques would make it possible to record from VTA neurons which do not comply with the ‘classical’ electrophysiological DA neuron phenotype.

The vast majority of cells in this study were recorded in the SNpc. Initially, SNpc DA neurons have been implicated in motor control which is nowadays regarded as an oversimplification. In fact, SNpc DA neurons also project along mesolimbic pathway thereby participating in reward-related behavior (Björklund & Dunnett, 2007). Additionally, there is an accumulating body of evidence that DA signaling in the CPu has

a larger impact on feeding than signaling in the NAc (Gao & Horvath, 2007; Palmiter, 2007; Szczypka *et al.*, 2001).

#### **4.3.2 Insulin signaling modulates the neuronal activity and alters the synaptic connectivity of mesencephalic dopaminergic neurons**

The role of insulin signaling in mesencephalic DA neurons was investigated using mice with a cell-specific ablation of the IR in Th-expressing neurons (Th<sup>ΔIR</sup>). One of the initial findings was that Th<sup>ΔIR</sup> mice had an obese, hyperphagic phenotype revealing a critical role for insulin signaling in Th-positive neurons in control of feeding. Upon acute AAV-Cre-mediated IR deletion in the VTA, mice exhibited a clear trend for hyperphagia, ruling out the possibility that other catecholaminergic circuits or neuroadaptive changes due to the lack of insulin signaling during development might be responsible for the observed alterations. Moreover, Th<sup>ΔIR</sup> mice exhibited altered cocaine-evoked locomotor activity and a tendency toward altered sensitivity to a sucrose solution supporting a direct role for insulin signaling in the brain-reward system (Könner *et al.*, 2011).

On a cellular level, previous studies could already demonstrate that IRs in mesencephalic neurons are fully functional (Figlewicz *et al.*, 2007). Similarly, activation of IRs led to the formation of PIP<sub>3</sub> following the activation of PI3K in mesencephalic DA neurons. In contrast, insulin's ability to activate PI3K was abolished in DA neurons of Th<sup>ΔIR</sup> mice (Könner *et al.*, 2011). Application of insulin to mesencephalic slices had a significant excitatory effect on DA neurons. This excitatory effect also persisted under conditions where synaptic transmissions was blocked suggesting that the observed effect is cell-intrinsic. Th-specific deletion of the IR on DA VTA/SN neurons abolished the aforementioned cell-autonomous effect on these cells, thus ruling out the possibility of nonspecific insulin-mediated activation of IGF-I receptors on these cells, as it has been previously suggested (Baserga *et al.*, 1997). Moreover, ablation of the IR results in a significant reduction of excitatory (glutamatergic) input. Changes in glutamatergic transmission following the use of drugs of abuse have been implicated in adaptations of the mesencephalic DA circuitry which can ultimately lead to the development of addictive behaviors (Schilström *et al.*, 2006). Thus, it can be hypothesized that under certain

conditions such as HFD-induced hyperinsulinaemia, increased insulin signaling in the DA circuitry might induce synaptic alterations promoting addictive behaviors.

Another finding in terms of insulin-responsiveness of DA neurons was that only a subset of DA neurons responded to insulin. The relative number of insulin-responsive DA neurons corresponds well with the percentage of DA neurons which have exhibited a strong PI3K activation suggesting that there is a relatively high threshold for immediate effects of insulin signaling on neuronal activity of DA neurons.

A potential mediator of insulin's effects on firing frequency is the PI3K pathway. The effect of insulin on the activity of DA neurons is also likely to be PI3K dependent, since wortmannin – a specific inhibitor of PI3K – was able to revert the excitatory effect of insulin. Previous studies have demonstrated that insulin signaling in the hypothalamic neurons leads to PI3K dependent activation of  $K_{ATP}$  channels resulting in cell-autonomous hyperpolarization (Klößener *et al.* , 2011; Plum *et al.* , 2006a). Since the findings in this study indicate that insulin leads to an increase in spontaneous firing in DA VTA/SN neurons, it is unlikely that  $K_{ATP}$ -channels are the downstream target of PI3K signaling in these cells. However at least two models can be hypothesized for how insulin signaling modulates DA neuronal function: i) transient receptor potential cation (TRPC) channels as a target of insulin signaling; and ii) insulin-mediated modulation of DAT and D2R function.

Only recently, it has been demonstrated that leptin through a JAK2-PI3K-PLC $\gamma$  pathway activates TRPC channels, which subsequently results in a depolarization of hypothalamic POMC neurons (Qiu *et al.* , 2010). However in this study, it could be demonstrated that insulin application to DA neurons leads to a decrease in membrane conductance arguing against the insulin signaling mediated activation of ion channels.

Another explanation for the observed effect might be the insulin-dependent increase in DA uptake, which could also lead to an increase in activity in VTA/SN neurons. It has previously been shown for rat SN DA neurons that extracellular DA acts on D2 autoreceptors and subsequently activates GIRKs, resulting in a decrease in the spontaneous firing activity (Uchida *et al.* , 2000). Moreover, it is well established that insulin application results in elevated expression levels of DAT mRNA in the VTA and SN

(Figlewicz *et al.* , 1994). Furthermore, insulin-dependent PI3K activation increases DA uptake, whereas inhibition of PI3K signaling reduces DAT surface expression and DA uptake in rat brain striatal synaptosomes and HEK293 cells stably transfected with the human DAT (Carvelli *et al.* , 2002). Taken together, these data suggests that insulin can modulate DAT activity on different levels via PI3K activation. Consistently, increased insulin-mediated DAT activity might lead to a higher DA clearance, resulting in the disinhibition of DA VTA/SN cells in a D2R-dependent mechanism. Furthermore, insulin and D2R signaling might overlap at some points. The open probability of GIRKs is strongly dependent on PIP<sub>2</sub> (Cho *et al.* , 2005). Thus, increased PI3K activity could locally alter the PIP<sub>2</sub> to PIP<sub>3</sub> ratio which might in turn decrease the sensitivity of GIRK channels for D2R dependent signaling via Gβγ protein. Additionally, insulin and D2R signaling might converge at the level of PKB regulation. PKB plays a key role in multiple cellular processes like transcription, glucose metabolism and ion channel function and is known to be activated via insulin dependent signaling (Plum *et al.* , 2006b). In contrast, PKB is negatively regulated in the late phase of D2R signaling via PKB binding to βArrestin 2 and PP2A (Beaulieu & Gainetdinov, 2011). Thus, insulin dependent signaling could serve as a modulator of D2R signaling on different levels.

Research over the last decade suggested a prominent role for D2R mediated signaling in the development of obesity since BMI is negatively correlated with D2R density in striatal areas (Volkow *et al.* , 2008; Wang *et al.* , 2001). Furthermore, diet-induced obesity is linked to deficits in mesolimbic dopamine neurotransmission, and obesity-prone rats exhibit reduced D2R expression levels (Geiger *et al.* , 2009, 2008; Johnson & Kenny, 2010).

### 4.3.3 Outlook

The work from this part of the study has provided substantial evidence for the role of insulin signaling in the mesencephalic DA circuitry. Here, I want to outline some future experiments that should be conducted to gain further insight into the cellular mechanisms of insulin's action in DA neurons and the functional neuroanatomy of the DA system with regard to feeding regulation:

- One of the main findings of this study was that insulin signaling increases the

activity of DA neurons. However, the downstream target responsible for that is unknown. Therefore, experiments are needed to identify the downstream target and the exact mechanism of insulin signaling.

- Based on the findings of this thesis, it can be hypothesized that insulin and D2R signaling might overlap at some points. Further experiments should be conducted to investigate a potential cross-talk between both signaling pathways.
- IRs and LepRs are expressed in DA as well as non-DA neurons in the mesencephalon (Figlewicz *et al.* , 2003). Since mesencephalic GABA interneurons are important parts of the DA circuitry in terms of feedback regulation of DA neurons it would be interesting to find out how these neurons are regulated by insulin and leptin signaling.
- The immediate effects of leptin and ghrelin on the activity of DA neurons are still a matter of debate (Abizaid *et al.* , 2006; Hommel *et al.* , 2006; Korotkova *et al.* , 2006). Experiments with the experimental setup used in this study should be conducted to clarify the role of leptin and ghrelin signaling in DA neurons.
- The study by Hommel *et al.* (2006) suggest that leptin signaling in DA neurons has an opposite effect on neuronal activity than insulin. Therefore, experiments should be conducted in order to find out if there is a cross-talk between insulin and leptin signaling on a cell-intrinsic or rather on a circuit level.
- Retrograde tracing techniques should be combined with electrophysiology in order to gain further insights in the functional neuroanatomy of the DA circuitry in control of energy homeostasis.
- Previous studies have shown that neurons postsynaptic to DA neurons, i.e. medium spiny neurons in the CPU, express IRs (Havrankova *et al.* , 1978). Therefore, neurons in the respective target areas of DA signaling should be investigated regarding the effects of insulin signaling.

- It would be interesting to see if HFD-induced obesity leads to insulin resistance or to increased insulin signaling, comparable to the situation in the VMH, within the mesencephalic DA circuitry.

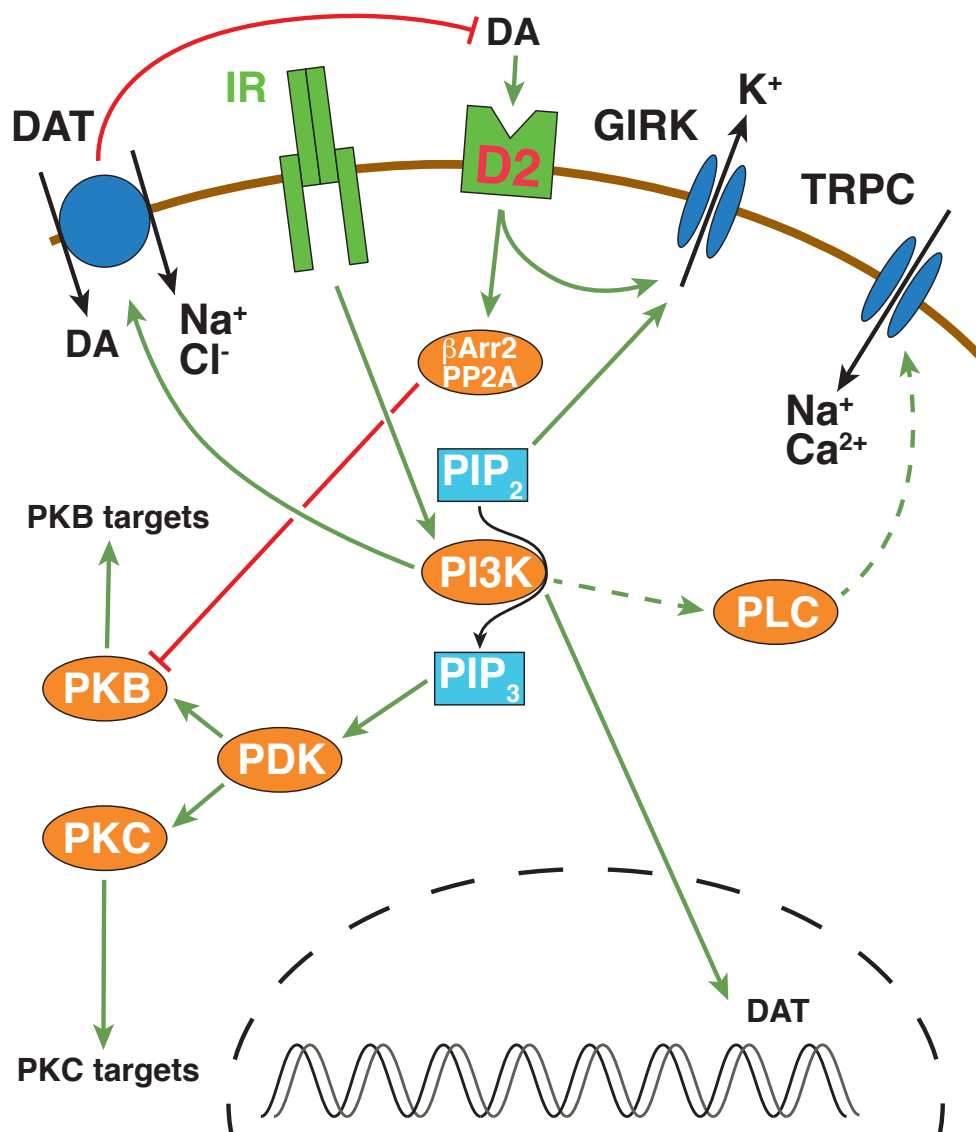


**Figure 4.2:** Proposed insulin signaling pathway in mesencephalic DA neurons. The D2R signaling pathway has been included to illustrate potential sites of cross-talk with IR signaling. *Green arrows* signify activation, *red arrows* inhibition; βArr2, β-arrestin 2; DA, dopamine; DAT, dopamine transporter; GIRK, G-protein activated inwardly rectifying potassium channel; IR, insulin receptor; PI3K, PI3 kinase; PIP<sub>2</sub>, phosphatidylinositol-4,5-bisphosphate; PIP<sub>3</sub>, phosphatidylinositol-3,4,5-trisphosphate; PKB, protein kinase B; PKC, protein kinase C; PLC, phospholipase C; PP2A, protein phosphatase 2A; TRPC, transient receptor potential channel.

## 4.4 Regulation of mesencephalic dopaminergic midbrain neurons by the obesity-associated *Fto* gene

In recent years genome-wide association studies identified a variety of genetic factors which could be linked to an individual's predisposition to obesity. Among these genetic variations, SNPs in the first intron of the *Fto* gene were the first to be unequivocally associated with obesity and showed a robust correlation with an increase in BMI (Frayling *et al.* , 2007). This finding was further substantiated by two studies in mice where the *Fto* gene was either ubiquitously deleted or overexpressed. Ablation of the *Fto* gene in mice resulted in growth retardation and increased energy expenditure. Moreover, *Fto* null mice are protected from obesity (Fischer *et al.* , 2009). Conversely, mice which had a bodywide overexpression of the *Fto* gene were overweight due to increased food consumption (Church *et al.* , 2010). In line with these findings, the highest *Fto* expression is found in the CNS with high levels in the hypothalamus pointing towards a pivotal role for *Fto* in feeding-related circuits (Gerken *et al.* , 2007; Olszewski *et al.* , 2011b).

The *Fto* gene product has been shown to be a dioxygenase with the ability to demethylate 3-methylthymine in single stranded DNA (Gerken *et al.* , 2007) pointing towards a role of *Fto* in DNA repair. Since oxygenases catalyze posttranslational hydroxylation and mediate histone demethylation (Jaakkola *et al.* , 2001; Klose *et al.* , 2006), transcriptional control represents another potential *Fto* function. In line with this hypothesis, a recent study by Olszewski *et al.* (2011a) suggests that *Fto* acts as a co-activator of the expression of certain feeding-related genes (POMC, oxytocin). Moreover, *In vitro* experiments showed that *Fto* has the ability to demethylate single stranded RNA which might represent an additional mechanism of expression control (Han *et al.* , 2010; Jia *et al.* , 2008). However, the exact mechanisms in which way the enzymatic function of *Fto* is linked to its role in the control of feeding and energy expenditure remains elusive.

### 4.4.1 *Fto* alters cocaine-induced responses of mesencephalic dopaminergic neurons

Immunohistochemical analysis of *Fto* distribution revealed that *Fto* is also expressed in extrahypothalamic feeding-related sites like the VTA and SN (Hess *et al.*, 2011; Ol-

szewski *et al.*, 2011b). In order to assess the role of the *Fto* gene in the mesencephalic DA circuit, complementary mouse models provided by Hess *et al.* (2011) were used.

Since the role of the DA circuitry in cocaine-mediated behavioral responses is well-established (Chiara & Imperato, 1988), behavioral experiments using the open field paradigm were conducted. In wildtype mice, cocaine induces a strong increase in locomotor activity and repeated cocaine administration leads to behavioral sensitization in terms of further increase in locomotor activity. In contrast, the response towards cocaine is blunted in *fto*-deficient mice and repeated cocaine administration does not lead to behavioral sensitization (Hess *et al.*, 2011). Subsequent analysis of cocaine-induced *c-fos* expression which is an indirect marker for neuronal activity further substantiated the aforementioned findings. In wildtype mice, a strong increase of transcriptional activity was detected in the VTA/SN and the CPu and NAc, the primary target areas of mesencephalic DA signaling. Similar to the behavior experiments, the cocaine-induced effect is blunted in *fto*-deficient mice (Hess *et al.*, 2011).

The effect of cocaine was further investigated on a cellular level in SN DA neurons. Being a potent re-uptake inhibitor via block of DAT, application of cocaine leads to the accumulation of extracellular dopamine which in turn activates D2 autoreceptors on DA neurons. Then, activation of D2Rs causes the opening of potassium channels via a g-protein signaling cascade (see section 1.4.2; Lacey *et al.*, 1990). As a result, cocaine initially hyperpolarizes DA neurons. Since DAT function is also abolished in the projection targets of DA neurons, cocaine leads to an increase in dopamine concentration thereby potentiating DA signaling in the CPu and NAc. In DA SN neurons, ablation of the *Fto* gene leads to profound alterations in cocaine-evoked responses. Whereas the activity in wildtype DA neurons was strongly inhibited by cocaine, the firing of DA neurons of *fto*-deficient mice was inhibited to a lesser extent. Furthermore in wildtype DA neurons, subsequent wash after cocaine treatment caused a rebound in spike frequency which was not observed in DA neurons of *fto*-deficient mice.

In summary, these experiments provide initial evidence for a critical role of the obesity-associated *Fto* gene in control of the DA circuitry.

#### 4.4.2 *Fto* regulates D<sub>2</sub>-receptor-dependent control of firing in mesencephalic DA neurons in a cell-autonomous manner

The differences in cocaine-induced inhibition of neuronal activity in DA neurons of wildtype and *Fto*-deficient mice suggest that ablation of the *Fto* gene attenuates D2R signaling in DA neurons. However, cocaine does not specifically block DAT but is also known to inhibit other monoamine transporters such as the serotonin transporter and voltage-gated sodium channels on presynaptic neurons which might render the observed effect in DA neurons secondary (Bonci *et al.* , 2003; Steffensen *et al.* , 2008). Therefore, in order to directly address D2R signaling in DA neurons, the selective D2R agonist quinpirole was used instead. Quinpirole inhibits DA neurons in a concentration dependent manner (see figure 5.5A,B) and application of quinpirole yielded the same differences in neuronal activity between both genotypes as in the previous experiments with cocaine. Quinpirole-evoked increases in membrane conductance turn out to be smaller in *Fto*-deficient mice compared to their wildtype littermates. Additionally, under conditions where D2Rs are pharmacologically inhibited, no rebound is detectable in wildtype mice after cocaine application, indirectly indicating that D2R signaling is impaired in *Fto*-deficient mice. Further support in favor of these findings come from quantitative PCR analyses in the VTA/SN showing that D2R mRNA levels are downregulated in *Fto*-deficient mice (M. Heß). Interestingly, mRNA levels of DAT and TH which heavily affect dopaminergic signaling are downregulated as well.

Previous studies have shown that the downstream target of D2R signaling are GIRK channels (Uchida *et al.* , 2000). However, the studies on D2R mediated GIRK activation are either conducted in heterologous expression systems such as *Xenopus* oocytes (Sahlholm *et al.* , 2008) or GIRK currents were isolated and characterized in voltage-clamp mode (Uchida *et al.* , 2000). Studies under physiological conditions demonstrating the impact of D2R mediated GIRK activity on neuronal firing are still lacking. Therefore, the contribution of GIRK channels to D2R mediated signaling was pharmacologically assessed in current-clamp recordings in control mice by using tertiapin-Q, a specific GIRK channel blocker. Co-application of tertiapin-Q reversed the membrane conductance and membrane potential to control values suggesting that D2R mediated changes in mem-

brane conductance are mainly caused by GIRK channels. Interestingly, co-application of tertiapin-Q is not sufficient to restore the firing rate of DA neurons to control values. Additional application of a D2R blocker is necessary to restore neuronal activity (see figure 5.5C,D).

Taken together, these findings suggest that D2R mediated changes in conductance density are mainly GIRK dependent and that D2R activation influences neuronal activity via more than one downstream target. D2R signaling is very complex and activates a large variety of downstream effectors via its G-proteins (see figure 1.4). Possible candidates which might play a role in the neuronal excitability are HCN channels which are modulated by intracellular cAMP levels. Additionally, L-type calcium channels ( $Ca_V$  1.3) which play a pivotal role in generating the pacemaker firing in DA neurons (Chan *et al.* , 2007) might be targeted by D2R-dependent signaling.

In order to rule out the possibility that the observed differences in D2R signaling in DA neurons between Fto-deficient and wildtype mice are dependent on additional circuits, experiments were conducted with a DA neuron specific knockout of the Fto gene ( $DAT^{\Delta Fto}$ ). Application of cocaine in  $DAT^{\Delta Fto}$  mice led to the same degree of cocaine induced inhibition of DA neuron activity as in mice with a whole body Fto knockout.

These findings clearly suggest that Fto alters D2R signaling in a cell-autonomous manner.

#### **4.4.3 Fto affects the pacemaker efficacy in mesencephalic dopaminergic neurons of cocaine-sensitized animals**

Behavioral experiments in the open field paradigm showed that Fto-deficiency blunts the cocaine induced increase in locomotor activity. Furthermore, lack of Fto prevents mice from developing behavioral sensitization toward repeated application of cocaine (M. Heß).

To further investigate the cellular changes after cocaine induced behavioral sensitization, perforated-patch clamp experiments were conducted in Fto-deficient and wildtype littermates. DA neurons of sensitized wildtype as well as Fto-deficient mice have a

smaller cell size than their naïve counterparts. Changes in DA neuron morphology have been previously described in mice which were subjected to repeated morphine treatment (Russo *et al.* , 2007). According to the authors of the study, chronic morphine treatment downregulates the IRS2-PKB(Akt) pathway which in turn decreases the cell size. Decreased cell size is associated with decreased levels of neurofilament proteins in the VTA, decreased axoplasmic transport from VTA DA neurons to other reward-related structures and a hypodopaminergic state. Thus, regulation of the cell size may play a pivotal role in regulating addictive behavior (Bolaños & Nestler, 2004; Nestler, 2004).

As previously stated, the vast majority of mesencephalic DA neurons *in vitro* exhibit a very precise pacemaker-like firing (see figure 3.7). One of the main findings concerning the impact of repeated cocaine application in Fto-deficient mice is that predominantly DA neurons in sensitized Fto-deficient mice fail to generate pacemaker-like activity. Trains of APs are often interrupted by sustained depolarizations with ‘spikelets’ riding on top. Analysis of basic electrophysiological parameters revealed that – in contrast to sensitized controls – sensitization in Fto-deficient mice leads to an increase in membrane conductance suggesting changes in the ion channel composition of the cell membrane. However, it remains elusive which ion channels might be responsible for the tremendous differences in sensitized Fto-deficient mice compared to their respective wildtype controls.

#### 4.4.4 Outlook

Collectively, the findings of this study reveal an Fto-dependent alteration in function of the mesencephalic DA circuitry. The results from electrophysiological recordings in Fto-deficient mice and conditional (DAT<sup>ΔFto</sup>) Fto-deficient mice clearly indicate an attenuation of D2R-mediated signaling in DA VTA/SN-neurons. This notion is further supported by behavioral experiments and quantitative realtime PCR. As already suggested by Olszewski *et al.* (2011a), Fto might serve as a co-activator for the expression of specific genes. Microarray expression data provides evidence in favor of this hypothesis, since the transcripts of D2R, DAT and TH are downregulated in Fto-deficient mice (M. Heß, Master-Thesis). Interestingly, the cocaine and amphetamine regulated

transcript (CART) which is implicated in the regulation of reward and feeding related behavior (Hunter *et al.* , 2004; Rogge *et al.* , 2008) exhibits the highest downregulation. The mechanism(s) through which Fto-deficiency functionally alters the mesencephalic DA circuitry appears to be complex. The results of this study provide the groundwork for understanding the role of Fto within the DA circuitry. Additional studies are necessary to further define this role:

- Metabolic phenotyping should be used to assess whether DA-specific Fto (Fto<sup>ΔDAT</sup>) ablation causes alterations in food intake
- D2R mediated signaling should be directly addressed using quinpirole in Fto<sup>ΔDAT</sup> mice to compare it to the whole body Fto knockouts.
- In order to understand the alterations in D2R signaling it is necessary to characterize the GIRK currents and further downstream targets of D2Rs in Fto-deficient mice.
- DAT mRNA has been shown to be downregulated in Fto-deficient mice. Therefore, it would be interesting to directly address DAT function in whole body and DAT<sup>ΔFto</sup> mice. DAT currents should be quantified using the experimental approach by Ingram *et al.* (2002).
- Medium spiny neurons (MSNs) are the postsynaptic targets of mesencephalic DA neurons. Since Fto is also expressed in the NAc, electrophysiological experiments should be conducted to clarify the role of the Fto gene in the neuronal downstream targets of DA signaling.

## 5 Appendix

### 5.1 SK currents decrease during whole cell recordings

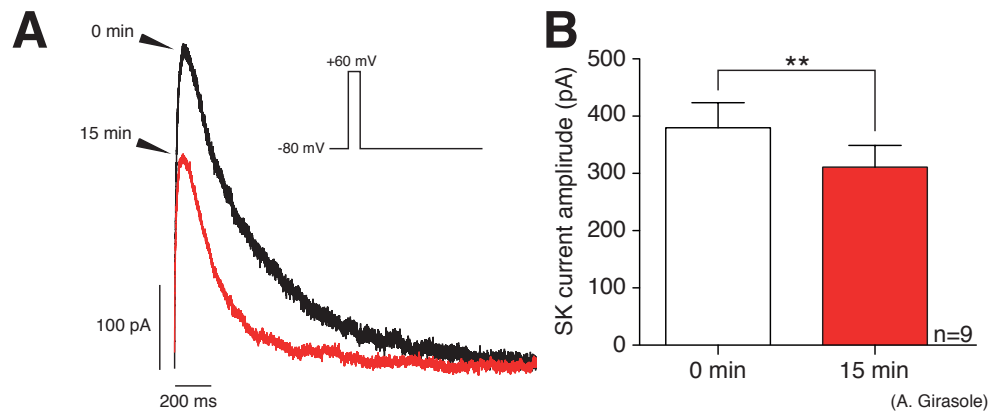


**Figure 5.1:** SK currents decrease during whole cell recordings in SNpc DA neurons. **(A)** Whole cell recording of SK currents in a DA neuron showing the rundown during a 15 min time period. **(B)** Quantification of the whole cell-dependent SK current rundown. Values are means  $\pm$  SEM. \*\*:  $p < 0.01$ . (recordings performed by A. Girasole).

## 5.2 Insulin activates the PI3-kinase pathway

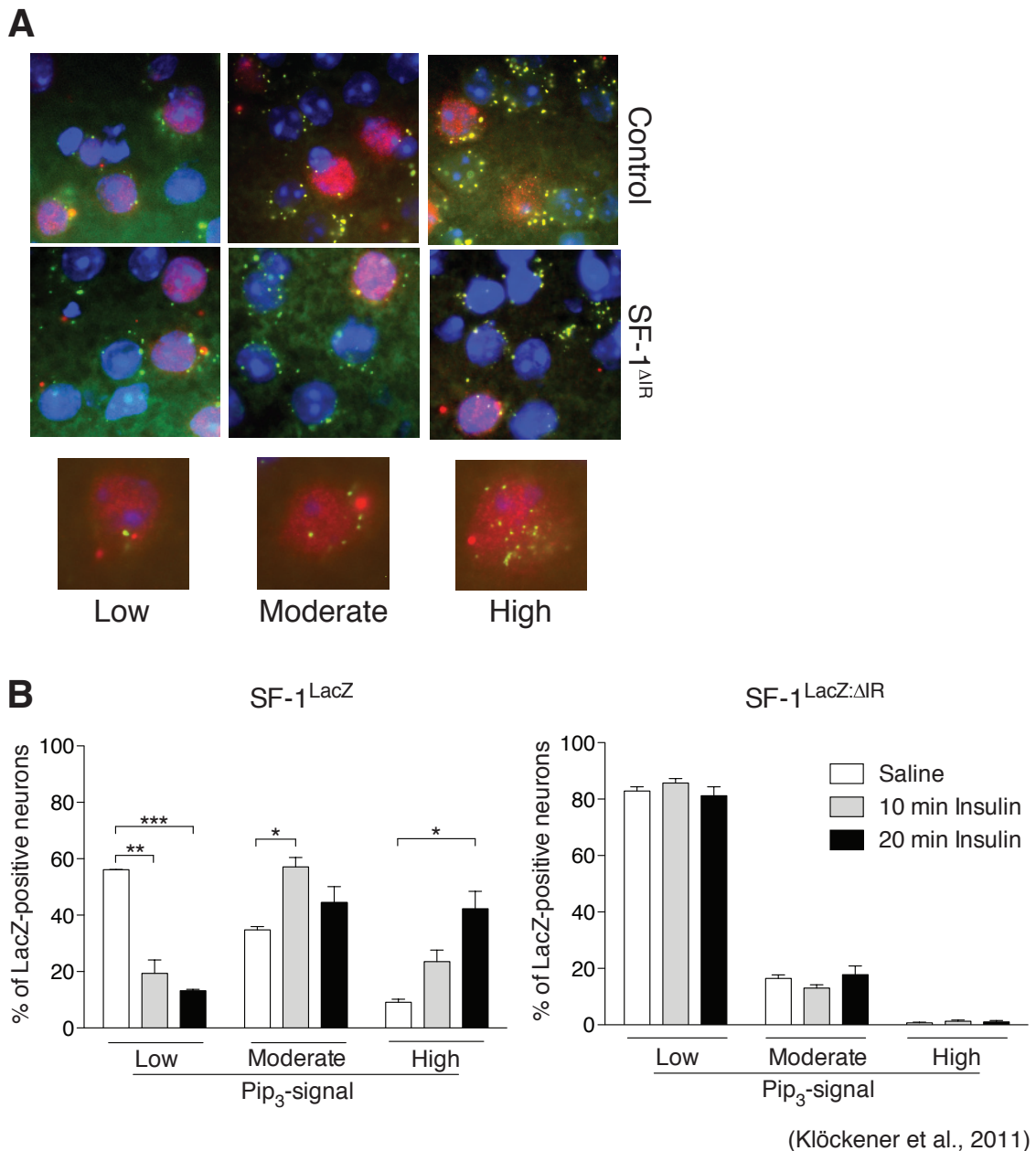


**Figure 5.2:** PIP<sub>3</sub> immunoreactivity of SF-1<sup>LacZ</sup> and SF-1<sup>LacZ:ΔIR</sup> reporter mice. **(A)** Double immunohistochemistry for lacZ and PIP<sub>3</sub> of VMH neurons of SF-1<sup>LacZ</sup> and SF-1<sup>LacZ:ΔIR</sup> reporter mice. A representative section is shown. Blue (DAPI), DNA; red, β-gal (SF-1 neurons); green, PIP<sub>3</sub>. **(B)** Quantification of PIP<sub>3</sub> immunoreactivity of SF-1 VMH neurons in SF-1<sup>LacZ</sup> (left) and SF-1<sup>LacZ:ΔIR</sup> (right) reporter mice after saline, or insulin stimulation for either 10 or 20 min. Values are means ± SEM of sections obtained from at least three mice per stimulation and genotype. 4400 neurons per genotype were counted and quantification was performed as described in methods (taken from Klößener *et al.*, 2011).

### 5.3 Population response of mesencephalic DA neurons upon insulin treatment

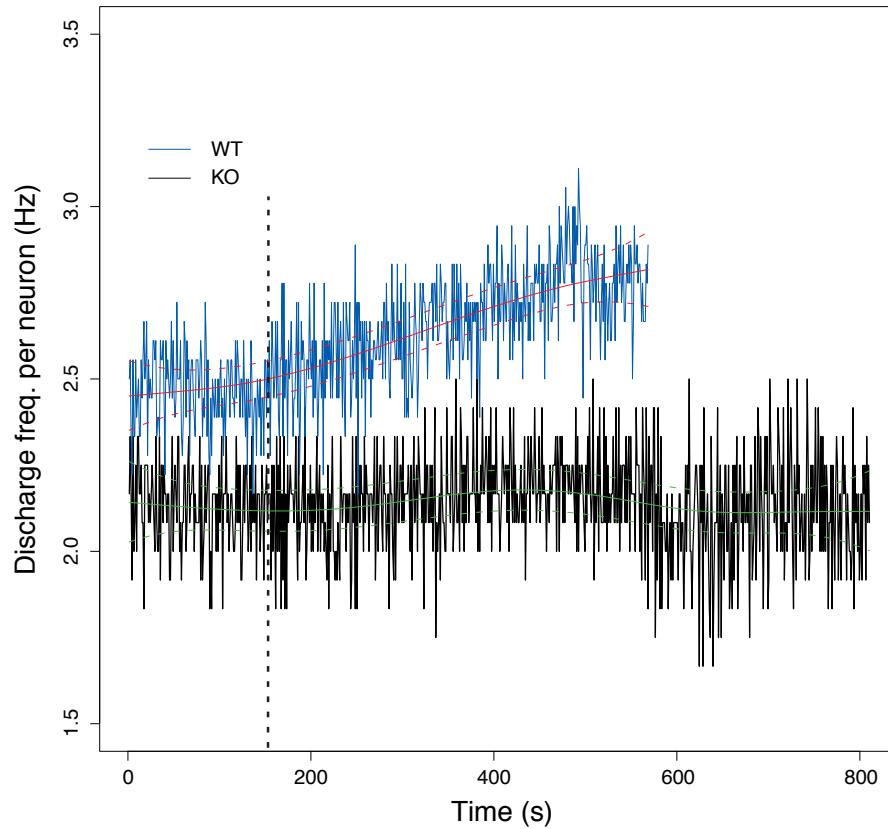


**Figure 5.3:** Population response of mesencephalic DA neurons upon insulin treatment. The diagram shows the time course of insulin's effect on mesencephalic DA neurons. The firing rate of all investigated wildtype ('responder' and 'non-responder') and the  $\text{Th}^{\Delta\text{IR}}$  neurons was pooled and statistically tested using a smoothing spline one-way ANOVA ([R]-script kindly provided by Ch. Pouzat). *Solid red and green lines, mean firing rate; dotted red and green lines, confidence bands; dotted black line, onset of insulin's effect.*

## 5.4 Fto regulates the activity of the dopaminergic circuitry

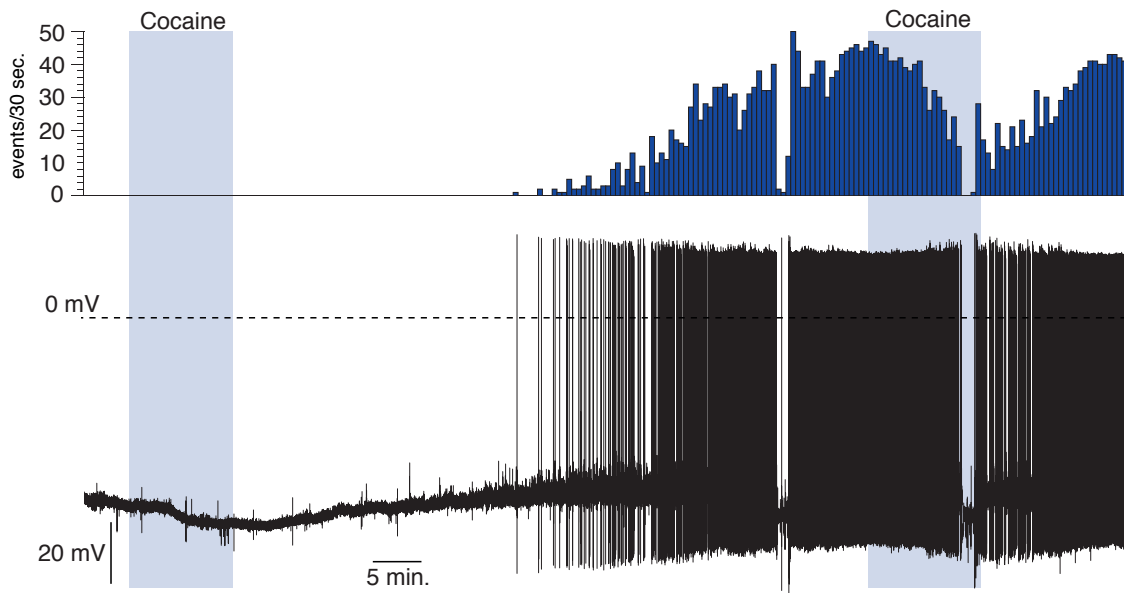


**Figure 5.4:** Perforated-patch recording of a initially silent SNpc DA neuron showing cocaine-induced rebound. *Top* Peristimulus histogram (bin width: 30s) and perforated-patch recording (*bottom*) of a SNpc DA neuron which was not spontaneously active during control. Approximately 25 – 30 min. after termination of the first cocaine application, the cell starts firing again. A second cocaine application reduced the firing of the cell by  $\sim 75\%$  and a consecutive wash restored the firing to values of the first wash. Blue bars indicate cocaine ( $10 \mu\text{M}$ ) perfusion. DA, dopaminergic; SNpc, substantia nigra *pars compacta*.

## 5.5 Fto regulates $D_2$ -receptor-dependent control of firing in mesencephalic DA neurons in a cell-autonomous manner

To directly address the role of Fto in controlling  $D_2R$ -mediated signaling, the selective  $D_2R$  agonist (-)quinpirole was used. Quinpirole concentrations ranging from 1 nM to 1000 nM were tested regarding the effect on membrane conductance density and membrane potential ( $E_M$ ). Quinpirole increases the membrane conductance density in a concentration-dependent manner and the same applies to the hyperpolarization of the membrane potential ( $E_M$ ; see figure 5.5A,B). Concentration-dependent effects of quinpirole can be described with a Hill-equation and yielded nearly the same results for conductance density and  $E_M$  (conductance density –  $EC_{50}$ : 27.7 nM, Hill-slope, 1.17;  $E_M$  –  $EC_{50}$ : 27.4 nM, Hill-slope: 1.28). Note that high concentrations of quinpirole (1000 nM)

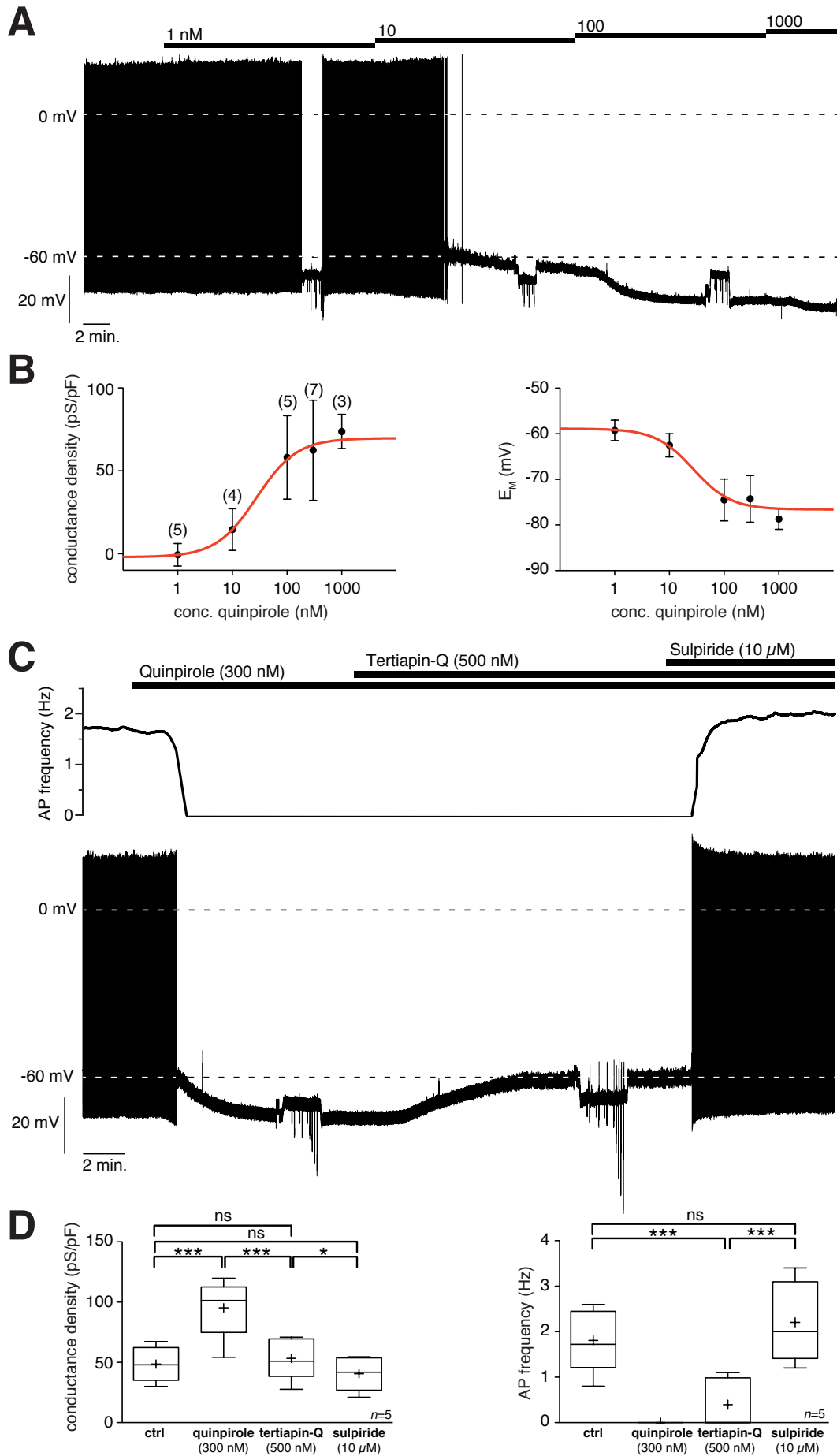
lead to the desensitization of D2R mediated signaling starting 5 – 7 min. after quinpirole application which becomes evident as a decrease in membrane hyperpolarization (data not shown).

D2Rs activate GIRKs via activation of the  $G\beta\gamma$  subunit of the inhibitory  $G\alpha_{i/o}$  protein (see 1.4.2). The specific GIRK-blocker tertiapin-Q was tested for its ability to reverse the quinpirole-mediated activation of D2Rs. Tertiapin-Q (500 nM) was able to reverse the effect of quinpirole (300 nM) on membrane conductance density (see figure 5.5D *left panel*; control:  $48.54 \pm 6.5$  pS/pF; quinpirole:  $95.2 \pm 11.0$  pS/pF; tertiapin-Q:  $53.3 \pm 7.8$  pS/pF;  $n=5$ ; control and tertiapin-Q conductance density are not significantly different). Additionally, tertiapin-Q led to a full recovery of  $E_M$  (see figure 5.5C; data not shown). However, the firing rate did not recover to control values during the application of tertiapin-Q. Additional application of  $10 \mu\text{M}$  (-) sulpiride – a specific D2R antagonist – increased the firing rate to control values (see figure 5.5C,D *right panel*; control:  $1.8 \pm 0.3$  Hz, quinpirole:  $0.0 \pm 0.0$  Hz, tertiapin-Q:  $0.4 \pm 0.2$  Hz, sulpiride:  $2.2 \pm 0.4$  Hz) and led to a further decrease in membrane conductance density ( $40.6 \pm 6.4$  pS/pF).

---

**Figure 5.5 (following page):** Characterization of the D2R mediated effects on SNpc DA neurons. (A) Perforated-patch recording of a SNpc DA neuron during increasing quinpirole concentrations (1 – 1000 nM). (B) Concentration-response curves for quinpirole (*left*: net conductance density; *right*:  $E_M$ ). (C) Perforated-patch recording of a DA neuron during quinpirole (300 nM) application and additional application of tertiapin-Q (500 nM) and sulpiride ( $10 \mu\text{M}$ ). (D) Effect of quinpirole and additional application of tertiapin-Q and sulpiride on membrane conductance density *left* and AP frequency (*right*). AP, action potential;  $E_M$ , membrane potential; D2R, dopamine type 2 receptor; DA, dopaminergic; SNpc, substantia nigra *pars compacta*. For details on box plots see Materials and Methods. \*\*\*:  $p < 0.001$ , \*:  $p < 0.05$ , n.s.:  $p \geq 0.05$ .

---



# List of Figures

1.1	Diagram of hypothalamic projections and the melanocortin system . . . . .	4
1.2	Overview of insulin and leptin signaling pathways . . . . .	8
1.3	Distribution of dopaminergic cell groups . . . . .	13
1.4	Overview of D1R and D2R signaling pathways . . . . .	17
1.5	Schematic drawings of the whole cell and perforated-patch configuration	22
1.6	Molecular properties of nystatin and amphotericin B . . . . .	25
1.7	Molecular properties of gramicidin . . . . .	27
3.1	Comparison of whole cell and perforated-patch recordings . . . . .	42
3.2	Comparison of spike-related parameters during whole cell and perforated-patch recordings . . . . .	43
3.3	Overview of the perforated-patch configuration . . . . .	45
3.4	Properties of SF-1 neurons . . . . .	49
3.5	Insulin effect on SF-1 neurons . . . . .	52
3.6	Alterations in synaptic connectivity in POMC neurons . . . . .	54
3.7	Properties of mesencephalic DA neurons . . . . .	57
3.8	Immunohistochemical characterization of Th-positive neurons of Th <sup>ΔIR</sup> and control mice. . . . .	59
3.9	Insulin increases the activity of mesencephalic DA neurons . . . . .	61
3.10	The insulin effect on mesencephalic DA neurons is cell-intrinsic . . . . .	63
3.11	Wortmannin reverses the excitatory effect of insulin on mesencephalic DA neurons . . . . .	64
3.12	Modified cocaine responsiveness in SNpc DA neurons of Fto <sup>-/-</sup> mice. . . . .	68
3.13	Fto regulates the activity of DA neurons via a D2R-dependent mechanism.	71
3.14	D2R-signaling is necessary for cocaine-induced rebound excitation. . . . .	73
3.15	Fto affects the pacemaker efficacy in DA neurons of cocaine-sensitized animals. . . . .	76

4.1	Wiring diagram of VMH SF-1 neurons . . . . .	86
4.2	Proposed insulin signaling pathway in mesencephalic DA neurons . . . . .	94
5.1	SK currents decrease during whole cell recordings . . . . .	101
5.2	PIP <sub>3</sub> immunoreactivity in SF-1 neurons . . . . .	102
5.3	Population response of mesencephalic DA neurons upon insulin treatment	103
5.4	Cocaine-induced rebound firing in a initially silent SNpc DA neuron . . .	104
5.5	Characterization of the D2R mediated effects on WT SNpc DA neurons .	105

# List of Tables

1.1	Properties of pore-forming compounds . . . . .	29
2.1	Mouse strains used for the thesis . . . . .	33
3.1	Comparison of initial values of basic electrophysiological parameters of mesencephalic DA neurons recorded in the perforated and whole cell configuration. . . . .	41
3.2	Comparison of the effects of amphotericin B and gramicidin on spike parameters of mesencephalic DA neurons . . . . .	46
3.3	Functional properties of SF-1 neurons (SF-1 <sup>GFP</sup> ) . . . . .	48
3.4	Comparison of functional properties of SF-1 <sup>GFP</sup> and SF-1 <sup>GFP:ΔIR</sup> . . . . .	51
3.5	Spike properties of mesencephalic DA neurons before and after insulin application . . . . .	62
3.6	Electrophysiological parameters of Fto <sup>+/+</sup> and Fto <sup>-/-</sup> SNpc DA neurons .	68
3.7	Basic electrophysiological properties of SNpc DA neurons of naïve and cocaine sensitized Fto <sup>+/+</sup> and Fto <sup>-/-</sup> mice . . . . .	75

# Bibliography

- ABIZAID, ALFONSO, LIU, ZHONG-WU, ANDREWS, ZANE B, SHANABROUGH, MARYA, BOROK, ERZSEBET, ELSWORTH, JOHN D, ROTH, ROBERT H, SLEEMAN, MARK W, PICCIOTTO, MARINA R, TSCHÖP, MATTHIAS H, GAO, XIAO-BING, & HORVATH, TAMAS L. 2006. Ghrelin modulates the activity and synaptic input organization of midbrain dopamine neurons while promoting appetite. *J clin invest*, **116**(12), 3229–39.
- ADAN, R A, CONE, R D, BURBACH, J P, & GISPEN, W H. 1994. Differential effects of melanocortin peptides on neural melanocortin receptors. *Mol pharmacol*, **46**(6), 1182–90.
- AKAGI, K, NAGAO, T, & URUSHIDANI, T. 1999. Responsiveness of beta-escin-permeabilized rabbit gastric gland model: effects of functional peptide fragments. *Am j physiol*, **277**(3 Pt 1), G736–44.
- AKAIKE, N, & HARATA, N. 1994. Nystatin perforated patch recording and its applications to analyses of intracellular mechanisms. *Jpn j physiol*, **44**(5), 433–73.
- ANDERSEN, O S, APELL, H J, BAMBERG, E, BUSATH, D D, KOEPPE, R E, SIGWORTH, F J, SZABO, G, URRY, D W, & WOOLLEY, A. 1999. Gramicidin channel controversy—the structure in a lipid environment. *Nat struct biol*, **6**(7), 609; discussion 611–2.
- ANDREOLI, T E. 1973. On the anatomy of amphotericin b-cholesterol pores in lipid bilayer membranes. *Kidney int*, **4**(5), 337–45.
- ASHCROFT, F M, & KAKEI, M. 1989. Atp-sensitive k<sup>+</sup> channels in rat pancreatic beta-cells: modulation by atp and mg<sup>2+</sup> ions. *The journal of physiology*, **416**(Sep), 349–67.
- BAGDADE, J D, BIERMAN, E L, & PORTE, D. 1967. The significance of basal insulin levels in the evaluation of the insulin response to glucose in diabetic and nondiabetic subjects. *J clin invest*, **46**(10), 1549–57.
- BALTHASAR, NINA, COPPARI, ROBERTO, MCMINN, JULIE, LIU, SHUN M, LEE, CHARLOTTE E, TANG, VINSEE, KENNY, CHRISTOPHER D, MCGOVERN, ROBERT A, CHUA, STREAMSON C, ELMQUIST, JOEL K, & LOWELL, BRADFORD B. 2004. Leptin receptor signaling in pomc neurons is required for normal body weight homeostasis. *Neuron*, **42**(6), 983–91.
- BANGHAM, AD, HORNE, RW, GLAUERT, AM, DINGLE, JT, & LUCY, JA. 1962. Action of saponin on biological cell membranes. *Nature*, **196**(Dec), 952–5.
- BANKS, A S, DAVIS, S M, BATES, S H, & MYERS, M G. 2000. Activation of downstream signals by the long form of the leptin receptor. *J biol chem*, **275**(19), 14563–72.
- BANKS, W, KASTIN, A, HUANG, W, & JASPAN... J. 1996. Leptin enters the brain by a saturable system independent of insulin. *Peptides*, Jan.

- BANKS, WILLIAM A. 2006. Blood-brain barrier and energy balance. *Obesity (silver spring)*, **14 Suppl 5**(Aug), 234S–237S.
- BASERGA, R, HONGO, A, RUBINI, M, PRISCO, M, & VALENTINIS, B. 1997. The igf-i receptor in cell growth, transformation and apoptosis. *Biochim biophys acta*, **1332**(3), F105–26.
- BAUKROWITZ, T, SCHULTE, U, OLIVER, D, HERLITZE, S, KRAUTER, T, TUCKER, S J, RUPPERSBERG, J P, & FAKLER, B. 1998. Pip2 and pip as determinants for atp inhibition of katp channels. *Science*, **282**(5391), 1141–4.
- BAURA, G, FOSTER, D, & JR. . . , D PORTE. 1993. Saturable transport of insulin from plasma into the central nervous system of dogs in vivo. a mechanism for regulated insulin delivery to the brain. *Journal of clinical . . .*, Jan.
- BEAN, BRUCE P. 2007. The action potential in mammalian central neurons. *Nat rev neurosci*, **8**(6), 451–65.
- BEAULIEU, JEAN-MARTIN, & GAINETDINOV, RAUL R. 2011. The physiology, signaling, and pharmacology of dopamine receptors. *Pharmacological reviews*, **63**(1), 182–217.
- BELGARDT, BENGT F, & BRÜNING, JENS C. 2010. Cns leptin and insulin action in the control of energy homeostasis. *Ann n y acad sci*, **1212**(Nov), 97–113.
- BELGARDT, BENGT F, HUSCH, ANDREAS, ROTHER, EVA, ERNST, MARIANNE B, WUNDERLICH, F THOMAS, HAMPEL, BRIGITTE, KLÖCKENER, TIM, ALESSI, DARIO, KLOPPENBURG, PETER, & BRÜNING, JENS C. 2008. Pdk1 deficiency in pomc-expressing cells reveals foxo1-dependent and -independent pathways in control of energy homeostasis and stress response. *Cell metabolism*, **7**(4), 291–301.
- BENTIVOGLIO, M, & MORELLI, M. 2005. Chapter i the organization and circuits of mesencephalic dopaminergic neurons and the distribution of dopamine receptors in the brain. *Handbook of chemical neuroanatomy*, Jan.
- BERTHOUD, HANS-RUDOLF. 2002. Multiple neural systems controlling food intake and body weight. *Neuroscience and biobehavioral reviews*, **26**(4), 393–428.
- BJÖRKLUND, ANDERS, & DUNNETT, STEPHEN B. 2007. Dopamine neuron systems in the brain: an update. *Trends neurosci.*, **30**(5), 194–202.
- BOLAÑOS, CARLOS A, & NESTLER, ERIC J. 2004. Neurotrophic mechanisms in drug addiction. *Neuromolecular med*, **5**(1), 69–83.
- BONCI, ANTONELLO, BERNARDI, GIORGIO, GRILLNER, PERNILLA, & MERCURI, NICOLA B. 2003. The dopamine-containing neuron: maestro or simple musician in the orchestra of addiction? *Trends pharmacol sci*, **24**(4), 172–7.
- BORGLAND, STEPHANIE L, TAHA, SHARIF A, SARTI, FEDERICA, FIELDS, HOWARD L, & BONCI, ANTONELLO. 2006. Orexin a in the vta is critical for the induction of synaptic plasticity and behavioral sensitization to cocaine. *Neuron*, **49**(4), 589–601.

- BROBECK, J. 1951. Localization of a "feeding center" in the hypothalamus of the rat. ... of the society for experimental biology ... , Jan.
- BROBECK, J, & TEPPERMAN, J. 1943. Experimental hypothalamic hyperphagia in the albino rat. *The yale journal of biology* ... , Jan.
- BRUCE-KELLER, ANNADORA J, KELLER, JEFFREY N, & MORRISON, CHRISTOPHER D. 2009. Obesity and vulnerability of the cns. *Biochim biophys acta*, **1792**(5), 395–400.
- BRÜNING, J C, GAUTAM, D, BURKS, D J, GILLETTE, J, SCHUBERT, M, ORBAN, P C, KLEIN, R, KRONE, W, MÜLLER-WIELAND, D, & KAHN, C R. 2000. Role of brain insulin receptor in control of body weight and reproduction. *Science*, **289**(5487), 2122–5.
- BURNS, R S, CHIUEH, C C, MARKEY, S P, EBERT, M H, JACOBOWITZ, D M, & KOPIN, I J. 1983. A primate model of parkinsonism: selective destruction of dopaminergic neurons in the pars compacta of the substantia nigra by n-methyl-4-phenyl-1,2,3,6-tetrahydropyridine. *Proc natl acad sci usa*, **80**(14), 4546–50.
- CABALLERO, BENJAMIN. 2007. The global epidemic of obesity: an overview. *Epidemiol rev*, **29**(Jan), 1–5.
- CALABRESI, PAOLO, PICCONI, BARBARA, TOZZI, ALESSANDRO, & FILIPPO, MASSIMILIANO DI. 2007. Dopamine-mediated regulation of corticostriatal synaptic plasticity. *Trends neurosci.*, **30**(5), 211–9.
- CAMERON, D L, WESSENDORF, M W, & WILLIAMS, J T. 1997. A subset of ventral tegmental area neurons is inhibited by dopamine, 5-hydroxytryptamine and opioids. *Neuroscience*, **77**(1), 155–66.
- CANTERAS, N S, SIMERLY, R B, & SWANSON, L W. 1994. Organization of projections from the ventromedial nucleus of the hypothalamus: a phaseolus vulgaris-leucoagglutinin study in the rat. *The journal of comparative neurology*, **348**(1), 41–79.
- CARLSSON, A, & FALCK, B. 1962. Cellular localization of brain monoamines. *Acta physiologica scandinavica*. ... , Jan.
- CARR, KENNETH D. 2002. Augmentation of drug reward by chronic food restriction: behavioral evidence and underlying mechanisms. *Physiology & behavior*, **76**(3), 353–64.
- CARVALHEIRA, JOSÉ B C, TORSONI, MÁRCIO A, UENO, MIRIAN, AMARAL, MARIA E, ARAÚJO, ELIANA P, VELLOSO, LÍCIO A, GONTIJO, JOSÉ A R, & SAAD, MARIO J A. 2005. Cross-talk between the insulin and leptin signaling systems in rat hypothalamus. *Obes res*, **13**(1), 48–57.
- CARVELLI, LUCIA, MORÓN, JOSÉ A, KAHLIG, KRISTOPHER M, FERRER, JASMINE V, SEN, NAMITA, LECHLEITER, JAMES D, LEEB-LUNDBERG, L M FREDRIK, MERRILL, GERALD, LAFER, EILEEN M, BALLOU, LISA M, SHIPPENBERG, TONI S, JAVITCH, JONATHAN A, LIN, RICHARD Z, & GALLI, AURELIO. 2002. Pi 3-kinase regulation of dopamine uptake. *J neurochem*, **81**(4), 859–69.

- CHAN, C SAVIO, GUZMAN, JAIME N, ILIJIC, EMA, MERCER, JEFF N, RICK, CAROLINE, TKATCH, TATIANA, MEREDITH, GLORIA E, & SURMEIER, D JAMES. 2007. 'rejuvenation' protects neurons in mouse models of parkinson's disease. *Nature*, **447**(7148), 1081–6.
- CHEN, H Y, TRUMBAUER, M E, CHEN, A S, WEINGARTH, D T, ADAMS, J R, FRAZIER, E G, SHEN, Z, MARSH, D J, FEIGNER, S D, GUAN, X-M, YE, Z, NARGUND, R P, SMITH, R G, DER PLOEG, L H T VAN, HOWARD, A D, MACNEIL, D J, & QIAN, S. 2004. Orexigenic action of peripheral ghrelin is mediated by neuropeptide y and agouti-related protein. *Endocrinology*, **145**(6), 2607–12.
- CHIARA, G DI, & IMPERATO, A. 1988. Drugs abused by humans preferentially increase synaptic dopamine concentrations in the mesolimbic system of freely moving rats. *Proc natl acad sci usa*, **85**(14), 5274–8.
- CHO, HANA, LEE, DOYUN, LEE, SUK HO, & HO, WON-KYUNG. 2005. Receptor-induced depletion of phosphatidylinositol 4,5-bisphosphate inhibits inwardly rectifying k+ channels in a receptor-specific manner. *Proc natl acad sci usa*, **102**(12), 4643–8.
- CHURCH, CHRIS, MOIR, LEE, MCMURRAY, FIONA, GIRARD, CHRISTOPHE, BANKS, GARETH T, TBOUL, LYDIA, WELLS, SARA, BRÜNING, JENS C, NOLAN, PATRICK M, ASHCROFT, FRANCES M, & COX, ROGER D. 2010. Overexpression of fto leads to increased food intake and results in obesity. *Nat genet*, **42**(12), 1086–92.
- CLARET, MARC, SMITH, MARK A, BATTERHAM, RACHEL L, SELMAN, COLIN, CHOUDHURY, AGHARUL I, FRYER, LEE G D, CLEMENTS, MELANIE, AL-QASSAB, HIND, HEFFRON, HELEN, XU, ALLISON W, SPEAKMAN, JOHN R, BARSH, GREGORY S, VIOLLET, BENOIT, VAULONT, SOPHIE, ASHFORD, MICHAEL L J, CARLING, DAVID, & WITHERS, DOMINIC J. 2007. Ampk is essential for energy homeostasis regulation and glucose sensing by pomc and agrp neurons. *J clin invest*, **117**(8), 2325–36.
- CLIFTON, IAN J, MCDONOUGH, MICHAEL A, EHRISMANN, DOMINIC, KERSHAW, NADIA J, GRANATINO, NICOLAS, & SCHOFIELD, CHRISTOPHER J. 2006. Structural studies on 2-oxoglutarate oxygenases and related double-stranded beta-helix fold proteins. *J inorg biochem*, **100**(4), 644–69.
- CONE, R D, LU, D, KOPPULA, S, VAGE, D I, KLUNGLAND, H, BOSTON, B, CHEN, W, ORTH, D N, POUTON, C, & KESTERSON, R A. 1996. The melanocortin receptors: agonists, antagonists, and the hormonal control of pigmentation. *Recent prog horm res*, **51**(Jan), 287–317; discussion 318.
- CONE, ROGER D. 2005. Anatomy and regulation of the central melanocortin system. *Nat neurosci*, **8**(5), 571–8.
- CONSIDINE, R V, SINHA, M K, HEIMAN, M L, KRIAUCIUNAS, A, STEPHENS, T W, NYCE, M R, OHANNESIAN, J P, MARCO, C C, MCKEE, L J, & BAUER, T L. 1996. Serum immunoreactive-leptin concentrations in normal-weight and obese humans. *N engl j med*, **334**(5), 292–5.

- COWLEY, M A, SMART, J L, RUBINSTEIN, M, CERDÁN, M G, DIANO, S, HORVATH, T L, CONE, R D, & LOW, M J. 2001. Leptin activates anorexigenic pomc neurons through a neural network in the arcuate nucleus. *Nature*, **411**(6836), 480–4.
- CROUZY, S, WOOLF, T B, & ROUX, B. 1994. A molecular dynamics study of gating in dioxolane-linked gramicidin a channels. *Biophys j*, **67**(4), 1370–86.
- DAHLSTRÖM, A, & FUXE, K. 1964. Evidence for the existence of monoamine-containing neurons in the central nervous system. i. demonstration of monoamines in the cell bodies of brain stem neurons. *Acta physiologica scandinavica*. . . , Jan.
- DE KRUIJFF, B, GERRITSEN, W J, OERLEMANS, A, DEMEL, R A, & VAN DEENEN, L L. 1974. Polyene antibiotic-sterol interactions in membranes of acholeplasma laidlawii cells and lecithin liposomes. i. specificity of the membrane permeability changes induced by the polyene antibiotics. *Biochim biophys acta*, **339**(1), 30–43.
- DENNIS, V W, STEAD, N W, & ANDREOLI, T E. 1970. Molecular aspects of polyene- and sterol-dependent pore formation in thin lipid membranes. *J. gen. physiol.*, **55**(3), 375–400.
- DHILLON, HARVEEN, ZIGMAN, JEFFREY M, YE, CHIANPING, LEE, CHARLOTTE E, MCGOVERN, ROBERT A, TANG, VINSEE, KENNY, CHRISTOPHER D, CHRISTIANSEN, LAURYN M, WHITE, RYAN D, EDELSTEIN, ELISABETH A, COPPARI, ROBERTO, BALTHASAR, NINA, COWLEY, MICHAEL A, CHUA, STREAMSON, ELMQUIST, JOEL K, & LOWELL, BRADFORD B. 2006. Leptin directly activates sf1 neurons in the vmh, and this action by leptin is required for normal body-weight homeostasis. *Neuron*, **49**(2), 191–203.
- DINA, CHRISTIAN, MEYRE, DAVID, GALLINA, SOPHIE, DURAND, EMMANUELLE, KÖRNER, ANTJE, JACOBSON, PETER, CARLSSON, LENA M S, KIESS, WIELAND, VATIN, VINCENT, LECOEUR, CECILE, DELPLANQUE, JÉRÔME, VAILLANT, EMMANUEL, PATTOU, FRANÇOIS, RUIZ, JUAN, WEILL, JACQUES, LEVY-MARCHAL, CLAIRE, HORBER, FRITZ, POTOCZNA, NATASCHA, HERCBERG, SERGE, STUNFF, CATHERINE LE, BOUGNÈRES, PIERRE, KOVACS, PETER, MARRE, MICHEL, BALKAU, BEVERLEY, CAUCHI, STÉPHANE, CHÈVRE, JEAN-CLAUDE, & FROGUEL, PHILIPPE. 2007. Variation in fto contributes to childhood obesity and severe adult obesity. *Nat genet*, **39**(6), 724–6.
- DODT, H U, & ZIEGLGÄNSBERGER, W. 1990. Visualizing unstained neurons in living brain slices by infrared dic-videomicroscopy. *Brain research*, **537**(1-2), 333–6.
- DOYON, C, DROUIN, G, & TRUDEAU... , V. 2001. Molecular evolution of leptin. *General and comparative* . . . , Jan.
- DUBOS, R J, & HOTCHKISS, R D. 1941. The production of bactericidal substances by aerobic sporulating bacilli. *J exp med*, **73**(5), 629–40.
- ELMQUIST, J, BJOERBAEK, C, & AHIMA... , R. 1998a. Distributions of leptin receptor mrna isoforms in the rat brain. *The journal of* . . . , Jan.

- ELMQUIST, J K, AHIMA, R S, ELIAS, C F, FLIER, J S, & SAPER, C B. 1998b. Leptin activates distinct projections from the dorsomedial and ventromedial hypothalamic nuclei. *Proc natl acad sci usa*, **95**(2), 741–6.
- EPSS, HEATHER L VAN. 2006. René dubos: unearthing antibiotics. *J exp med*, **203**(2), 259.
- FADEL, J, & DEUTCH, A Y. 2002. Anatomical substrates of orexin-dopamine interactions: lateral hypothalamic projections to the ventral tegmental area. *Neuroscience*, **111**(2), 379–87.
- FAN, J S, & PALADE, P. 1998. Perforated patch recording with beta-escin. *Pflugers arch*, **436**(6), 1021–3.
- FIGLEWICZ, D P, SZOT, P, CHAVEZ, M, WOODS, S C, & VEITH, R C. 1994. Intraventricular insulin increases dopamine transporter mrna in rat vta/substantia nigra. *Brain research*, **644**(2), 331–4.
- FIGLEWICZ, D P, HIGGINS, M S, NG-EVANS, S B, & HAVEL, P J. 2001. Leptin reverses sucrose-conditioned place preference in food-restricted rats. *Physiology & behavior*, **73**(1-2), 229–34.
- FIGLEWICZ, D P, EVANS, S B, MURPHY, J, HOEN, M, & BASKIN, D G. 2003. Expression of receptors for insulin and leptin in the ventral tegmental area/substantia nigra (vta/sn) of the rat. *Brain research*, **964**(1), 107–15.
- FIGLEWICZ, DIANNE P, & BENOIT, STEPHEN C. 2009. Insulin, leptin, and food reward: update 2008. *Am j physiol regul integr comp physiol*, **296**(1), R9–R19.
- FIGLEWICZ, DIANNE P, BENNETT, JENNIFER, EVANS, SCOTT B, KAIYALA, KARL, SIPOLS, ALFRED J, & BENOIT, STEPHEN C. 2004. Intraventricular insulin and leptin reverse place preference conditioned with high-fat diet in rats. *Behav neurosci*, **118**(3), 479–87.
- FIGLEWICZ, DIANNE P, BENNETT, JENNIFER L, NALEID, AMY MACDONALD, DAVIS, CHARLES, & GRIMM, JEFFREY W. 2006. Intraventricular insulin and leptin decrease sucrose self-administration in rats. *Physiology & behavior*, **89**(4), 611–6.
- FIGLEWICZ, DIANNE P, NALEID, AMY MACDONALD, & SIPOLS, ALFRED J. 2007. Modulation of food reward by adiposity signals. *Physiology & behavior*, **91**(5), 473–8.
- FINKELSTEIN, A, & HOLZ, R. 1973. Aqueous pores created in thin lipid membranes by the polyene antibiotics nystatin and amphotericin b. *Membranes*, **2**(Jan), 377–408.
- FISCHER, JULIA, KOCH, LINDA, EMMERLING, CHRISTIAN, VIERKOTTEN, JEANETTE, PETERS, THOMAS, BRÜNING, JENS C, & RÜTHER, ULRICH. 2009. Inactivation of the fto gene protects from obesity. *Nature*, **458**(7240), 894–8.
- FLORESCO, STAN B, WEST, ANTHONY R, ASH, BRIAN, MOORE, HOLLY, & GRACE, ANTHONY A. 2003. Afferent modulation of dopamine neuron firing differentially regulates tonic and phasic dopamine transmission. *Nature neuroscience*, **6**(9), 968–73.

- FRAYLING, TIMOTHY M, TIMPSON, NICHOLAS J, WEEDON, MICHAEL N, ZEGGINI, ELEFTHERIA, FREATHY, RACHEL M, LINDGREN, CECILIA M, PERRY, JOHN R B, ELLIOTT, KATHERINE S, LANGO, HANA, RAYNER, NIGEL W, SHIELDS, BEVERLEY, HARRIES, LORNA W, BARRATT, JEFFREY C, ELLARD, SIAN, GROVES, CHRISTOPHER J, KNIGHT, BRIDGET, PATCH, ANN-MARIE, NESS, ANDREW R, EBRAHIM, SHAH, LAWLOR, DEBBIE A, RING, SUSAN M, BEN-SHLOMO, YOAV, JARVELIN, MARJO-RIITTA, SOVIO, ULLA, BENNETT, AMANDA J, MELZER, DAVID, FERRUCCI, LUIGI, LOOS, RUTH J F, BARROSO, INÊS, WAREHAM, NICHOLAS J, KARPE, FREDRIK, OWEN, KATHARINE R, CARDON, LON R, WALKER, MARK, HITMAN, GRAHAM A, PALMER, COLIN N A, DONEY, ALEX S F, MORRIS, ANDREW D, SMITH, GEORGE DAVEY, HATTERSLEY, ANDREW T, & MCCARTHY, MARK I. 2007. A common variant in the *fto* gene is associated with body mass index and predisposes to childhood and adult obesity. *Science*, **316**(5826), 889–94.
- FREDERICH, R, HAMANN, A, & ANDERSON... , S. 1995. Leptin levels reflect body lipid content in mice: evidence for diet-induced resistance to leptin action. *Nature medicine*, Jan.
- FREDRIKSSON, ROBERT, HÄGGLUND, MARIA, OLSZEWSKI, PAWEŁ K, STEPHANSSON, OLGA, JACOBSSON, JOSEFIN A, OLSZEWSKA, AGNIESZKA M, LEVINE, ALLEN S, LINDBLOM, JONAS, & SCHIÖTH, HELGI B. 2008. The obesity gene, *fto*, is of ancient origin, up-regulated during food deprivation and expressed in neurons of feeding-related nuclei of the brain. *Endocrinology*, **149**(5), 2062–71.
- FREEMAN, A S, MELTZER, L T, & BUNNEY, B S. 1985. Firing properties of substantia nigra dopaminergic neurons in freely moving rats. *Life sci*, **36**(20), 1983–94.
- FULTON, STEPHANIE, PISSIOS, PAVLOS, MANCHON, RAMON PINOL, STILES, LINSEY, FRANK, LAUREN, POTHOS, EMMANUEL N, MARATOS-FLIER, ELEFTHERIA, & FLIER, JEFFREY S. 2006. Leptin regulation of the mesoaccumbens dopamine pathway. *Neuron*, **51**(6), 811–22.
- GAO, QIAN, & HORVATH, TAMAS L. 2007. Neurobiology of feeding and energy expenditure. *Annu. rev. neurosci.*, **30**(Jan), 367–98.
- GAROFALO, R. 2002. Genetic analysis of insulin signaling in drosophila. *Trends in endocrinology and metabolism*, Jan.
- GEIGER, B M, HABURCAK, M, AVENA, N M, MOYER, M C, HOEBEL, B G, & POTHOS, E N. 2009. Deficits of mesolimbic dopamine neurotransmission in rat dietary obesity. *Neuroscience*, **159**(4), 1193–9.
- GEIGER, BRENDA M, BEHR, GERALD G, FRANK, LAUREN E, CALDERA-SIU, ANGELA D, BEINFELD, MARGERY C, KOKKOTOU, EFI G, & POTHOS, EMMANUEL N. 2008. Evidence for defective mesolimbic dopamine exocytosis in obesity-prone rats. *Faseb j*, **22**(8), 2740–6.
- GEISLER, STEFANIE, DERST, CHRISTIAN, VEH, RÜDIGER W, & ZAHM, DANIEL S. 2007. Glutamatergic afferents of the ventral tegmental area in the rat. *J neurosci*, **27**(21), 5730–43.

- GERKEN, THOMAS, GIRARD, CHRISTOPHE A, TUNG, YI-CHUN LORAINÉ, WEBBY, CELIA J, SAUDEK, VLADIMIR, HEWITSON, KIRSTY S, YEO, GILES S H, McDONOUGH, MICHAEL A, CUNLIFFE, SHARON, MCNEILL, LUKE A, GALVANOVSKIS, JURIS, RORSMAN, PATRIK, ROBINS, PETER, PRIEUR, XAVIER, COLL, ANTHONY P, MA, MARCELLA, JOVANOVIĆ, ZORICA, FAROOQI, I SADAË, SEDGWICK, BARBARA, BARROSO, INÊS, LINDAHL, TOMAS, PONTING, CHRIS P, ASHCROFT, FRANCES M, O'RAHILLY, STEPHEN, & SCHOFIELD, CHRISTOPHER J. 2007. The obesity-associated fto gene encodes a 2-oxoglutarate-dependent nucleic acid demethylase. *Science*, **318**(5855), 1469–72.
- GIROS, B, SOKOLOFF, P, MARTRES, M P, RIOU, J F, EMORINE, L J, & SCHWARTZ, J C. 1989. Alternative splicing directs the expression of two d2 dopamine receptor isoforms. *Nature*, **342**(6252), 923–6.
- GOTO, YUKIORI, & GRACE, ANTHONY A. 2005. Dopaminergic modulation of limbic and cortical drive of nucleus accumbens in goal-directed behavior. *Nature neuroscience*, **8**(6), 805–12.
- GRACE, A A. 1991. Phasic versus tonic dopamine release and the modulation of dopamine system responsivity: a hypothesis for the etiology of schizophrenia. *Neuroscience*, **41**(1), 1–24.
- GRACE, A A, & BUNNEY, B S. 1984. The control of firing pattern in nigral dopamine neurons: single spike firing. *J neurosci*, **4**(11), 2866–76.
- GRACE, A A, & BUNNEY, B S. 1985. Opposing effects of striatonigral feedback pathways on midbrain dopamine cell activity. *Brain research*, **333**(2), 271–84.
- GRACE, A A, & ONN, S P. 1989. Morphology and electrophysiological properties of immunocytochemically identified rat dopamine neurons recorded in vitro. *J. neurosci.*, **9**(10), 3463–81.
- GRACE, ANTHONY A, FLORESCO, STAN B, GOTO, YUKIORI, & LODGE, DANIEL J. 2007. Regulation of firing of dopaminergic neurons and control of goal-directed behaviors. *Trends neurosci.*, **30**(5), 220–7.
- GREENGARD, P. 2001. The neurobiology of slow synaptic transmission. *Science*, **294**(5544), 1024–30.
- GREENGARD, P, ALLEN, P B, & NAIRN, A C. 1999. Beyond the dopamine receptor: the darpp-32/protein phosphatase-1 cascade. *Neuron*, **23**(3), 435–47.
- HAMILL, O P, MARTY, A, NEHER, E, SAKMANN, B, & SIGWORTH, F J. 1981. Improved patch-clamp techniques for high-resolution current recording from cells and cell-free membrane patches. *Pflügers archiv*, **391**(2), 85–100.
- HAN, ZHIFU, NIU, TIANHUI, CHANG, JUNBIAO, LEI, XIAOGUANG, ZHAO, MINGYAN, WANG, QIANG, CHENG, WEI, WANG, JINJING, FENG, YI, & CHAI, JIJIE. 2010. Crystal structure of the fto protein reveals basis for its substrate specificity. *Nature*, **464**(7292), 1205–9.

- HAVRANKOVA, J, ROTH, J, & BROWNSTEIN, M. 1978. Insulin receptors are widely distributed in the central nervous system of the rat. *Nature*, **272**(5656), 827–9.
- HE, WU, LAM, TONY K T, OBICI, SILVANA, & ROSSETTI, LUCIANO. 2006. Molecular disruption of hypothalamic nutrient sensing induces obesity. *Nature neuroscience*, **9**(2), 227–33.
- HERNANDEZ, L, & HOEBEL, B G. 1988. Food reward and cocaine increase extracellular dopamine in the nucleus accumbens as measured by microdialysis. *Life sci*, **42**(18), 1705–12.
- HERVÉ, D, & GIRAULT, JA. 2005. Signal transduction of dopamine receptors. *Dopamine*, Jan.
- HERVEY, G. 1959. The effects of lesions in the hypothalamus in parabiotic rats. *The journal of physiology*, Jan.
- HETHERINGTON, AW. 1940. Hypothalamic lesions and adiposity in the rat. *The anatomical record*, Jan.
- HETHERINGTON, AW. 1944. Non-production of hypothalamic obesity in the rat by lesions rostral or dorsal to the ventro-medial hypothalamic nuclei. *The journal of comparative neurology*, Jan.
- HILL, J, WILLIAMS, K, YE, C, LUO, J, BALTHASAR, N, COPPARI, R, COWLEY, M, CANTLEY, L, LOWELL, B, & ELMQUIST, J. 2008. Acute effects of leptin require pi3k signaling in hypothalamic proopiomelanocortin neurons in mice. *J clin invest*, **118**(5), 1796–1805.
- HOMMEL, JONATHAN D, TRINKO, RICHARD, SEARS, ROBERT M, GEORGESCU, DAN, LIU, ZONG-WU, GAO, XIAO-BING, THURMON, JEREMY J, MARINELLI, MICHELA, & DILEONE, RALPH J. 2006. Leptin receptor signaling in midbrain dopamine neurons regulates feeding. *Neuron*, **51**(6), 801–10.
- HORN, R, & MARTY, A. 1988. Muscarinic activation of ionic currents measured by a new whole-cell recording method. *J. gen. physiol.*, **92**(2), 145–59.
- HUNTER, RICHARD G, PHILPOT, KELLY, VICENTIC, ALEKSANDRA, DOMINGUEZ, GERALDINA, HUBERT, GEORGE W, & KUCHAR, MICHAEL J. 2004. Cart in feeding and obesity. *Trends endocrinol metab*, **15**(9), 454–9.
- HUXLEY, RACHEL R, ANSARY-MOGHADDAM, ALIREZA, CLIFTON, PETER, CZERNICHOW, SEBASTIEN, PARR, CHRISTINE L, & WOODWARD, MARK. 2009. The impact of dietary and lifestyle risk factors on risk of colorectal cancer: a quantitative overview of the epidemiological evidence. *Int j cancer*, **125**(1), 171–80.
- HYMAN, STEVEN E, MALENKA, ROBERT C, & NESTLER, ERIC J. 2006. Neural mechanisms of addiction: the role of reward-related learning and memory. *Annu. rev. neurosci.*, **29**(Jan), 565–98.

- IBRAHIM, N, BOSCH, M, SMART, J, QIU, J, & . . . , M RUBINSTEIN. 2003. Hypothalamic proopiomelanocortin neurons are glucose responsive and express katp channels. *Endocrinology*, Jan.
- IKEDA, Y, LUO, X, ABBUD, R, NILSON, J H, & PARKER, K L. 1995. The nuclear receptor steroidogenic factor 1 is essential for the formation of the ventromedial hypothalamic nucleus. *Mol endocrinol*, **9**(4), 478–86.
- INGRAM, SUSAN L, PRASAD, BALAKRISHNA M, & AMARA, SUSAN G. 2002. Dopamine transporter-mediated conductances increase excitability of midbrain dopamine neurons. *Nature neuroscience*, **5**(10), 971–8.
- IVERSEN, SUSAN D, & IVERSEN, LESLIE L. 2007. Dopamine: 50 years in perspective. *Trends neurosci.*, **30**(5), 188–93.
- JAAKKOLA, P, MOLE, D R, TIAN, Y M, WILSON, M I, GIELBERT, J, GASKELL, S J, AV, KRIEGSHEIM, HEBESTREIT, H F, MUKHERJI, M, SCHOFIELD, C J, MAXWELL, P H, PUGH, C W, & RATCLIFFE, P J. 2001. Targeting of hif-alpha to the von hippel-lindau ubiquitylation complex by o2-regulated prolyl hydroxylation. *Science*, **292**(5516), 468–72.
- JERLHAG, ELISABET, EGECIOGLU, EMIL, DICKSON, SUZANNE L, ANDERSSON, MALIN, SVENSSON, LENNART, & ENGEL, JÖRGEN A. 2006. Ghrelin stimulates locomotor activity and accumbal dopamine-overflow via central cholinergic systems in mice: implications for its involvement in brain reward. *Addict biol*, **11**(1), 45–54.
- JIA, GUIFANG, YANG, CAI-GUANG, YANG, SHANGDONG, JIAN, XING, YI, CHENGQI, ZHOU, ZHIQIANG, & HE, CHUAN. 2008. Oxidative demethylation of 3-methylthymine and 3-methyluracil in single-stranded dna and rna by mouse and human fto. *Febs lett*, **582**(23-24), 3313–9.
- JOHNSON, PAUL M, & KENNY, PAUL J. 2010. Dopamine d2 receptors in addiction-like reward dysfunction and compulsive eating in obese rats. *Nature neuroscience*, **13**(5), 635–41.
- JONES, S, & KAUER, J A. 1999. Amphetamine depresses excitatory synaptic transmission via serotonin receptors in the ventral tegmental area. *J neurosci*, **19**(22), 9780–7.
- KARSCHIN, C, DISSMANN, E, STÜHMER, W, & KARSCHIN, A. 1996. Irk(1-3) and girk(1-4) inwardly rectifying k+ channel mrnas are differentially expressed in the adult rat brain. *J. neurosci.*, **16**(11), 3559–70.
- KAUER, JULIE A. 2004. Learning mechanisms in addiction: synaptic plasticity in the ventral tegmental area as a result of exposure to drugs of abuse. *Annu rev physiol*, **66**(Jan), 447–75.
- KAUER, JULIE A, & MALENKA, ROBERT C. 2007. Synaptic plasticity and addiction. *Nat rev neurosci*, **8**(11), 844–58.

- KEBABIAN, J W, & CALNE, D B. 1979. Multiple receptors for dopamine. *Nature*, **277**(5692), 93–6.
- KENNEDY, GC. 1953. The role of depot fat in the hypothalamic control of food intake in the rat. *Proc r soc lond, b, biol sci*, **140**(901), 578–96.
- KHAN, F A, GOFORTH, P B, ZHANG, M, & SATIN, L S. 2001. Insulin activates atp-sensitive k(+) channels in pancreatic beta-cells through a phosphatidylinositol 3-kinase-dependent pathway. *Diabetes*, **50**(10), 2192–8.
- KHAN, Z U, MRZLJAK, L, GUTIERREZ, A, DE LA CALLE, A, & GOLDMAN-RAKIC, P S. 1998. Prominence of the dopamine d2 short isoform in dopaminergic pathways. *Proc natl acad sci usa*, **95**(13), 7731–6.
- KILLIAN, J A, PRASAD, K U, HAINS, D, & URRY, D W. 1988. The membrane as an environment of minimal interconversion. a circular dichroism study on the solvent dependence of the conformational behavior of gramicidin in diacylphosphatidylcholine model membranes. *Biochemistry*, **27**(13), 4848–55.
- KITAI, S T, SHEPARD, P D, CALLAWAY, J C, & SCROGGS, R. 1999. Afferent modulation of dopamine neuron firing patterns. *Curr opin neurobiol*, **9**(6), 690–7.
- KLEINBERG, M E, & FINKELSTEIN, A. 1984. Single-length and double-length channels formed by nystatin in lipid bilayer membranes. *J membr biol*, **80**(3), 257–69.
- KLÖCKENER, TIM, HESS, SIMON, BELGARDT, BENGT F, PAEGER, LARS, VERHAGEN, LINDA A W, HUSCH, ANDREAS, SOHN, JONG-WOO, HAMPEL, BRIGITTE, DHILLON, HARVEEN, ZIGMAN, JEFFREY M, LOWELL, BRADFORD B, WILLIAMS, KEVIN W, ELMQUIST, JOEL K, HORVATH, TAMAS L, KLOPPENBURG, PETER, & BRÜNING, JENS C. 2011. High-fat feeding promotes obesity via insulin receptor/pi3k-dependent inhibition of sf-1 vmh neurons. *Nature neuroscience*, Jun.
- KLOPPENBURG, PETER, ZIPFEL, WARREN R, WEBB, WATT W, & HARRIS-WARRICK, RONALD M. 2007. Heterogeneous effects of dopamine on highly localized, voltage-induced ca2+ accumulation in identified motoneurons. *J neurophysiol*, **98**(5), 2910–7.
- KLOSE, ROBERT J, YAMANE, KENICHI, BAE, YANGJIN, ZHANG, DIANZHENG, ERDJUMENT-BROMAGE, HEDIYE, TEMPST, PAUL, WONG, JIEMIN, & ZHANG, YI. 2006. The transcriptional repressor jhdm3a demethylates trimethyl histone h3 lysine 9 and lysine 36. *Nature*, **442**(7100), 312–6.
- KOBAYASHI, S, KITAZAWA, T, SOMLYO, A V, & SOMLYO, A P. 1989. Cytosolic heparin inhibits muscarinic and alpha-adrenergic ca2+ release in smooth muscle. physiological role of inositol 1,4,5-trisphosphate in pharmacomechanical coupling. *J biol chem*, **264**(30), 17997–8004.
- KOMORI, T, MORIKAWA, Y, NANJO, K, & SENBA, E. 2006. Induction of brain-derived neurotrophic factor by leptin in the ventromedial hypothalamus. *Neuroscience*, **139**(3), 1107–15.

- KONISHI, M, & WATANABE, M. 1995. Resting cytoplasmic free ca<sup>2+</sup> concentration in frog skeletal muscle measured with fura-2 conjugated to high molecular weight dextran. *J. gen. physiol.*, **106**(6), 1123–50.
- KÖNNER, A CHRISTINE, JANOSCHEK, RUTH, PLUM, LEONA, JORDAN, SABINE D, ROTHER, EVA, MA, XIAOSONG, XU, CHUN, ENRIORI, PABLO, HAMPSEL, BRIGITTE, BARSH, GREGORY S, KAHN, C RONALD, COWLEY, MICHAEL A, ASHCROFT, FRANCES M, & BRÜNING, JENS C. 2007. Insulin action in agrp-expressing neurons is required for suppression of hepatic glucose production. *Cell metab*, **5**(6), 438–49.
- KÖNNER, A CHRISTINE, HESS, SIMON, TOVAR, SULAY, MESAROS, ANDREA, SÁNCHEZ-LASHERAS, CARMEN, EVERS, NADINE, VERHAGEN, LINDA A W, BRÖNNEKE, HELLA S, KLEINRIDDEES, ANDRÉ, HAMPSEL, BRIGITTE, KLOPPENBURG, PETER, & BRÜNING, JENS C. 2011. Role for insulin signaling in catecholaminergic neurons in control of energy homeostasis. *Cell metabolism*, **13**(6), 720–8.
- KOROTKOVA, T M, BROWN, R E, SERGEEVA, O A, PONOMARENKO, A A, & HAAS, H L. 2006. Effects of arousal- and feeding-related neuropeptides on dopaminergic and gabaergic neurons in the ventral tegmental area of the rat. *Eur j neurosci*, **23**(10), 2677–85.
- KOROTKOVA, TATIANA M, SERGEEVA, OLGA A, ERIKSSON, KRISTER S, HAAS, HELMUT L, & BROWN, RITCHIE E. 2003. Excitation of ventral tegmental area dopaminergic and nondopaminergic neurons by orexins/hypocretins. *J neurosci*, **23**(1), 7–11.
- KRÜGEL, UTE, SCHRAFT, THOMAS, KITTNER, HOLGER, KIESS, WIELAND, & ILLES, PETER. 2003. Basal and feeding-evoked dopamine release in the rat nucleus accumbens is depressed by leptin. *Eur j pharmacol*, **482**(1-3), 185–7.
- KYZOZIS, A, & REICHLING, D B. 1995. Perforated-patch recording with gramicidin avoids artifactual changes in intracellular chloride concentration. *J neurosci methods*, **57**(1), 27–35.
- LACEY, M G, MERCURI, N B, & NORTH, R A. 1989. Two cell types in rat substantia nigra zona compacta distinguished by membrane properties and the actions of dopamine and opioids. *J. neurosci.*, **9**(4), 1233–41.
- LACEY, M G, MERCURI, N B, & NORTH, R A. 1990. Actions of cocaine on rat dopaminergic neurones in vitro. *Br j pharmacol*, **99**(4), 731–5.
- LAMMEL, STEPHAN, HETZEL, ANDREA, HÄCKEL, OLGA, JONES, IAN, LISS, BIRGIT, & ROEPER, JOCHEN. 2008. Unique properties of mesoprefrontal neurons within a dual mesocorticolimbic dopamine system. *Neuron*, **57**(5), 760–73.
- LINDAU, M, & FERNANDEZ, J M. 1986. Ige-mediated degranulation of mast cells does not require opening of ion channels. *Nature*, **319**(6049), 150–3.
- LISS, B, BRUNS, R, & ROEPER, J. 1999. Alternative sulfonylurea receptor expression defines metabolic sensitivity of k-atp channels in dopaminergic midbrain neurons. *Embo j*, **18**(4), 833–46.

- LLINÁS, R, & YAROM, Y. 1981. Properties and distribution of ionic conductances generating electroresponsiveness of mammalian inferior olivary neurones in vitro. *The journal of physiology*, **315**(Jun), 569–84.
- LODGE, D J, & GRACE, A A. 2006. The laterodorsal tegmentum is essential for burst firing of ventral tegmental area dopamine neurons. *Proc natl acad sci usa*, **103**(13), 5167–72.
- LOGRASSO, P V, MOLL, F, & CROSS, T A. 1988. Solvent history dependence of gramicidin a conformations in hydrated lipid bilayers. *Biophys j*, **54**(2), 259–67.
- LUCHSINGER, JOSE A, & MAYEUX, RICHARD. 2007. Adiposity and alzheimer's disease. *Curr alzheimer res*, **4**(2), 127–34.
- LUO, X, IKEDA, Y, & PARKER, K L. 1994. A cell-specific nuclear receptor is essential for adrenal and gonadal development and sexual differentiation. *Cell*, **77**(4), 481–90.
- MAJDIC, GREGOR, YOUNG, MORAG, GOMEZ-SANCHEZ, ELISE, ANDERSON, PAUL, SZCZEPANIAK, LIDIA S, DOBBINS, ROBERT L, MCGARRY, J DENIS, & PARKER, KEITH L. 2002. Knockout mice lacking steroidogenic factor 1 are a novel genetic model of hypothalamic obesity. *Endocrinology*, **143**(2), 607–14.
- MARGOLIS, ELYSSA B, LOCK, HAGAR, HJELMSTAD, GREGORY O, & FIELDS, HOWARD L. 2006. The ventral tegmental area revisited: is there an electrophysiological marker for dopaminergic neurons? *The journal of physiology*, **577**(Pt 3), 907–24.
- MARGOLIS, ELYSSA B, MITCHELL, JENNIFER M, ISHIKAWA, JUNKO, HJELMSTAD, GREGORY O, & FIELDS, HOWARD L. 2008. Midbrain dopamine neurons: projection target determines action potential duration and dopamine d(2) receptor inhibition. *J. neurosci.*, **28**(36), 8908–13.
- MARKS, J L, PORTE, D, STAHL, W L, & BASKIN, D G. 1990. Localization of insulin receptor mrna in rat brain by in situ hybridization. *Endocrinology*, **127**(6), 3234–6.
- MARSHALL, NB, & MAYER, J. 1956. Specificity of gold thioglucose for ventromedial hypothalamic lesions and hyperphagia. *Nature*, **178**(4547), 1399–400.
- MIKI, T, LISS, B, MINAMI, K, SHIUCHI, T, & SARAYA, A. 2001. Atp-sensitive k channels in the hypothalamus are essential for the maintenance of glucose . . . *Nature neuroscience*, Jan.
- MINAMI, T, OOMURA, Y, & SUGIMORI, M. 1986. Electrophysiological properties and glucose responsiveness of guinea-pig ventromedial hypothalamic neurones in vitro. *The journal of physiology*, **380**(Nov), 127–43.
- MIRSHAMSI, SHIRIN, LAIDLAW, HILARY A, NING, KE, ANDERSON, ERIN, BURGESS, LAURA A, GRAY, ALEXANDER, SUTHERLAND, CALUM, & ASHFORD, MICHAEL L J. 2004. Leptin and insulin stimulation of signalling pathways in arcuate nucleus neurones: P13k dependent actin reorganization and katp channel activation. *Bmc neuroscience*, **5**(1), 54.

- MISSALE, C, NASH, S R, ROBINSON, S W, JABER, M, & CARON, M G. 1998. Dopamine receptors: from structure to function. *Physiol rev*, **78**(1), 189–225.
- MITCHELL, JOHN B O, & SMITH, JAMES. 2003. D-amino acid residues in peptides and proteins. *Proteins*, **50**(4), 563–71.
- MORTON, G J, CUMMINGS, D E, BASKIN, D G, BARSH, G S, & SCHWARTZ, M W. 2006. Central nervous system control of food intake and body weight. *Nature*, **443**(7109), 289–95.
- MOSHER, CATHERINE E, SLOANE, RICHARD, MOREY, MIRIAM C, SNYDER, DENISE CLUTTER, COHEN, HARVEY J, MILLER, PAIGE E, & DEMARK-WAHNEFRIED, WENDY. 2009. Associations between lifestyle factors and quality of life among older long-term breast, prostate, and colorectal cancer survivors. *Cancer*, **115**(17), 4001–9.
- MOUNTJOY, K G, MORTRUD, M T, LOW, M J, SIMERLY, R B, & CONE, R D. 1994. Localization of the melanocortin-4 receptor (mc4-r) in neuroendocrine and autonomic control circuits in the brain. *Mol endocrinol*, **8**(10), 1298–308.
- MUST, A, SPADANO, J, COAKLEY, E H, FIELD, A E, COLDITZ, G, & DIETZ, W H. 1999. The disease burden associated with overweight and obesity. *Jama*, **282**(16), 1523–9.
- MYERS, V B, & HAYDON, D A. 1972. Ion transfer across lipid membranes in the presence of gramicidin a. ii. the ion selectivity. *Biochim biophys acta*, **274**(2), 313–22.
- NESTLER, ERIC J. 2004. Molecular mechanisms of drug addiction. *Neuropharmacology*, **47 Suppl 1**(Jan), 24–32.
- NEUHOFF, HENRIKE, NEU, AXEL, LISS, BIRGIT, & ROEPER, JOCHEN. 2002. I(h) channels contribute to the different functional properties of identified dopaminergic subpopulations in the midbrain. *J. neurosci.*, **22**(4), 1290–302.
- NICHOLS, COLIN G. 2006. Katp channels as molecular sensors of cellular metabolism. *Nature*, **440**(7083), 470–6.
- NISWENDER, K D, MORTON, G J, STEARNS, W H, RHODES, C J, MYERS, M G, & SCHWARTZ, M W. 2001. Intracellular signalling. key enzyme in leptin-induced anorexia. *Nature*, **413**(6858), 794–5.
- NISWENDER, KEVIN D, & SCHWARTZ, MICHAEL W. 2003. Insulin and leptin revisited: adiposity signals with overlapping physiological and intracellular signaling capabilities. *Frontiers in neuroendocrinology*, **24**(1), 1–10.
- NISWENDER, KEVIN D, MORRISON, CHRISTOPHER D, CLEGG, DEBORAH J, OLSON, RYAN, BASKIN, DENIS G, MYERS, MARTIN G, SEELEY, RANDY J, & SCHWARTZ, MICHAEL W. 2003. Insulin activation of phosphatidylinositol 3-kinase in the hypothalamic arcuate nucleus: a key mediator of insulin-induced anorexia. *Diabetes*, **52**(2), 227–31.

- NOWEND, K L, ARIZZI, M, CARLSON, B B, & SALAMONE, J D. 2001. D1 or d2 antagonism in nucleus accumbens core or dorsomedial shell suppresses lever pressing for food but leads to compensatory increases in chow consumption. *Pharmacol biochem behav*, **69**(3-4), 373–82.
- OLSZEWSKI, PAWEL K, FREDRIKSSON, ROBERT, ERIKSSON, JENNY D, MITRA, ANAYA, RADOMSKA, KATARZYNA J, GOSNELL, BLAKE A, SOLVANG, MARIA N, LEVINE, ALLEN S, & SCHIÖTH, HELGI B. 2011a. Fto colocalizes with a satiety mediator oxytocin in the brain and upregulates oxytocin gene expression. *Biochem biophys res commun*, **408**(3), 422–6.
- OLSZEWSKI, PAWEL K, RADOMSKA, KATARZYNA J, GHIMIRE, KEDAR, KLOCKARS, ANICA, INGMAN, CAROLINE, OLSZEWSKA, AGNIESZKA M, FREDRIKSSON, ROBERT, LEVINE, ALLEN S, & SCHIÖTH, HELGI B. 2011b. Fto immunoreactivity is widespread in the rodent brain and abundant in feeding-related sites, but the number of fto-positive cells is not affected by changes in energy balance. *Physiol behav*, **103**(2), 248–53.
- O'RAHILLY, STEPHEN. 2009. Human genetics illuminates the paths to metabolic disease. *Nature*, **462**(7271), 307–14.
- OSMOND, JESSICA M, MINTZ, JAMES D, DALTON, BRIAN, & STEPP, DAVID W. 2009. Obesity increases blood pressure, cerebral vascular remodeling, and severity of stroke in the zucker rat. *Hypertension*, **53**(2), 381–6.
- OVERTON, P G, & CLARK, D. 1997. Burst firing in midbrain dopaminergic neurons. *Brain res brain res rev*, **25**(3), 312–34.
- PALMITER, RICHARD D. 2007. Is dopamine a physiologically relevant mediator of feeding behavior? *Trends neurosci.*, **30**(8), 375–81.
- PARKER, K L, & SCHIMMER, B P. 1997. Steroidogenic factor 1: a key determinant of endocrine development and function. *Endocr rev*, **18**(3), 361–77.
- PARTON, LAURA E, YE, CHIAN PING, COPPARI, ROBERTO, ENRIORI, PABLO J, CHOI, BRIAN, ZHANG, CHEN-YU, XU, CHUN, VIANNA, CLAUDIA R, BALTHASAR, NINA, LEE, CHARLOTTE E, ELMQUIST, JOEL K, COWLEY, MICHAEL A, & LOWELL, BRADFORD B. 2007. Glucose sensing by pomc neurons regulates glucose homeostasis and is impaired in obesity. *Nature*, **449**(7159), 228–32.
- PAXINOS, & FRANKLIN. 2008. The mouse brain in stereotaxic coordinates, compact, third edition: The coronal plates and diagrams.
- PELLEYMOUNTER, M, CULLEN, M, BAKER, M, & HECHT... R. 1995. Effects of the obese gene product on body weight regulation in ob/ob mice. *Science*, Jan.
- PLUM, L, MA, X, HAMPEL, B, BALTHASAR, N, & COPPARI, R. 2006a. Enhanced pip3 signaling in pomc neurons causes katp channel activation and leads to diet-sensitive ... *Journal of clinical investigation*, Jan.

- PLUM, LEONA, BELGARDT, BENGT F, & BRÜNING, JENS C. 2006b. Central insulin action in energy and glucose homeostasis. *J clin invest*, **116**(7), 1761–6.
- POLONSKY, K. 2005. Insulin secretion in vivo. *Joslin's diabetes mellitus*, Jan.
- POPKIN, B M, & GORDON-LARSEN, P. 2004. The nutrition transition: worldwide obesity dynamics and their determinants. *Int j obes relat metab disord*, **28 Suppl 3**(Nov), S2–9.
- QIU, JIAN, FANG, YUAN, RØNNEKLEIV, OLIVE K, & KELLY, MARTIN J. 2010. Leptin excites proopiomelanocortin neurons via activation of trpc channels. *J. neurosci.*, **30**(4), 1560–5.
- RAE, J, COOPER, K, GATES, P, & WATSKY, M. 1991. Low access resistance perforated patch recordings using amphotericin b. *Journal of neuroscience methods*, **37**(1), 15–26.
- RICHARDS, C D, SHIROYAMA, T, & KITAI, S T. 1997. Electrophysiological and immunocytochemical characterization of gaba and dopamine neurons in the substantia nigra of the rat. *Neuroscience*, **80**(2), 545–57.
- ROBINSON, T E, & BERRIDGE, K C. 1993. The neural basis of drug craving: an incentive-sensitization theory of addiction. *Brain res brain res rev*, **18**(3), 247–91.
- ROGGE, G, JONES, D, HUBERT, G W, LIN, Y, & KUCHAR, M J. 2008. Cart peptides: regulators of body weight, reward and other functions. *Nat rev neurosci*, **9**(10), 747–58.
- RUSSELL, J M, EATON, D C, & BRODWICK, M S. 1977. Effects of nystatin on membrane conductance and internal ion activities in aplysia neurons. *J membr biol*, **37**(2), 137–56.
- RUSO, SCOTT J, BOLANOS, CARLOS A, THEOBALD, DAVID E, DECAROLIS, NATHAN A, RENTHAL, WILLIAM, KUMAR, ARVIND, WINSTANLEY, CATHARINE A, RENTHAL, NORA E, WILEY, MATTHEW D, SELF, DAVID W, RUSSELL, DAVID S, NEVE, RACHAEL L, EISCH, AMELIA J, & NESTLER, ERIC J. 2007. Irs2-akt pathway in midbrain dopamine neurons regulates behavioral and cellular responses to opiates. *Nature neuroscience*, **10**(1), 93–9.
- SAHLHOLM, KRISTOFFER, NILSSON, JOHANNA, MARCELLINO, DANIEL, FUXE, KJELL, & ARHEM, PETER. 2008. Voltage-dependence of the human dopamine d2 receptor. *Synapse*, **62**(6), 476–80.
- SARANTOPOULOS, CONSTANTINE, MCCALLUM, J BRUCE, KWOK, WAI-MENG, & HOGAN, QUINN. 2004. Beta-escin diminishes voltage-gated calcium current rundown in perforated patch-clamp recordings from rat primary afferent neurons. *Journal of neuroscience methods*, **139**(1), 61–8.
- SARGES, R, & WITKOP, B. 1965. Gramicidin a. v. the structure of valine- and isoleucine-gramicidin a. *J am chem soc*, **87**(May), 2011–20.
- SATO, S, KREUTZ, R, WILM, C, GANTEN, D, & PFITZER, G. 1994. Augmented agonist-induced  $Ca^{2+}$ -sensitization of coronary artery contraction in genetically hypertensive rats. evidence for altered signal transduction in the coronary smooth muscle cells. *J clin invest*, **94**(4), 1397–403.

- SAWYER, D B, KOEPPE, R E, & ANDERSEN, O S. 1990. Gramicidin single-channel properties show no solvent-history dependence. *Biophys j*, **57**(3), 515–23.
- SCHILSTRÖM, BJÖRN, YAKA, RAMI, ARGILLI, EMANUELA, SUVARNA, NEESHA, SCHUMANN, JOHANNA, CHEN, BILLY T, CARMAN, MELISSA, SINGH, VINEETA, MAILLIARD, WILLIAM S, RON, DORIT, & BONCI, ANTONELLO. 2006. Cocaine enhances nmda receptor-mediated currents in ventral tegmental area cells via dopamine d5 receptor-dependent redistribution of nmda receptors. *J neurosci*, **26**(33), 8549–58.
- SCHUBERT, MARKUS, GAUTAM, DINESH, SURJO, DAVID, UEKI, KOJIHIKO, BAUDLER, STEPHANIE, SCHUBERT, DOMINIC, KONDO, TATSUYA, ALBER, JENS, GALLDIKS, NORBERT, KÜSTERMANN, ECKEHARDT, ARNDT, SASKIA, JACOBS, ANDREAS H, KRONE, WILHELM, KAHN, C RONALD, & BRÜNING, JENS C. 2004. Role for neuronal insulin resistance in neurodegenerative diseases. *Proc natl acad sci usa*, **101**(9), 3100–5.
- SCHULTZ, W. 1998. Predictive reward signal of dopamine neurons. *Journal of neurophysiology*, **80**(1), 1–27.
- SCHULTZ, W, DAYAN, P, & MONTAGUE, P R. 1997. A neural substrate of prediction and reward. *Science*, **275**(5306), 1593–9.
- SCHULTZ, WOLFRAM. 2007. Behavioral dopamine signals. *Trends neurosci.*, **30**(5), 203–10.
- SCHWARTZ, M, WOODS, S, JR, D PORTE, & SEELEY, R. 2000. Central nervous system control of food intake. *Nature*, Jan.
- SCHWARTZ, MICHAEL W, & PORTE, DANIEL. 2005. Diabetes, obesity, and the brain. *Science*, **307**(5708), 375–9.
- SHINODA, K, LEI, H, YOSHII, H, NOMURA, M, NAGANO, M, SHIBA, H, SASAKI, H, OSAWA, Y, NINOMIYA, Y, & NIWA, O. 1995. Developmental defects of the ventromedial hypothalamic nucleus and pituitary gonadotroph in the ftz-f1 disrupted mice. *Dev dyn*, **204**(1), 22–9.
- SHYNG, S L, & NICHOLS, C G. 1998. Membrane phospholipid control of nucleotide sensitivity of katp channels. *Science*, **282**(5391), 1138–41.
- SIRTORI, C R. 2001. Aescin: pharmacology, pharmacokinetics and therapeutic profile. *Pharmacol res*, **44**(3), 183–93.
- SMITH, I D, & GRACE, A A. 1992. Role of the subthalamic nucleus in the regulation of nigral dopamine neuron activity. *Synapse*, **12**(4), 287–303.
- SPANSWICK, D, SMITH, M, GROPPA, V, & LOGAN, S. 1997. Leptin inhibits hypothalamic neurons by activation of atp-sensitive potassium channels. *Nature*, Jan.
- SPANSWICK, D, SMITH, M A, MIRSHAMSI, S, ROUTH, V H, & ASHFORD, M L. 2000. Insulin activates atp-sensitive k+ channels in hypothalamic neurons of lean, but not obese rats. *Nat neurosci*, **3**(8), 757–8.

- STANLEY, B G, KYRKOULI, S E, LAMPERT, S, & LEIBOWITZ, S F. 1986. Neuropeptide y chronically injected into the hypothalamus: a powerful neurochemical inducer of hyperphagia and obesity. *Peptides*, **7**(6), 1189–92.
- STEFFENSEN, SCOTT C, TAYLOR, SETH R, HORTON, MALIA L, BARBER, ELISE N, LYLE, LAURA T, STOBBS, SARAH H, & ALLISON, DAVID W. 2008. Cocaine disinhibits dopamine neurons in the ventral tegmental area via use-dependent blockade of gaba neuron voltage-sensitive sodium channels. *Eur j neurosci*, **28**(10), 2028–40.
- STERN, J E. 2001. Electrophysiological and morphological properties of pre-autonomic neurones in the rat hypothalamic paraventricular nucleus. *The journal of physiology*, **537**(Pt 1), 161–77.
- STERNSON, SCOTT M, SHEPHERD, GORDON M G, & FRIEDMAN, JEFFREY M. 2005. Topographic mapping of vmh → arcuate nucleus microcircuits and their reorganization by fasting. *Nature neuroscience*, **8**(10), 1356–63.
- STRAUSS, U, HERBRIK, M, MIX, E, SCHUBERT, R, & ROLFS, A. 2001. Whole-cell patch-clamp: true perforated or spontaneous conventional recordings? *Pflugers arch*, **442**(4), 634–8.
- SZCZYPKA, M S, RAINEY, M A, KIM, D S, ALAYNICK, W A, MARCK, B T, MATSUMOTO, A M, & PALMITER, R D. 1999. Feeding behavior in dopamine-deficient mice. *Proc natl acad sci usa*, **96**(21), 12138–43.
- SZCZYPKA, M S, KWOK, K, BROTH, M D, MARCK, B T, MATSUMOTO, A M, DONAHUE, B A, & PALMITER, R D. 2001. Dopamine production in the caudate putamen restores feeding in dopamine-deficient mice. *Neuron*, **30**(3), 819–28.
- TAJIMA, Y, ONO, K, & AKAIKE, N. 1996. Perforated patch-clamp recording in cardiac myocytes using cation-selective ionophore gramicidin. *Am j physiol*, **271**(2 Pt 1), C524–32.
- TANIGUCHI, CULLEN M, EMANUELLI, BRICE, & KAHN, C RONALD. 2006. Critical nodes in signalling pathways: insights into insulin action. *Nat rev mol cell biol*, **7**(2), 85–96.
- TARASOV, ANDREI, DUSONCHET, JULIEN, & ASHCROFT, FRANCES. 2004. Metabolic regulation of the pancreatic beta-cell atp-sensitive k<sup>+</sup> channel: a pas de deux. *Diabetes*, **53 Suppl 3**(Dec), S113–22.
- TERAMOTO, NORIYOSHI, TOMODA, TOSHIHISA, YUNOKI, TAKAKAZU, & ITO, YUSHI. 2006. Different glibenclamide-sensitivity of atp-sensitive k<sup>+</sup> currents using different patch-clamp recording methods. *Eur j pharmacol*, **531**(1-3), 34–40.
- TOSHINAI, KOJI, DATE, YUKARI, MURAKAMI, NOBORU, SHIMADA, MITSUSHI, MONDAL, MUHTASHAN S, SHIMBARA, TAKUYA, GUAN, JIAN-LIAN, WANG, QING-PING, FUNAHASHI, HISAYUKI, SAKURAI, TAKESHI, SHIODA, SEIJI, MATSUKURA, SHIGERU, KANGAWA, KENJI, & NAKAZATO, MASAMITSU. 2003. Ghrelin-induced food intake is mediated via the orexin pathway. *Endocrinology*, **144**(4), 1506–12.

- UCHIDA, S, AKAIKE, N, & NABEKURA, J. 2000. Dopamine activates inward rectifier k<sup>+</sup> channel in acutely dissociated rat substantia nigra neurones. *Neuropharmacology*, **39**(2), 191–201.
- UNGERSTEDT, U. 1971. Adipsia and aphagia after 6-hydroxydopamine induced degeneration of the nigro-striatal dopamine system. *Acta physiol scand suppl*, **367**(Jan), 95–122.
- UNGLESS, M A, WHISTLER, J L, MALENKA, R C, & BONCI, A. 2001. Single cocaine exposure in vivo induces long-term potentiation in dopamine neurons. *Nature*, **411**(6837), 583–7.
- URRY, D W. 1971. The gramicidin a transmembrane channel: a proposed pi(l,d) helix. *Proc natl acad sci usa*, **68**(3), 672–6.
- URRY, D W, GOODALL, M C, GLICKSON, J D, & MAYERS, D F. 1971. The gramicidin a transmembrane channel: characteristics of head-to-head dimerized (l,d) helices. *Proc natl acad sci usa*, **68**(8), 1907–11.
- URRY, D W, TRAPANE, T L, & PRASAD, K U. 1983. Is the gramicidin a transmembrane channel single-stranded or double-stranded helix? a simple unequivocal determination. *Science*, **221**(4615), 1064–7.
- VAN DEN POL, A N, & CASSIDY, J R. 1982. The hypothalamic arcuate nucleus of rat—a quantitative golgi analysis. *J comp neurol*, **204**(1), 65–98.
- VEATCH, W R, FOSSEL, E T, & BLOUT, E R. 1974. The conformation of gramicidin a. *Biochemistry*, **13**(26), 5249–56.
- VOLKOW, N D, & FOWLER, J S. 2000. Addiction, a disease of compulsion and drive: involvement of the orbitofrontal cortex. *Cereb cortex*, **10**(3), 318–25.
- VOLKOW, NORA D, WANG, GENE-JACK, TELANG, FRANK, FOWLER, JOANNA S, THANOS, PANAYOTIS K, LOGAN, JEAN, ALEXOFF, DAVID, DING, YU-SHIN, WONG, CHRISTOPHER, MA, YEMING, & PRADHAN, KITH. 2008. Low dopamine striatal d2 receptors are associated with prefrontal metabolism in obese subjects: possible contributing factors. *Neuroimage*, **42**(4), 1537–43.
- WALLACE, B A. 1990. Gramicidin channels and pores. *Annu rev biophys biophys chem*, **19**(Jan), 127–57.
- WANG, G J, VOLKOW, N D, LOGAN, J, PAPPAS, N R, WONG, C T, ZHU, W, NETUSIL, N, & FOWLER, J S. 2001. Brain dopamine and obesity. *Lancet*, **357**(9253), 354–7.
- WILLIAMS, KEVIN W, MARGATHO, LISANDRA O, LEE, CHARLOTTE E, CHOI, MICHELLE, LEE, SYANN, SCOTT, MICHAEL M, ELIAS, CAROL F, & ELMQUIST, JOEL K. 2010. Segregation of acute leptin and insulin effects in distinct populations of arcuate proopiomelanocortin neurons. *J neurosci*, **30**(7), 2472–9.
- WISE, ROY A. 2006. Role of brain dopamine in food reward and reinforcement. *Philos trans r soc lond, b, biol sci*, **361**(1471), 1149–58.

- WISE, ROY A. 2009. Roles for nigrostriatal—not just mesocorticolimbic—dopamine in reward and addiction. *Trends neurosci.*, **32**(10), 517–24.
- WOLFART, J, NEUHOFF, H, FRANZ, O, & ROEPER, J. 2001. Differential expression of the small-conductance, calcium-activated potassium channel sk3 is critical for pacemaker control in dopaminergic midbrain neurons. *J. neurosci.*, **21**(10), 3443–56.
- WOODS, S C, LOTTER, E C, MCKAY, L D, & PORTE, D. 1979. Chronic intracerebroventricular infusion of insulin reduces food intake and body weight of baboons. *Nature*, **282**(5738), 503–5.
- XU, BAOJI, GOULDING, EVAN H, ZANG, KELING, CEPOI, DAVID, CONE, ROGER D, JONES, KEVIN R, TECOTT, LAURENCE H, & REICHARDT, LOUIS F. 2003. Brain-derived neurotrophic factor regulates energy balance downstream of melanocortin-4 receptor. *Nature neuroscience*, **6**(7), 736–42.
- YAFFE, KRISTINE. 2007. Metabolic syndrome and cognitive disorders: is the sum greater than its parts? *Alzheimer dis assoc disord*, **21**(2), 167–71.
- YAU, W M, WIMLEY, W C, GAWRISCH, K, & WHITE, S H. 1998. The preference of tryptophan for membrane interfaces. *Biochemistry*, **37**(42), 14713–8.
- YE, J, ZHANG, J, XIAO, C, & KONG, J. 2006. Patch-clamp studies in the cns illustrate a simple new method for obtaining viable neurons in rat . . . . *Journal of neuroscience methods*, **158**(Jan), 251–259.
- YUNG, W H, HÄUSSER, M A, & JACK, J J. 1991. Electrophysiology of dopaminergic and non-dopaminergic neurones of the guinea-pig substantia nigra pars compacta in vitro. *J. physiol. (lond.)*, **436**(May), 643–67.
- ZHANG, Y, PROENCA, R, MAFFEI, M, & BARONE. . . , M. 1994. Positional cloning of the mouse obese gene and its human homologue. *Nature*, Jan.
- ZHOU, Q Y, & PALMITER, R D. 1995. Dopamine-deficient mice are severely hypoactive, adipsic, and aphagic. *Cell*, **83**(7), 1197–209.
- ZOLLES, GERD, KLÖCKER, NIKOLAJ, WENZEL, DANIELA, WEISSER-THOMAS, JUTTA, FLEISCHMANN, BERND K, ROEPER, JOCHEN, & FAKLER, BERND. 2006. Pacemaking by hcn channels requires interaction with phosphoinositides. *Neuron*, **52**(6), 1027–36.

# Danksagung

An dieser Stelle möchte ich die Gelegenheit nutzen, mich bei allen zu bedanken, die mich während der letzten Jahre auf so vielfältige Weise bei meiner Promotion unterstützt haben, im Besonderen gilt mein Dank:

- **Prof. Dr. Peter Kloppenburg** für seine uneingeschränkte Unterstützung während meiner Doktorarbeit. Besonders möchte ich mich dafür bedanken, dass ich jederzeit alle erdenklichen Ressourcen des Labors nutzen konnte und ich bezüglich der verschiedenen Projekte sämtliche Freiheiten in Bezug auf Versuchsplanung und -durchführung hatte.
- **Prof. Dr. Jens Brüning** möchte ich dafür danken, dass ich die Möglichkeit bekommen habe, an den verschiedenen 'Maus'-Projekten mitarbeiten zu können. Weiterhin möchte ich mich für die Erstellung des Zweitgutachtens bedanken.
- **Helmut Wratil** möchte ich für die phantastischste technische Unterstützung bedanken, die man sich nur vorstellen kann. Ohne ihn wäre die Arbeit in dieser Form mit Sicherheit nicht möglich gewesen. Weiterhin möchte ich mich für die großartigen 'HiFi-Seminare' bedanken.
- Meinem Bruder **Martin** für die exzellente Zusammenarbeit beim 'Fto-Projekt' und die vielen sehr hilfreichen Anregungen beim Zusammenschreiben. Ich kann mich wirklich sehr glücklich schätzen, dass es der Zufall so wollte und wir – hoffentlich auch in Zukunft – zusammen an diversen Projekten arbeiten können.
- **Christine Könner** für die großartige Zusammenarbeit beim 'Insulin'-Projekt und das geduldige Korrekturlesen meiner Arbeit. Danke auch für eine lustige Zeit während der Schweiz-Exkursion und dem BC-Praktikum.
- **Tim Klöckener** für eine phantastische Zusammenarbeit im Rahmen des 'SF-1'-Projektes. Wenn es auch manchmal nicht den Anschein hatte, war es mir dennoch eine große Freude.
- *The very talented Ally Girasole for providing additional data on SK currents and many enjoyable moments in the lab. Hope, you had a fun time at our lab!*
- **Andi Pippow** danke ich für das Korrekturlesen meiner Arbeit und dass er sich immer mit großer Geduld meiner Fragen, insbesondere bezüglich IGOR und [R], angenommen hat. Meinem 'Setup Mitbewohner' **Lars Paeger** danke ich für diverse unterhaltsame Mauerbier und die morgendlichen UniFit-Qualen; **Cathleen Rotte** danke ich für das Protokoll-Führen in meiner Disputation und das recht kurzfristige Korrekturlesen meiner Arbeit. Bei **Moritz Paehler** möchte ich mich für viele unterhaltsame Stunden im Lab und die Einführung ins 'Maus-Patchen'

danken. Weiterhin danke ich allen Kollegen/Freunden im **Kloppenburg und Brüning Lab** möchte für eine entspannte und überaus angenehme Arbeitsatmosphäre bedanken.

- **Andreas Husch** danke ich für die Einführung ins *Patchen* die vielen unterhaltenden Gespräche über Musik im Allgemeinen und Speziellen und natürlich(!) San Diego 2007 und Chicago 2009!
- *Dr. Bruce Johnson for his great lectures during his stay in Cologne and many enjoyable conversations.*
- *Prof. Dr. Ron Harris-Warrick for many enjoyable conversations and for being a true inspiration.*
- Mein ganz besonderer Dank gilt meinen Eltern **Ingrid** und **Erich Heß**, die mich immer bedingungslos unterstützt haben und an mich geglaubt haben. Danke!
- Meiner **Kathi** für ihre Liebe und dafür, dass sie mir meine – zuweilen promotionsbedingten – Gemütsschwankungen mit größtem Verständnis nachgesehen hat und mir während der ganzen Zeit immer Halt gegeben hat.

— *All's Well That Ends Well* —

# Erklärung

Ich versichere, dass ich die von mir vorgelegte Dissertation selbständig angefertigt, die benutzten Quellen und Hilfsmittel vollständig angegeben und die Stellen der Arbeit – einschließlich Tabellen, Karten und Abbildungen –, die anderen Werken im Wortlaut oder dem Sinn nach entnommen sind, in jedem Einzelfall als Entlehnung kenntlich gemacht habe; dass diese Dissertation noch keiner anderen Fakultät oder Universität zur Prüfung vorgelegen hat; dass sie – abgesehen von unten angegebenen Teilpublikationen – noch nicht veröffentlicht worden ist sowie, dass ich eine solche Veröffentlichung vor Abschluss des Promotionsverfahrens nicht vornehmen werde.

Die Bestimmungen der Promotionsordnung sind mir bekannt. Die von mir vorgelegte Dissertation ist von Prof. Dr. Peter Kloppenburg betreut worden.

Köln, den 15.08.2011

---

(Simon Heß)

# Teilpublikationen

## Artikel

ERNST, M B, WUNDERLICH, C M, HESS, S, PAEHLER, M, MESAROS, A, KORALOV, S B, KLEINRIDDER, A, HUSCH, A, MÜNZBERG, H, HAMPEL, B, ALBER, J, KLOPPENBURG, P, BRÜNING, J C, WUNDERLICH F T. 2009. Enhanced Stat3 activation in POMC neurons provokes negative feedback inhibition of leptin and insulin signaling in obesity. *J. Neurosci.*, **29**(37), 11582–93.

HUSCH, A, HESS, S, KLOPPENBURG, P. 2008. Functional parameters of voltage-activated Ca<sup>2+</sup> currents from olfactory interneurons in the antennal lobe of *Periplaneta americana*. *J. Neurophysiol.*, **99**(1), 320–332.

KLÖCKENER, T, HESS, S, BELGARDT, B F, PAEGER, L, VERHAGEN, L A, HUSCH, A, SOHN, J W, HAMPEL, B, DHILLON, H, ZIGMAN, J, LOWELL, B B, WILLIAMS, K W, ELMQUIST, J K, HORVATH, T L, KLOPPENBURG, P, BRÜNING, J C. 2011. High-fat Feeding Promotes Obesity via Insulin Receptor/PI3k-Dependent Inhibition of SF-1 VMH Neurons. *Nat. Neurosci.*, **14**(7), 911–18.

KÖNNER, A C, HESS, S, TOVAR, S, MESAROS, A, SÁNCHEZ-LASHERAS, C, EVERS, N, VERHAGEN, L A W, BRÖNNEKE, H S, KLEINRIDDER, A, HAMPEL, B, KLOPPENBURG, P, BRÜNING, J C. 2011. Role for Insulin Signaling in Catecholaminergic Neurons in Control of Energy Homeostasis. *Cell Metab.*, **13**(6), 720–8.

HESS, M E\*, HESS, S\*, KOCH, L\*, BRÖNNECKE, H S, VERHAGEN, L A, DIETRICH, M O, JORDAN, S D, BELGARDT, B F, FRANZ, T, HORVATH, T L, RÜTHER, U, KLOPPENBURG, P, BRÜNING, J C. 2011. The Obesity-Associated Fto Gene Regulates Activity of the Dopaminergic Midbrain Circuitry. *Nat. Neurosci.* (submitted) .

---

\*These authors contributed equally to the study.

TOVAR, S, PAEGER, L, HESS, S, REDEMANN, N, BRÖNNEKE, H S, HAMPEL, B, ACKERMANN, J, WUNDERLICH, F T, RHAMOUNI, K, KLOPPENBURG, P, BRÜNING, J C. 2011.  $K_{ATP}$ -Channel-dependent Glucose Sensing in the Locus Coeruleus controls Energy Homeostasis via Regulation of Sympathetic Innervation of Brown Adipose Tissue. *Cell Metab.* (submitted).

PIPPOW, A, PAEHLER, M, HESS, S, PAEGER, L, JOUCLA, S, KLÖCKENER, T, POUZAT, C, BRÜNING, J C, KLOPPENBURG, P. 2011. High fat diet decreases neural activity in anorexigenic POMC neurons of the nucleus arcuatus by altering  $Ca^{2+}$  handling properties. (in preparation).

NEUHAUS, J, BARIS, O, HESS, S, MOSER, N, SCHRÖDER H J, CHINTA, S J, ANDERSEN, J K, KLOPPENBURG, P, WIESNER, R J. 2011. Catecholamine metabolism is sufficient to drive the generation of mitochondrial DNA deletions – implications for the selective loss of dopaminergic neurons in Parkinsons disease and aging. (in preparation).

## Poster

HESS, S, HUSCH, A, KLOPPENBURG, P. 2007. Pharmacological Characterization of Voltage-gated Calcium Currents in Olfactory Interneurons of *Periplaneta Americana*. *Proceedings of the 31<sup>th</sup> Göttingen Neurobiology Conference and the 7<sup>th</sup> Meeting of the German Neuroscience Society.*

DEMMEER, H, HESS, S, HUSCH, A, PAEHLER, M, KLOPPENBURG, P. 2007. Physiological and morphological characterization of interneurons in the insect olfactory pathway. *Annual Meeting of the Society for Neuroscience (SfN). Abstract, San Diego, CA*

PIPPOW, A, DEMMEER, H, FUSCA, D, HESS, S, HUSCH, A, PAEHLER, M, WRATIL, H, POUZAT, C, KLOPPENBURG, P. 2008. Distinct calcium handling properties of identified insect olfactory interneurons. *Annual Meeting of the Society for Neuroscience (SfN). Abstract, Washington, DC*

HESS, S, HUSCH, A, PAEHLER, M, PIPPOW, A, WRATIL, H, BELGARDT, B F, KLÖCKENER, T, ROTHER, E, BRÜNING, J C, KLOPPENBURG, P. 2009. Functional parameters of identified neurons in the arcuate nucleus of the hypothalamus. *Annual Meeting of the Society for Neuroscience (SfN). Abstract, Chicago, IL*

PIPPOW, A, PAEHLER, M, PAEGER, L, HESS, S, KLÖCKENER, T, VOGT, M, POUZAT, C, BRÜNING, J C, KLOPPENBURG, P. 2010. High fat induced obesity impairs intrinsic properties of anorexigenic POMC neurons in the hypothalamus. *CECAD Meeting 2010*

HESS, S, KLÖCKENER, T, HAMPEL, B, BRÜNING, J C, KLOPPENBURG, P. 2011. Direct Action of Insulin on Steroidogenic Factor 1 positive Neurons in the Ventromedial Hypothalamus. *Proceedings of the 33<sup>th</sup> Göttingen Neurobiology Conference and the 9<sup>th</sup> Meeting of the German Neuroscience Society.*

# Curriculum Vitae

*Dipl. Biol. Simon Heß*

Universität zu Köln  
Biozentrum Köln  
Zoologisches Institut  
Zülpicher Straße 47b  
50674 Köln  
Tel.: +49 (0)221 470-5207  
Email: simon.hess@uni-koeln.de  
Geburtsdatum/ -ort: 19.09.1978 in Adenau  
Staatsangehörigkeit: deutsch

## AUSBILDUNG

---

- 2007 – 2011 **Universität zu Köln, Zoologisches Institut**  
Doktorarbeit im Labor von Prof. Dr. Peter Kloppenburg. Thema:  
„Towards Defining the Role of CNS Circuits in Control of Energy  
Homeostasis“.
- 1999 – 2006 **Universität zu Köln**  
Studium Biologie, Fächer: Zoologie, Entwicklungsbiologie, Biochemie  
Diplom in Biologie (November 2006), Note: sehr gut „mit  
Auszeichnung“, Thema: „Modification of Calcium Currents in  
Interneurons of the Antennal Lobe of *Periplaneta americana* by  
Selected Organic Calcium Channel Blockers“  
Vordiplom in Biologie (April 2003)
- 1998 – 1999 **DRK Eifel-Mosel-Hunsrück Rettungsdienst gGmbH**  
Zivildienst
- 1989 – 1998 **St. Matthias Gymnasium Gerolstein** (Abitur)

## BERUFLICHE TÄTIGKEITEN

---

- 2007 – 2011 **Universität zu Köln, Zoologisches Institut**  
WM (2007 – 2011): Praktikum Tierphysiologie, Physiologie des  
Menschen, Anfängerkurs “Biologie IIIA”  
WHK (2007): Praktikum Tierphysiologie
- 2005 – 2006 **Universität zu Köln, Zoologisches Institut**  
SHK: Praktikum Tierphysiologie
- 2005 **Universität zu Köln, Institut für Genetik**  
SHK: Tierpflege Aquarienanlage. Prof. Tautz

Köln, den 15. August 2011 \_\_\_\_\_  
(Simon Heß)

# Curriculum Vitae

*Dipl. Biol. Simon Heß*

University of Cologne  
Cologne Biocenter  
Institute for Zoology  
Zülpicher Straße 47b  
50674 Cologne, Germany  
tel.: +49 (0)221 470-5207  
email: simon.hess@uni-koeln.de  
date and place of birth: 9-19-1978 in Adenau  
citizenship: German

## EDUCATION

---

- 2007 – 2011 **University of Cologne, Institute for Zoology**  
PhD thesis in the lab of Prof. Dr. Peter Kloppenburg: „Towards Defining the Role of CNS Circuits in Control of Energy Homeostasis“.
- 1999 – 2006 **University of Cologne**  
Study in biology, main courses: zoology, developmental biology, biochemistry  
Diploma in biology (November 2006), grade: sehr gut „with distinction“, Title: „Modification of Calcium Currents in Interneurons of the Antennal Lobe of *Periplaneta americana* by Selected Organic Calcium Channel Blockers“  
Intermediate diploma in biology (April 2003)
- 1998 – 1999 **DRK Eifel-Mosel-Hunsrück Rettungsdienst gGmbH**  
alternative civilian service
- 1989 – 1998 **St. Matthias Gymnasium Gerolstein** (university entrance diploma)

## PROFESSIONAL QUALIFICATIONS

---

- 2007 – 2011 **University of Cologne, Institute for Zoology**  
scientific assistant (WM; 2007 – 2011): Lab course in animal physiology, Human physiology, Beginner lab course „Biologie IIIA“  
graduate assistant (WHK; 2007): Lab course in animal physiology
- 2005 – 2006 **University of Cologne, Institute for Zoology**  
student assistant (SHK): Lab course in animal physiology
- 2005 **University of Cologne, Institute for Genetics**  
student assistant (SHK): Animal care fish tanks. Prof. Tautz

Cologne, August 15, 2011 \_\_\_\_\_  
(Simon Heß)